

PONTE SULLO STRETTO DI MESSINA



PROGETTO DEFINITIVO

EUROLINK S.C.p.A.

IMPREGILO S.p.A. (MANDATARIA)
SOCIETÀ ITALIANA PER CONDOTTE D'ACQUA S.p.A. (MANDANTE)
COOPERATIVA MURATORI E CEMENTISTI - C.M.C. DI RAVENNA SOC. COOP. A.R.L. (MANDANTE)
SACYR S.A.U. (MANDANTE)
ISHIKAWAJIMA - HARIMA HEAVY INDUSTRIES CO. LTD (MANDANTE)
A.C.I. S.C.P.A. - CONSORZIO STABILE (MANDANTE)

<p>IL PROGETTISTA COWI Ing. E.M. Veje Dott. Ing. E. Pagani Ordine Ingegneri Milano n° 15408</p> 	<p>IL CONTRAENTE GENERALE</p> <p>Project Manager (Ing. P.P. Marcheselli)</p>	<p>STRETTO DI MESSINA Direttore Generale e RUP Validazione (Ing. G. Fiammenghi)</p>	<p>STRETTO DI MESSINA Amministratore Delegato (Dott. P. Ciucci)</p>
--	--	---	---

<p><i>Unità Funzionale</i> <i>Tipo di sistema</i> <i>Raggruppamento di opere/attività</i> <i>Opera - tratto d'opera - parte d'opera</i> <i>Titolo del documento</i></p>	<p>OPERA DI ATTRAVERSAMENTO SOTTOSTRUTTURE BLOCCHI DI ANCORAGGIO Geotechnical Design Reports Calabria Anchor Block – evaluation of block behaviour via 3D FE analyses and of bearing capacity, Annex</p>	<p>PF0067_F0</p>
---	--	-------------------------

CODICE	C	G	1	0	0	0	P	C	L	D	P	S	T	B	4	B	C	0	0	0	0	0	0	3	F0
--------	---	---	---	---	---	---	---	---	---	---	---	---	---	---	---	---	---	---	---	---	---	---	---	---	----

REV	DATA	DESCRIZIONE	REDATTO	VERIFICATO	APPROVATO
F0	20-06-2011	EMISSIONE FINALE	GL	LC	SR

		<p align="center">Ponte sullo Stretto di Messina PROGETTO DEFINITIVO</p>		
<p>Calabria Anchor Block – evaluation of block behaviour via 3D FE analyses and of bearing capacity, Annex</p>	<p><i>Codice documento</i> PF0067_F0_ANX</p>		<p><i>Rev</i> F0</p>	<p><i>Data</i> 20-06-2011</p>

		Ponte sullo Stretto di Messina PROGETTO DEFINITIVO		
Calabria Anchor Block – evaluation of block behaviour via 3D FE analyses and of bearing capacity, Annex	<i>Codice documento</i> PF0067_F0_ANX	<i>Rev</i> F0	<i>Data</i> 20-06-2011	

INDEX

1	EXECUTIVE SUMMARY	5
2	SOIL PROFILE AND GEOTECHNICAL CHARACTERISATION	11
3	3D NUMERICAL ANALYSIS OF THE CALABRIA ANCHOR BLOCK	15
3.1	Soil model	15
3.1.1	Geometrical soil model	15
3.1.2	Constitutive soil model	16
3.1.3	Soil parameters	18
3.2	Structural elements	20
3.2.1	Anchor Block	20
3.2.2	Diaphragm walls	20
3.2.3	Retaining Anchors	21
3.3	Calculation steps of analysis	24
3.3.1	Effect of excavation around the block	27
4	RESULTS OF THE 3D ANALYSES	28
4.1	Application of the design forces	28
4.2	Load-displacement curves: increase of external loads	32
4.3	Msf-displacement curves: ϕ' – c' reduction analyses	33
4.4	Plaxis 3D foundation output	34
4.4.1	Soil stress state	34
4.4.2	Mesh displacements	35
4.4.3	Water pressure distribution	35
5	CONCLUSIONS	37
6	FIGURES	40
	APPENDIX A – Updated cable forces obtained from global IBDAS model version 3.3b	99
	APPENDIX B – Updated cable forces obtained from global IBDAS model version 3.3f	102
	REFERENCES	105

		<p align="center">Ponte sullo Stretto di Messina PROGETTO DEFINITIVO</p>		
<p>Calabria Anchor Block – evaluation of block behaviour via 3D FE analyses and of bearing capacity, Annex</p>	<p><i>Codice documento</i> PF0067_F0_ANX</p>		<p><i>Rev</i> F0</p>	<p><i>Data</i> 20-06-2011</p>

		Ponte sullo Stretto di Messina PROGETTO DEFINITIVO		
Calabria Anchor Block – evaluation of block behaviour via 3D FE analyses and of bearing capacity, Annex	<i>Codice documento</i> PF0067_F0_ANX	<i>Rev</i> F0	<i>Data</i> 20-06-2011	

1 EXECUTIVE SUMMARY

This report describes the static 3D finite element analyses of the behaviour of the Calabria Anchor Block carried out using the commercial code Plaxis 3D Foundation. The calculations are based on both drawings and cable forces provided in the Tender Design; account is also given for the influence of the cable forces computed from the global IBDAS model version 3.3b and 3.3f.

The analyses carried out to evaluate earthquake-induced block displacements and safety against sliding, rotation and bearing capacity failure are described in the companion report “Calabria anchor block: earthquake-induced displacements and safety against ultimate limit states”.

Chapter 2 describes the soil profile on the Calabria shore (Figure 1). Starting from ground level and moving downwards the following units are encountered: *Depositi Costieri* (Coastal Deposits); *Ghiaie di Messina* (Messina Gravel)/*Sedimenti dei terrazzi* (Terrace Deposits); *Depositi Continentali* (Continental Deposits)/*Calcarenite di Vinco* (Vinco Calcarenite); *Conglomerato di Pezzo* (Pezzo Conglomerate); *Cristallino* (Crystalline bedrock). For the Calabria Anchor Block, the relevant geological unit is the Pezzo Conglomerate, with a weathered shallow layer ($20\text{ m} < z < 40\text{ m}$), overlain by the Terrace Deposits of small thickness. A plan view at the site of the Calabria Anchor Block is shown in Figure 2. The two longitudinal sections and the cross section indicated in Figure 2 are shown in Figure 3, Figure 4 and Figure 5. Table 1 summarises the main mechanical parameters obtained from the geotechnical characterisation for the relevant layers.

Chapter 3 describes the geometry of the 3D model of the Calabria Anchor Block, details the constitutive models adopted for the soil and the structural elements, and summarises the calculation steps of the finite element analyses.

The soil model is described in section 3.1. The geometry of the model of the subsoil (section 3.1.1) consists of a layer of gravel and sand, corresponding to the Coastal Plain Deposits and the Messina Gravel, a layer of weathered Pezzo Conglomerate, and a layer of Pezzo Conglomerate in place. In the numerical model (Figures 11, 12, and 13) the layers are inclined on the horizontal in the east-west direction, parallel to the coastline; the ground level is horizontal at + 118 m a.s.l.; the initial pore water pressure distribution is hydrostatic with a hydraulic head at +102 m a.s.l. The constitutive model adopted for the soil (section 3.1.2) is an elastic-plastic rate independent model with isotropic hardening (Hardening Soil) available in the library of the code *Plaxis*. The calibration

		Ponte sullo Stretto di Messina PROGETTO DEFINITIVO		
Calabria Anchor Block – evaluation of block behaviour via 3D FE analyses and of bearing capacity, Annex	<i>Codice documento</i> PF0067_F0_ANX	<i>Rev</i> F0	<i>Data</i> 20-06-2011	

of the constitutive model (section 3.1.3) was carried out using the results from the cross hole test carried out at the site and from published results of compression triaxial tests. In particular, the cross-hole test was used to evaluate the shear modulus at small strains G_0 and to describe its variation with effective stress. The remaining soil parameters were selected to obtain a satisfactory description of the soil non-linearity observed in the triaxial tests. The Hardening Soil parameters for the three layers are summarised in Table 3 and Table 4.

The numerical models of the structural elements is described in section 3.2. The Anchor Block (section 3.2.1) has the shape of a trapezoid-based prism (Figure 11); in the numerical model the bottom boundary of the block is defined by a stepped profile. The anchor block has two pairs of empty chambers, to host the main cables from the Messina Bridge and to be filled with ballast material, respectively. Table 5 summarises the mechanical parameters adopted in the analyses for the anchor block concrete, the ballast material and the "empty material", all modelled as linear elastic. The diaphragm walls supporting the excavation (section 3.2.2) have a thickness of 1.0 m and a variable length according to the shape of the block. In the model, the depth of the toe of the walls is essentially the same as in the design, while the head of the walls is uniformly located at +118 m a.s.l. The diaphragm walls are modelled as anisotropic Plaxis WALL elements. To simulate the lack of connection beams between the panels of the diaphragm walls, E_2 Young modulus and G_{23} shear modulus (Figure 18) have been reduced by an order of magnitude. Table 6 summarizes the geometrical and mechanical properties of the diaphragm walls. The model includes 7 levels of retaining anchors along the east and the west side of the pit and 4 levels of anchors along its north and south side (section 3.2.3). The retaining anchors are modelled as Plaxis SPRING elements, located, with a 5.0 m spacing in plan, i.e. twice (or more) the design spacing, so that each spring represents at least two retaining anchors. A connecting beam is inserted in the model at the elevation of each level of retaining anchors to distribute the load from the anchors to the retaining wall. SPRING elements simulate anchors in a simplified way, without taking into account anchor – soil interaction. The skin resistance of the retaining anchors has been determined using to eqn. (10) (Bustamante and Doix method (1985), - *repetitive and selective injection*) and the soil properties and the SPT results of the grouted soil layers. The stiffness of the anchor bars has been computed for a variable number of strands per bar (between 7 and 11) with a nominal diameter of 15.2 mm. The limit displacement of the anchor bars has been calculated using eqn. (11). Table 7 summarises the geometrical characteristics and the strength and stiffness properties of the retaining anchors. A non-linear stiffness has been assigned to each spring through a force-displacement (T-u) diagram (Figure 17), including a pre-tension value T_{pret} of the anchors. Table 8

		Ponte sullo Stretto di Messina PROGETTO DEFINITIVO		
Calabria Anchor Block – evaluation of block behaviour via 3D FE analyses and of bearing capacity, Annex	<i>Codice documento</i> PF0067_F0_ANX	<i>Rev</i> F0	<i>Data</i> 20-06-2011	

summarizes the stiffness properties assigned to the springs in the numerical model; the u_{mod} values were determined using eqn. (12). Table 9 summarises the properties of the connection beam.

The following sequence of computation steps was used in the analyses (section 3.3):

1. computation of the initial stress state, by means of the K_0 -procedure;
2. activation of diaphragm walls and corresponding interface elements (Figure 19);
3. excavation of the soil, in 7 progressive drops, to reach the anchor block base; simultaneous activation of the corresponding retaining anchors levels, connection beam and pre-tension of the anchors. For all excavation stages with dredge level below ground water level (i.e. below +102 m a.s.l.) seepage occurs towards the inside of the pit; in these stages, the pore pressure distribution of the soil clusters below dredge line and within the area of the pit has been interpolated between the external groundwater level (+102 m a.s.l.) and the groundwater level corresponding to dredge level (Figure 58 and 57);
4. progressive activation of the anchor block from the bottom up in 11 steps. In each step the excavated clusters are first reactivated as "fluid concrete", with very low value of shear stiffness, and then their properties changed to "solid concrete", while the next layer of "fluid concrete" element is activated. At the end of the construction of the anchor block, the ballast material fills the rear chambers of the block, while the "empty material" fills the front chambers. Figure 25 show the 3D model of the anchor block, before and after filling the chambers. Before application of the external loads, the provisional retaining systems are removed and the general hydrostatic groundwater conditions are reinstated (Figure 58).
5. application of external loads; the forces transmitted by the cables to the Calabria Anchor Block are those provided by the structural analyses of the tender design, for three different load combinations. Table 10 summarises the load cases and the corresponding values of the acting forces. The direction of the force is inclined 15 degrees upwards; the versus is towards the sea shore. The lowest value of the force (SILS) is reached in 10 incremental load steps; 1 further load step is needed to reach the SLS2 force and three further steps to reach the highest value of the force (ULS).
6. a) increase external loads. The external loads are further increased, up to a final value of about 8500 MN, or about twice the ULS force value and about 2.7 times the SILS force value.
 b) $\varphi' - c'$ reduction. Starting from the values of forces corresponding to SILS, SLS2 and ULS loading conditions, $\varphi' - c'$ reduction analyses are carried out. In these analyses the

		Ponte sullo Stretto di Messina PROGETTO DEFINITIVO		
Calabria Anchor Block – evaluation of block behaviour via 3D FE analyses and of bearing capacity, Annex	<i>Codice documento</i> PF0067_F0_ANX	<i>Rev</i> F0	<i>Data</i> 20-06-2011	

strength properties of the soils are progressively reduced, as per eqn. (13) and (14).

To evaluate the effect of the uppermost layer of soil on the computed displacements of the block under the applied loads, one *comparative* analysis has been carried out (section 3.3.1), in which before the application of the external loads, a 4 m deep excavation extending 25 m around the block in plane was modelled (Figure 27).

Chapter 4 describes the results of the 3D finite element analysis.

The displacement of the anchor block under the external loads (section 4.1) is a translation towards the seashore (z-direction), and a downward rotation in the y-z plane (Figures 26 and 27). Figure 30 shows the translation of a North South section of the anchor block near its centre of gravity, obtained assigning to all points of the section the average values of the displacements in the z- and y- directions computed for the 12469 nodes of the anchor block. The average displacement is equal to about 8 mm, with a slope of about 8 degrees on the horizontal, directed upwards. Figure 31 shows the roto-translation of the same section of the anchor block. The displacement of the centre of gravity is still equal to about 8 mm, with an inclination of 13° on the horizontal, while the average rotation θ_G around point G is equal to about $3 \cdot 10^{-3}$ degrees.

Ten points of the anchor block were selected to process output; their location is given in Figure 31 and Table 12.

Table 13 and Table 14 summarize the displacements computed for each of the ten points at the end of three steps, corresponding to SILS, SLS2 and ULS load values. The load-displacement curves obtained for the ten selected points are plotted in Figure 34; Figure 35 and Figure 36 show the horizontal (z-direction) and vertical (y-direction) load-displacement curves, while Figure 37 shows the horizontal (x-direction, orthogonal to the force) load-displacement curves. Figure 37 compares the load-displacement curves obtained from the standard and comparative analyses. The displacements were reset to zero before application of the external loads. The results show

- 1) The anchor block displacement under the external loads is a translation towards the sea shore (z-direction), and a downward rotation in the y-z plane (Figure 28 - Figure 30).
- 2) For all three load combinations, the horizontal displacement of the block under the external loads is less than 10 mm, the vertical upward displacement is less than 2 mm, while the horizontal displacement in the x-direction (orthogonal to the force) is practically equal to zero.
- 3) Table 16 summarizes the rotation angles corresponding to the SILS, SLS2 and ULS values of the external load, while Figure 38 shows the evolution of the y-z plane and x-z plane rotations versus the increasing external load. The rotation values in the y-z plane are of the order of the

		Ponte sullo Stretto di Messina PROGETTO DEFINITIVO		
Calabria Anchor Block – evaluation of block behaviour via 3D FE analyses and of bearing capacity, Annex	<i>Codice documento</i> PF0067_F0_ANX	<i>Rev</i> F0	<i>Data</i> 20-06-2011	

thousandth of degree (the positive value of rotation is directed toward the seashore), while they are essentially equal to zero in the x-y direction. The rotations in the x-z plane are small, showing a slight effect of the inclination of the soil layers on the response of the anchor block.

- 4) The results of *comparative* analysis show a relatively small influence of the uppermost 4 m of soil on the response of the anchor block (Figure 40). Anyway, full refilling of the area surrounding the anchor block is recommended at least up to an elevation of 118 m a.s.l.
- 5) The average direction of the block movement is directed upwards, with a slope of about 10° on the horizontal (Table 17).
- 6) A limit value of the load that can be applied to the anchor block (section 4.2) can be evaluated using a hyperbolic fit of the load displacement curves (Figure 39), as per eqn. (15) and (16). The resulting value of the limit load is about 11000 MN, or a safety factor against increasing external forces of about 2.75 for ULS load and of about 3.5 for SILS load.
- 7) The $\phi' - c'$ reduction analyses carried out starting from the configuration corresponding to the SILS, SLS2 and ULS values of applied loads, yield a safety factor M_{sf} of about 3 for all three loading conditions (Figure 40). The $\phi' - c'$ reduction analyses carried out for the comparative analyses yield a safety factor M_{sf} of about 2.5 (Figure 42).

The state of stress in the soil during the main steps of the analysis is discussed in section 4.4.1., with reference to two sections through the centre of gravity of the anchor block, one longitudinal and one transversal. Figure 45, Figure 46 and Figure 47 show the contours of relative shear stress, defined as in eqn. (17), in the initial conditions, at the end of excavation, and at the end of block construction, respectively; Figure 48 shows the distribution of relative shear stress at the end of the ULS load application, with the active earth pressure fully mobilised on the south side and the passive earth pressure still far from being completely activated on the north side. Figure 49 and Figure 50 show the vertical total stresses σ_y and the horizontal total stresses (σ_z or σ_x) induced by ULS load condition; Figure 51 and Figure 52 show the vertical total stresses σ_y and the horizontal total stresses σ_z on a horizontal section at an elevation of 105.05 m a.s.l.

The computed displacements of the soil and of the anchor block are presented in section 4.4.2., with reference to the ULS loading condition (Figures 51 to 55). The maximum anchor block displacement is equal to about 11 mm (top of the block), while the core block displacement is equal to about 8 mm. During the excavation, a seepage process is induced from the outside of the pit toward the inside. The pore pressure distribution (section 4.4.3) assigned to the soil clusters at the end of the last excavation step is shown in Figure 58, still along longitudinal and transversal sections; the corresponding groundwater head profile is shown in Figure 59.

		Ponte sullo Stretto di Messina PROGETTO DEFINITIVO		
Calabria Anchor Block – evaluation of block behaviour via 3D FE analyses and of bearing capacity, Annex	<i>Codice documento</i> PF0067_F0_ANX	<i>Rev</i> F0	<i>Data</i> 20-06-2011	

Appendix A and Appendix B. Updated cable forces obtained from global IBDAS model version 3.3b and version 3.3f

The forces transmitted by the main cables to the Calabria Anchor Block have been re-evaluated using the global IBDAS model version 3.3b and version 3.3f. The worst load combinations were selected for each limit state (SILS, SLS2 and ULS) for both static and seismic conditions, using 6 different criteria (Table A.1 – Table A.2 for IBDAS 3.3b, Table B.1 – Table B.2 for IBDAS 3.3f). For both IBDAS model versions, a low difference is observed between the Tender Design and the updated (IBDAS) cable forces, the ratio being in the range of 1.05 to 0.96 for IBDAS 3.3b (Table A.3) and in the range of 1.07 to 0.93 for IBDAS 3.3f (Table B.3); the higher value refers to the ULS load combination, while the lower is obtained for the SILS load combination. For the Ultimate Limit State (ULS) cable forces provided by the Tender Design, referred to in the 3D FE analyses, are 5% higher than the corresponding IBDAS 3.3b values and 7% higher than the corresponding IBDAS 3.3f values, this resulting in a conservative estimate of the behaviour of the Calabria Anchor Block. Performance of the anchor block under SILS and SLS2 load cases are also discussed in § 4.

		Ponte sullo Stretto di Messina PROGETTO DEFINITIVO		
Calabria Anchor Block – evaluation of block behaviour via 3D FE analyses and of bearing capacity, Annex	<i>Codice documento</i> PF0067_F0_ANX	<i>Rev</i> F0	<i>Data</i> 20-06-2011	

2 SOIL PROFILE AND GEOTECHNICAL CHARACTERISATION

Figure 1 shows the soil profile on the Calabria shore. Starting from the ground level and moving downwards the following units are encountered:

- Coastal Deposits (*Depositi Costieri*). Sand and gravel with very little or no fine content, with a thickness varying between a minimum of 5 m towards inner land and a maximum of 45 m towards the sea shore. At this location, these deposits are generally coarser in the first 15 to 20 m b.g.l. and become sandier with depth; towards inner land these deposits are generally sandier. Occasionally, silty peaty layers appear in the lower part of the formation.
- Messina Gravel / Terrace Deposits (*Ghiaie di Messina / Sedimenti dei terrazzi*). Gravel and sand, with very occasional silty layers; difficult to distinguish from the Coastal Deposits and of small thickness, at times totally absent, so that the Coastal Deposits rest directly above the underlying Continental Deposits / Vinco Calcarenite.
- Continental Deposits / Vinco Calcarenite (*Depositi Continentali / Calcarenite di Vinco*). Clayey-sandy deposit, consisting of layers of silt or silt and sand, with significant gravel content / Bio-calcarenite and fossiliferous calcarenite, with thin silty layers.
- Pezzo Conglomerate (*Conglomerato di Pezzo*). Soft rock, consisting of clasts of different dimensions in a moderately cemented silty-sandy matrix and sandstone. The thickness of this formation is larger than 200 m.
- Crystalline bedrock (*Cristallino*). Tectonised granite.

The geotechnical site investigations carried out between 1988 and 1992 together with the geological and geophysical investigations performed for the Preliminary Design make it possible to define in more detail the soil profile in the area of the Calabria Anchor Block, characterised by significant variations of the level of the soil layers in the direction parallel to the coastline and to a lesser extent in the direction orthogonal to the coastline.

Figure 2 shows a plan view of the site together with the location of the available site investigations; Figure 3, Figure 4 and Figure 5 show the cross section and the two longitudinal sections indicated in Figure 2.

The ground level at the location of the Calabria Anchor Block is between +114 m and +127 m a.s.l.; the sea shore is at a distance of about 900 m from the anchor block. The groundwater level varies between about +95 m a.s.l. in the north-west corner of the anchor block to about +107 m a.s.l. in the south-east corner.

		Ponte sullo Stretto di Messina PROGETTO DEFINITIVO		
Calabria Anchor Block – evaluation of block behaviour via 3D FE analyses and of bearing capacity, Annex	<i>Codice documento</i> PF0067_F0_ANX	<i>Rev</i> F0	<i>Data</i> 20-06-2011	

The sections in Figures 3 to 5 show that, at the location of the Anchor Block, the Coastal Deposits and Messina Gravel, difficult to distinguish from one another and in the following considered as one layer, have a thickness that varies between a minimum of 7 m towards the north-east corner and a maximum of 18 m towards the south-east corner of the anchor block area. They overlie the Pezzo Conglomerate, weathered in its upper 20 m, and then not weathered below. Pezzo Conglomerate extend over a thickness of about 130 m.

It follows that for the Calabria Anchor Block the relevant geological unit is the Pezzo Conglomerate, with a weathered shallow layer ($20 \text{ m} < z < 40 \text{ m}$), overlain by the Terrace Deposits of small thickness.

The permeability of the Coastal Deposits was evaluated by pumping tests carried out from a well located in the area of the Calabria Tower and extending 33 m b.g.l., and by Lefranc permeability tests carried out in two boreholes at depths between about 5 m b.g.l. and 45 m b.g.l. The value of the horizontal permeability resulting from the more reliable well pumping tests is $k_h = 2.6 \cdot 10^{-3} \text{ m/s}$; the measured value of the ratio between vertical and horizontal permeability ranges between $k_v/k_h = 0.10$ and $k_v/k_h = 0.17$. The permeability of the Pezzo Conglomerate was evaluated by Lugeon tests carried out in one of the boreholes used for Lefranc tests, at pressures of 1, 2, and 3 atm, between depths of 48 to 58 m b.g.l. The results show values of permeability possibly decreasing with depth, with an average value of $2.3 \cdot 10^{-2} \text{ m/s}$.

Standard and large penetration tests provided high values of N_{SPT} and N_{LPT} in the Coastal Deposits, although a large scatter was observed (Figure 6); an estimate of the coefficient of earth pressure at rest is $K_0 = 0.43 - 0.47$. The Pezzo Conglomerate is cemented and geologically relatively old (Miocene); it is likely that the geological history of the formation includes mechanical overconsolidation. An estimate of the values of the coefficient of earth pressure at rest is $K_0 = 0.6 \div 0.9$.

The relative density of the Coastal Deposits and Messina Gravel was estimated from the SPT and LPT results using the procedure proposed by Cubrinovski and Ishihara (1999): values of $D_R = 40 \%$ to 70% were obtained as shown in Figure 7. The angle of shearing resistance $\varphi' = 41^\circ - 44^\circ$ was then evaluated through the relationship proposed by Schmertmann (1975) (Figure 7).

The shear strength parameters of the Pezzo Conglomerate were obtained from the results of large diameter (865 mm) plate loading tests carried out in the area of the Calabria Anchor Block. These were carried out at three different depths of 5, 11.85, and 16 m b.g.l. within a 2.5 m diameter shaft. The results were interpreted adopting the available solutions for the limiting pressure, q_u , of a circular shallow foundations (Berezantzev, 1964):

		Ponte sullo Stretto di Messina PROGETTO DEFINITIVO		
Calabria Anchor Block – evaluation of block behaviour via 3D FE analyses and of bearing capacity, Annex	<i>Codice documento</i> PF0067_F0_ANX	<i>Rev</i> F0	<i>Data</i> 20-06-2011	

$$q_u = C_K c' + B_K \gamma D + A_K \gamma \frac{B}{2} \quad (1)$$

in which $\gamma = 20 \text{ kN/m}^3$ is the unit weight of the soil, c' is the cohesion of the soil, $B = 0.865 \text{ m}$ is the diameter of the plate, $D = 0$ is the depth of the plate and A_K , B_K and C_K are capacity factors depending on the friction angle ϕ' .

The values of q_u were obtained directly for the test carried out at 5 m b.g.l. which was taken to failure, and extrapolated with a hyperbolic law for the other two tests. In this manner, for any given value of ϕ' it is possible to calculate the corresponding value of c' .

Figure 8 shows the values of c' obtained at depths between 5 and 16 m b.g.l. assuming that the friction angle is in the range $\phi' = 38^\circ \div 42^\circ$. For depths larger than 16 m b.g.l. it is conservative to assume that c' is constant and equal to its value at 16 m b.g.l.; this assumption is consistent with the existence at the top of the Pezzo conglomerate unit of a layer of weathered conglomerate, also shown by the shear wave velocity profiles of the following section. In this type of materials, an increase of cohesion with depth does not affect the friction angle (Jamiolkowski *et al.*, 1991).

The stiffness characteristics of the deposits were obtained from one cross-hole test carried out in the vicinity of the Calabria Anchor Block (AC-BH1), using three boreholes reaching a maximum depth of 100 m b.g.l., at a distance of 5 m from one another. The results of the cross-hole test in terms of shear wave velocity V_s versus depth are given in

Figure 9. In

Figure 10 the same results are shown as profiles of small strain shear modulus G_0 . This has been obtained from the shear wave velocity as:

$$G_0 = \rho V_s^2 \quad (2)$$

The three data sets refer to the values obtained in each of the three boreholes, while the continuous line is the average of the three data at each depth.

The G_0 profile with depth shows three different trends: for $0 \text{ m} < z < 20 \text{ m}$ G_0 increases rapidly from 190 MPa to 1200 MPa; for $20 \text{ m} < z < 40 \text{ m}$ G_0 varies from about 1200 MPa to about 1400 MPa; below $z = 40 \text{ m}$ the data are more dispersed with an average value of 2000 MPa. Table 1 summarises the main mechanical parameters obtained from the geotechnical characterisation discussed above.

		Ponte sullo Stretto di Messina PROGETTO DEFINITIVO		
Calabria Anchor Block – evaluation of block behaviour via 3D FE analyses and of bearing capacity, Annex	<i>Codice documento</i> PF0067_F0_ANX		<i>Rev</i> F0	<i>Data</i> 20-06-2011

Table 1: Summary of main mechanical parameters from geotechnical characterization

layer	depth (m bgl)	K_0	φ'_p (°)	c' (kPa)	K_n (m/s)	G_0 (MPa)
Coastal Deposits.	0÷20	0.43÷0.47	41÷42	---	2.6×10^{-3}	190÷1200
Weathered Conglomerate	20÷40	0.6÷0.9	40	35-70	2.3×10^{-2}	1200÷1400
Pezzo Conglomerate	>40	0.6÷0.9	40	70	2.3×10^{-2}	2000

		Ponte sullo Stretto di Messina PROGETTO DEFINITIVO		
Calabria Anchor Block – evaluation of block behaviour via 3D FE analyses and of bearing capacity, Annex	<i>Codice documento</i> PF0067_F0_ANX	<i>Rev</i> F0	<i>Data</i> 20-06-2011	

3 3D NUMERICAL ANALYSIS OF THE CALABRIA ANCHOR BLOCK

The Calabria Anchor Block consists of a massive block, with the shape of a trapezoid-based prism (Figure 11). The dimensions in plane of the upper rectangle are 98 x 87.5 m²; the lower rectangle at the base has dimensions of 98 x 25 m². The upper part of the block will be positioned at +118 m a.s.l.; the lower part at +77 m a.s.l., resulting in a maximum height of construction of 41 m (Figure 12).

The excavation will be supported by diaphragm walls constructed in 1.0 m thick and 2.5 m wide panels, around the rectangular shaped pit. The length of the diaphragm walls varies according to the shape of the block and, to some extent, according to the ground level. The maximum depth of the walls reaches +70 m a.s.l., while the wall top is mostly located at +114 m a.s.l.

The excavation will be supported also by several levels of pre-stressed anchors, varying in number along the different sides of the pit, according to the depth of the excavation. Generally, for each level, one or two anchors are planned for each diaphragm wall, with an horizontal spacing of 2.5 m or less.

3.1 Soil model

3.1.1 Geometrical soil model

The grain size similarity of the Coastal deposits and of the Messina gravel makes it difficult to distinguish clearly the two layers. Therefore, the subsoil model used to analyse the construction and performance of the Anchor Block has only three layers: the first one is a gravel and sand layer, modelling the Coastal Plain Deposit and the Messina Gravel; the second and the third layer refer to the Pezzo conglomerate; the upper layer corresponds to the weathered conglomerate, the lower layer to the conglomerate in place. The layers are inclined on the horizontal in the east-west direction, parallel to the coastline.

In the numerical model the geometry of the layers is identified using two soil columns, referring to the east and the west sides of the excavation pit, respectively. Table 2 reports the values of the elevation assigned to the bed of each layer. In the numerical model, ground level is horizontal at +118 m a.s.l.; the groundwater head H is located at an average value of +102 m a.s.l and the initial distribution of pore water pressure is hydrostatic.

		Ponte sullo Stretto di Messina PROGETTO DEFINITIVO		
Calabria Anchor Block – evaluation of block behaviour via 3D FE analyses and of bearing capacity, Annex	<i>Codice documento</i> PF0067_F0_ANX	<i>Rev</i> F0	<i>Data</i> 20-06-2011	

Table 2: numerical simulation: soil columns

layer bed	east side elevation (m a.s.l.)	west side elevation (m a.s.l.)
Coastal Deposit	+110	+102
Weathered Conglomerate	+92	+80
Pezzo Conglomerate	undefined	undefined

Figure 13 shows an axonometric view of the 3D model used for the analyses, extending 500x500 m² in plan and 200 m below the ground level and consisting of about 60 thousands elements. Figure 14 shows a view of the finite elements mesh from above, while Figure 15 shows two longitudinal sections of the same mesh.

3.1.2 Constitutive soil model

The behaviour of the Anchor Block was studied through finite element analyses performed using the Plaxis 3D Foundation code. The mechanical behaviour of the soil was described using the Hardening Soil constitutive model available in the model library of the code. The model is capable of reproducing soil non-linearity due to the occurrence of plastic strains from the beginning of the loading process. The computed non linear stress-strain relationship has initial tangent modulus equal to E'_0 ; upon unloading, the model assumes elastic behaviour with Young's modulus E'_0 , thus reproducing a significant change in stiffness. In the model, soil stiffness depends on the effective stress state.

The calibration of the constitutive model was carried out using the results from the cross hole test carried out at the site and from published results of compression triaxial tests carried out on large-diameter reconstituted samples of gravelly soils (Tanaka et al., 1987). The cross-hole test was used to evaluate the shear modulus at small strains G_0 and to describe its variation with effective stress. The remaining soil parameters were selected to obtain a satisfactory description of the soil non-linearity observed in the triaxial tests.

Hardening soil model is an elastic-plastic rate independent model with isotropic hardening. The elastic behaviour is defined by isotropic elasticity through a stress-dependent Young's modulus:

$$E' = E^{\text{ref}} \left(\frac{c' \cdot \cot \phi' + \sigma'_3}{c' \cdot \cot \phi' + p^{\text{ref}}} \right)^m \quad (3)$$

where σ'_3 is the minimum principal effective stress, c' is the cohesion, ϕ' is the angle of shearing

		Ponte sullo Stretto di Messina PROGETTO DEFINITIVO	
Calabria Anchor Block – evaluation of block behaviour via 3D FE analyses and of bearing capacity, Annex	<i>Codice documento</i> PF0067_F0_ANX	<i>Rev</i> F0	<i>Data</i> 20-06-2011

resistance, $p^{\text{ref}} = 100 \text{ kPa}$ is a reference pressure; E^{ref} and m are model parameters.

The model has two yield surfaces f_s and f_v with independent isotropic hardening depending on distortional plastic strain $\gamma^p = (2 \cdot \varepsilon^p_1 - \varepsilon^p_v)$ and on volumetric plastic strains ε^p_v , respectively; the two surfaces have the following equations:

$$f_s = \frac{1}{E'_{50}} \frac{q}{(1 - 0.9 \cdot q/q_f)} - \frac{2q}{E'} - \gamma^p = 0 \quad (4)$$

$$f_v = \frac{\tilde{q}^2}{\alpha^2} + p'^2 - p_c'^2 = 0 \quad (5)$$

In eqn. (4), E'_{50} is given by an expression similar to eqn. (3), but, in contrast to E' , it is not used within a concept of elasticity. Hardening of the f_s surface is isotropic and depends on the plastic distortional strain $\gamma^p = (2 \cdot \varepsilon^p_1 - \varepsilon^p_v)$.

In eqn. (5), p' is the mean effective stress; \tilde{q} is a generalised deviator stress, that accounts for the dependence of strength on the intermediate principal effective stress σ'_2 ; α controls the shape of the f_v surface in the \tilde{q} - p' plane and can be related to the coefficient of earth pressure at rest K_0 for normally consolidated states. The hardening parameter p'_c is the size of the current f_v surface and is related to the plastic volumetric strains ε^p_v through the hardening law, written in the incremental form as:

$$d\varepsilon^p_v = \frac{\beta}{p^{\text{ref}}} \left(\frac{p'_c}{p^{\text{ref}}} \right)^m \cdot dp'_c \quad (6)$$

where β is a parameter that controls the variation of p'_c with the plastic volumetric strains. In the model formulation implemented in *Plaxis*, the parameter E'_{oad} , which is related to β , has to be specified. This is the constrained modulus for one-dimensional plastic loading, and depends on the maximum principal effective stress σ'_1 through the relationship:

$$E'_{\text{oad}} = E^{\text{ref}}_{\text{oad}} \cdot \left(\frac{c' \cdot \cot \varphi' + \sigma'_1}{c' \cdot \cot \varphi' + p^{\text{ref}}} \right)^m \quad (7)$$

where σ'_1 is the maximum principal effective stress.

The initial value of the hardening parameter p'_c is related to the one-dimensional vertical yield stress, and can therefore be specified by assigning a value for the overconsolidation ratio OCR. It is worth mentioning that OCR has to be regarded as a yield stress ratio (YSR) defined in the framework of strain hardening plasticity, so that values of $\text{OCR} > 1$ can be specified also for geologically normally consolidated soil deposits exhibiting a yield stress larger than the in situ stress.

		Ponte sullo Stretto di Messina PROGETTO DEFINITIVO		
Calabria Anchor Block – evaluation of block behaviour via 3D FE analyses and of bearing capacity, Annex	<i>Codice documento</i> PF0067_F0_ANX	<i>Rev</i> F0	<i>Data</i> 20-06-2011	

The flow rule is associated for states lying on the surface f_v , while a non associated flow rule is used for states on the surface f_s . The latter is derived from the theory of stress dilatancy by Rowe (1962): the mobilised dilatancy angle ψ_m depends on the current stress state through the angle of mobilised friction ϕ'_m and the angle of friction at constant volume ϕ'_{cv} :

$$\sin \psi_m = \frac{\sin \phi'_m - \sin \phi'_{cv}}{1 - \sin \phi'_m \sin \phi'_{cv}} \quad (8)$$

In turn, ϕ'_{cv} can be obtained from the angle of shearing resistance ϕ' and the angle of dilatancy ψ at failure:

$$\sin \phi'_{cv} = \frac{\sin \phi' - \sin \psi}{1 - \sin \phi' \sin \psi} \quad (9)$$

Figure 16 shows the shape of the yield surfaces f_v and f_s and schematically indicates their evolution.

For plastic loading from isotropic stress states, the model predicts a non linear stress-strain relationship with tangent initial modulus equal to E' . Therefore, values of E' were related to the shear modulus at small-strain G_0 obtained from the cross-hole test carried out in the site. In particular, values of E'^{ref} and m were obtained by best fitting the cross-hole test results using eqn. (3) and assuming $\nu' = 0.2$.

For the Coastal Deposits, the remaining model parameters $E'_{50}{}^{ref}$ and $E'_{oed}{}^{ref}$, were calibrated on the results of triaxial compression tests carried out on large-diameter reconstituted samples of gravelly soils (Tanaka et al., 1987). Figure 17 shows a comparison between model simulation and Tanaka test results. For the Pezzo Conglomerate, the stiffness decay with shear strain was described using ratios of $E'^{ref} / E'_{50}{}^{ref} = 2$ and of $E'_{50}{}^{ref} / E'_{oed}{}^{ref} = 1.0$ and a value for the angle of dilatancy at failure $\psi = 0$.

3.1.3 Soil parameters

The mechanical properties of the soil layers in the Hardening Soil Model are summarised in Table 3 and Table 4.

For the Coastal Deposit, a non zero value of cohesion has been introduced to simulate non zero values of stiffness at shallow depths (see

Figure 10); this low value of cohesion, anyway, does not significantly affect the behaviour of the layer in terms of strength.

		Ponte sullo Stretto di Messina PROGETTO DEFINITIVO		
Calabria Anchor Block – evaluation of block behaviour via 3D FE analyses and of bearing capacity, Annex	<i>Codice documento</i> PF0067_F0_ANX	<i>Rev</i> F0	<i>Data</i> 20-06-2011	

For the layer of weathered Pezzo Conglomerate a reduced value of cohesion, $c' = 35$ kPa, was assumed consistently with the indications of the plate loading tests; besides, according to the altered conditions of the conglomerate, a value of K_0 of 0.47 has been assigned to the layer, which is consistent with the behaviour of a granular soil rather than a soft rock.

Figure 10 shows the profile of G_0 against depth b.g.l. The continuous black lines in the figure represent the prediction of G_0 obtained using eqn. (3) with the values of c' , φ' , K_0 , E'^{ref} and m reported in Table 3 and Table 4. Values of E'^{ref} and m were obtained by best fitting the cross-hole test results and assuming $\nu' = 0.2$.

A good agreement for the stiffness decay in the Coastal Deposits with the shear strain was obtained using ratios of $E'^{ref} / E'_{50}{}^{ref}$ and of $E'^{ref} / E'_{oed}{}^{ref}$ equal to 7; lower ratios have been used for Pezzo Conglomerate. For all soil layers the value of the angle of dilatancy ψ at failure was taken to be zero.

A yield stress ratio $YSR = 2$ was given to all soil layers to reproduce numerically the observed high values of yield stress for granular soils.

Table 3: numerical simulation: physical and mechanic properties of soil layers

layer	Model	γ (kN/m ³)	c' (kPa)	φ' (°)	YSR	$K_{0,NC}$	K_0	ν
Coastal Deposit	Hardening soil	20	4.2	40	2.0	0.357	0.470	0.2
Weathered Conglomerate	Hardening soil	20	35	40	2.0	0.357	0.470	0.2
Pezzo Conglomerate	Hardening soil	20	70	40	2.0	0.357	0.600	0.2

Table 4: numerical simulation: stiffness parameters of soil layers

layer	E'^{ref} (MPa)	m	$E'^{ref}/E'_{50}{}^{ref}$	$E'^{ref}/E'_{oed}{}^{ref}$	$E'_{50}{}^{ref}$ (MPa)	$E'_{oed}{}^{ref}$ (MPa)
Coastal Deposit	1920	1.0	7	7	274	274
Weathered Conglomerate	2520	0.2	3	3	840	840
Pezzo Conglomerate	4800	0.0	2	2	2400	2400

		Ponte sullo Stretto di Messina PROGETTO DEFINITIVO		
Calabria Anchor Block – evaluation of block behaviour via 3D FE analyses and of bearing capacity, Annex	<i>Codice documento</i> PF0067_F0_ANX	<i>Rev</i> F0	<i>Data</i> 20-06-2011	

3.2 Structural elements

3.2.1 Anchor Block

The Calabria Anchor Block consist of a massive block, with the shape of a trapezoid-based prism (Figure 11). The dimensions in plane of the upper rectangle are 98 x 87.5 m²; the lower rectangle at the base has dimensions of 98 x 25 m². The upper part of the block will be at +118 m a.s.l.; the lower part at +77 m a.s.l., resulting in a maximum height of the construction of 41 m.

In the numerical model, due to some limitations of Plaxis 3D code, the Calabria Anchor Block has been defined with a step profile.

The geometrical design of the anchor block includes two pairs of empty chambers; two of them are meant for the installation of the main cables of the Messina Bridge; the other two should be filled with ballast material.

The mechanical behaviour of the anchor block concrete, of the ballast material and of the "empty material" is described as linear elastic. Table 5 summarises the mechanical properties of the linear elastic materials adopted in the analyses for the different parts of the block.

Table 5: numerical simulation: properties for the linear-elastic materials

material	γ (kN/m ³)	E (kPa)	ν
concrete	25.0	3.00E+07	0.15
ballast	20.0	3.00E+07	0.15
<i>empty material</i>	0.0	3.00E+08	0.15

3.2.2 Diaphragm walls

The rectangular shaped excavation pit has external dimensions, in plan, of 100 x 89.5 m², including 1 m of wall thickness. Because of the shape of the anchor block, the depth of the toe of the diaphragm walls varies along the perimeter of the excavation, between +94.0 m a.s.l. (in the north and south sides of the excavation) and +70.0 m a.s.l. (in the central part of the east and of the west side of the excavation). The top of the walls is also variable, lying between +114 m a.s.l. and +127 m a.s.l. (in the south-east corner of the excavation), depending on the initial ground level and on the different depth of the planned pre-excavation.

In the model, the depth of the toe of the walls essentially the same as in the design, while the head of the walls is uniformly located at +118 m a.s.l. This corresponds to a 4 m deeper excavation in

		Ponte sullo Stretto di Messina PROGETTO DEFINITIVO		
Calabria Anchor Block – evaluation of block behaviour via 3D FE analyses and of bearing capacity, Annex	<i>Codice documento</i> PF0067_F0_ANX	<i>Rev</i> F0	<i>Data</i> 20-06-2011	

the most part of the pit, while it is only slightly non conservative (with respect to the excavation process) in the south-east corner of the excavation.

The diaphragm walls are modelled as Plaxis WALL elements. These are shell elements, with thickness $d = 1$ m and weight $\gamma = 25$ kN/m³. To define the mechanical properties of the wall, the code requires 5 stiffness values (Figure 18), namely E_1 , E_2 , G_{12} , G_{13} , G_{23} , and the Poisson ratio ν_{12} . The stiffness value of concrete ($E = 30$ GPa) has been assigned to the E_1 Young modulus; G_{12} and G_{13} shear moduli have been determined considering ν_{12} equal to 0.15. To simulate the lack of connection between the panels of the diaphragm walls, E_2 Young modulus and G_{23} shear modulus (Figure 18) have been reduced by one order of magnitude. This results in an anisotropic behaviour of the WALL elements.

Table 6 summarises the geometrical and mechanical properties of the diaphragm walls.

Table 6: numerical simulation: parameters for the diaphragm walls

d (m)	γ (kN/m ³)	E_1 (kPa)	E_2 (kPa)	ν	G_{12} (kPa)	G_{13} (kPa)	G_{23} (kPa)
1.00	25.0	3.00E+07	3.00E+06	0.15	1.30E+07	1.30E+07	1.30E+06

3.2.3 Retaining Anchors

Several levels of retaining anchors, varying in number along the different sides of the pit according to the depth of excavation, cooperate with the diaphragm walls to support the excavation. Generally, for each level, one or two retaining anchors are planned for each diaphragm wall, resulting in an horizontal spacing of 2.5 m or less. The retaining anchors have an inclination on the horizontal of 15 degrees and will be pre-stressed.

The geometrical disposition of the retaining anchors in the numerical model is substantially based on the tender design of the excavation, and consists of 7 levels of retaining anchors along the east and the west side of the pit, characterised by a higher depth of excavation, and 4 levels of anchors along the north and the south side of the pit.

The skin resistance of the retaining anchors has been determined using the following equation:

$$T_{lim} = \pi \cdot d_g \cdot L_g \cdot \tau \quad (10)$$

Where $d_g = \alpha \cdot d$ is the actual diameter of the grouted body, α is a parameter depending on the grouting technology and on the mechanical characteristics of the grouted soil layer, d is the nominal diameter of the grout body (= 0.15 m), L_g is the grout body length, and τ is the shear

		Ponte sullo Stretto di Messina PROGETTO DEFINITIVO		
Calabria Anchor Block – evaluation of block behaviour via 3D FE analyses and of bearing capacity, Annex	<i>Codice documento</i> PF0067_F0_ANX	<i>Rev</i> F0	<i>Data</i> 20-06-2011	

strength between the grout body and the soil, also depending on the grouting technology and on the soil properties. With reference to the method proposed by Bustamante and Doix (1985), depending on the soil properties and to the SPT test results, and considering a *repetitive and selective injection* for the grouted body, values of $\alpha = 1.5$ (for Coastal Deposits) and $\alpha = 1.2$ (for Weathered and Pezzo Conglomerate), and conservative values of $\tau = 0.20$ MPa (for Coastal Deposits), $\tau = 0.35$ MPa (for Weathered Conglomerate) and $\tau = 0.45$ MPa (for Pezzo Conglomerate) have been obtained for the parameters of eqn. (10).

The anchor bar stiffness has been determined based on the number of strands composing each bar; a number of 7 to 11 strands, with a nominal diameter of 15.2 mm, and a value of the Young's modulus of steel of 210 GPa have been considered. The limit displacement of the anchor bars has been calculated as:

$$u_{lim} = \frac{T_{lim} \cdot L_{bar}}{E_{steel} \cdot A_{bar}} \quad (11)$$

Table 7 summarises the geometrical characteristics and the strength and stiffness properties of the retaining anchors.

Table 7: geometrical and mechanical properties for the retaining anchors

anchor	elevation (m a.s.l)	bar length (m)	grout body length (m)	grout body soil layer	T_{lim} (kN)	number of strands	$E_{steel}A_{bar}$ (kN)	u_{lim} (m)
East/West – L.1	118.00	46	8	Coastal Dep.	1131	8	3.06E+05	0.170
East/West – L.2	110.00	43	11	Coastal Dep.	1555	10	3.83E+05	0.175
East/West – L.3	105.50	36	12	Weath. Cong.	2375	10	3.83E+05	0.223
East/West – L.4	99.45	29	12	Weath. Cong.	2375	10	3.83E+05	0.180
East/West – L.5	94.50	23	12	Weath. Cong.	2375	11	4.21E+05	0.130
East/West – L.6	88.05	18	12	Pezzo Cong.	3054	11	4.21E+05	0.130
East/West – L.7	84.25	16	12	Pezzo Cong.	3054	11	4.21E+05	0.116
North/South – L.1	118.00	20	8	Coastal Dep.	1131	7	2.68E+05	0.084
North/South – L.2	110.00	20	12	Coastal Dep.	1696	7	2.68E+05	0.127
North/South – L.3	105.50	20	11	Weath. Cong.	2177	8	3.06E+05	0.142
North/South – L.4	99.45	20	12	Weath. Cong.	2375	8	3.06E+05	0.155

The retaining anchors are modelled as Plaxis SPRINGS elements. These elements simulate anchors in a simplified way, without taking into account anchor – soil interaction. A bi-linear

		Ponte sullo Stretto di Messina PROGETTO DEFINITIVO		
Calabria Anchor Block – evaluation of block behaviour via 3D FE analyses and of bearing capacity, Annex	<i>Codice documento</i> PF0067_F0_ANX	<i>Rev</i> F0	<i>Data</i> 20-06-2011	

stiffness has been assigned to each spring through a force-displacement (T-u) diagram (Figure 19, left side). A pre-tension value T_{pret} of the anchors was defined in the analyses, dividing the limit skin resistance by a factor in between 3.0 and 3.7.

For computational reasons, the springs have been located, in plan, with a 5.0 m spacing, i.e. two times (or more) the designed spacing; so each spring represents at least two retaining anchors. This has been considered in the definition of the anchor properties by doubling the limit skin resistance of each anchor. In addition, a connecting beam was inserted in the model at the elevation of each level of retaining anchors to simulate an homogeneous distribution of the forces on the retaining wall.

Figure 19 (right side) shows the force-displacement (T-u) relationship adopted for the pre-tensioned springs. Table 8 summarizes the stiffness properties assigned to the springs in the numerical model; the u_{mod} values have been determined referring to the equation:

$$u_{mod} = \left(1 - \frac{T_{pret}}{T_{lim}}\right) \cdot u_{lim} \quad (12)$$

Table 9 summarises the stiffness properties assigned to the BEAM elements (Figure 20), modelling the connecting beam between the 5 m spaced springs. The geometrical dimensions of the beam have been chosen so as to reduce by about 10 times the free horizontal displacement of a point placed between two anchors.

		Ponte sullo Stretto di Messina PROGETTO DEFINITIVO	
Calabria Anchor Block – evaluation of block behaviour via 3D FE analyses and of bearing capacity, Annex	<i>Codice documento</i> PF0067_F0_ANX	<i>Rev</i> F0	<i>Data</i> 20-06-2011

Table 8: numerical simulation: properties for the retaining anchors

anchor	$T_{lim,model}$ (kN)	$T_{pret,model}$ (kN)	U_{mod} (m)
East/West – L.1	2262	700	0.117
East/West – L.2	3110	900	0.124
East/West – L.3	4750	1300	0.162
East/West – L.4	4750	1500	0.123
East/West – L.5	4750	1600	0.086
East/West – L.6	6107	1800	0.092
East/West – L.7	6107	1800	0.082
North/South – L.1	2262	500	0.066
North/South – L.2	3393	600	0.104
North/South – L.3	4354	750	0.118
North/South – L.4	4750	750	0.131

Table 9: numerical simulation: parameters for the connection beam

b (m)	h (m)	A (m ²)	γ (kN/m ³)	E (kPa)	I_2 (m ⁴)	I_3 (m ⁴)
2.50	0.50	1.25	0.0	3.00E+07	0.651	0.026

3.3 Calculation steps of analysis

3D finite element analysis of the Calabria Block Anchor was carried out adopting the following main sequence of steps:

1. computation of the initial stress state;
 2. activation of diaphragm walls;
 3. progressive excavation of the soil to reach the anchor block base; simultaneous activation of the retaining anchors levels;
 4. progressive activation of the anchor block;
 5. application of loads;
 6.
 - a) increase of external loads
 - b) ϕ' – c' reduction
1. The initial stress state of the soil has been assigned to the layers by means of the K_0 -procedure; in this way the desired value of the K_0 coefficient and of the yield stress ratio YSR

		Ponte sullo Stretto di Messina PROGETTO DEFINITIVO		
Calabria Anchor Block – evaluation of block behaviour via 3D FE analyses and of bearing capacity, Annex	<i>Codice documento</i> PF0067_F0_ANX	<i>Rev</i> F0	<i>Data</i> 20-06-2011	

have been generated. A following nil step has been implemented to ensure equilibrium of the forces in the whole soil mass.

2. The activation of the diaphragm walls is concurrent to the activation of the corresponding interface elements, whose strength parameter are 0.67 times the strength parameter of the surrounding soil. The fully activated diaphragm walls are shown in Figure 21.
3. The excavation of the soil has been modelled by means of 7 progressive drops, each reaching the elevation of a retaining anchor level (i.e. +110 m a.s.l., +105.5 m a.s.l., +99.45 m a.s.l., +94.5 m a.s.l., +88.05 m a.s.l., +84.25 m a.s.l and +76.65 m a.s.l. or the deepest excavation level, see Table 7). The construction sequence is the following: a) activate the retaining anchor level, activate corresponding connection beam and pre-tension of the anchors; b) excavate down to the following elevation.

The shape of the excavation matches the design shape of the anchor block, resulting in a stepped profile prism. Figure 22 shows an axonometric zoomed view of the fully completed excavation; Figure 23 shows two sections of the excavation and Figure 24 shows the whole of the retaining structures (walls, anchors, beams).

Starting from an elevation of +102 m a.s.l. the excavation induces seepage from outside into the pit. Due to limitations of the Plaxis 3D code, the 3D seepage process cannot be solved. Nevertheless, it is possible to change the water pressure distribution of the soil clusters where the seepage process takes place. During the excavation, the pore pressure distribution of the soil clusters above the pit area has been interpolated between the external groundwater level (+102 m a.s.l.) and the groundwater head corresponding to the elevation of the excavation. Calibration analyses performed with Plaxis 2D, showed that the seepage process induce deviations of pore water pressure from the hydrostatic distribution to an elevation of about 0 m a.s.l.. No changes have been adopted for clusters outside the excavation pit area.

The initial pore water pressure regime has been restored at the end of the construction phases of the anchor block (see § 4.4.3 and Figure 58 - Figure 60).

4. The progressive construction of the anchor block is modelled activating progressively the concrete clusters in 11 steps, each characterised by a height of about 4 m.

To simulate the initial fluid conditions of the concrete and the consequent horizontal pressure on the diaphragm walls, a "fluid concrete" material has been defined with a very low shear stiffness G . Hence, the construction sequence of the anchor block is defined as follows: a) activation of the lowest level of excavation clusters with "fluid concrete" properties; b)

		Ponte sullo Stretto di Messina PROGETTO DEFINITIVO		
Calabria Anchor Block – evaluation of block behaviour via 3D FE analyses and of bearing capacity, Annex	<i>Codice documento</i> PF0067_F0_ANX	<i>Rev</i> F0	<i>Data</i> 20-06-2011	

substitution of “fluid concrete” properties with “solid concrete” properties in the lower clusters and simultaneous activation of the excavation clusters immediately above, again with “fluid concrete” properties. This sequence of phases is repeated until the construction reaches the top of the anchor block; c) substitution of “fluid concrete” properties in the uppermost clusters of the anchor block.

Finally, to model the part of the structure above the elevation of +118 m a.s.l., in the area of the cables chambers, a distributed vertical load, with a value of 65 kPa, is applied.

At the end of the construction of the anchor block, the ballast material fills the rear chambers of the block, while the “empty material” fills the front chambers, in which the main cables of the bridge are to be installed.

Figure 25 show the 3D model of the anchor block, before and after filling of the chambers.

Before applying the external loads, two further steps have been introduced: a) removal of the provisional retaining systems, by deactivation all the retaining anchor levels and corresponding connecting beams; b) reinstatement of the original groundwater level, as described in the previous indention.

5. The cable forces considered in computations for the Calabria Anchor Block are those provided by the structural analyses of the tender design, for three different load combinations. Table 10 summarises the loading conditions and the corresponding values of the acting forces. The direction of the forces is of 15 degrees to the horizontal, upwards; the versus is towards the sea. In § 4 the influence of the cable forces computed using the global IBIDAS model version 3.3b (Table A.1 – Table A.2) and version 3.3f (Table B.1 – Table B.2) is also discussed.

Table 10: Cable forces in the Calabria Anchor Block (tender design)

Load case	F (MN)
SILS	3142
SLS2	3232
ULS	3933

The global force, divided between the two main cables, has been decomposed in its horizontal and vertical components and applied on the block. The two points of application are located in the convergence node of the cables of the bridge, as indicated in the tender design. The lower value of the force (SILS) has been reached in 10 incremental load steps; 1 further load step has been defined to reach the SLS2 force and three further steps to reach

		Ponte sullo Stretto di Messina PROGETTO DEFINITIVO		
Calabria Anchor Block – evaluation of block behaviour via 3D FE analyses and of bearing capacity, Annex	<i>Codice documento</i> PF0067_F0_ANX	<i>Rev</i> F0	<i>Data</i> 20-06-2011	

the highest value of the force (ULS).

Before application of the forces, the computed displacements of the anchor block have been reset to zero.

Figure 26 shows the anchor block model with the external forces applied; for sake of clarity, the "empty material" has been switched off.

- 6(a) The external loads have been further increased, up to a final value of about 8500 MN, which is about 2 times the ULS force value and about 2.7 times the SILS force value.
- 6(b) Starting from SILS, SLS2 and ULS force values, three $\varphi' - c'$ reduction analyses have been carried out. In these analyses the strength properties of the soils are progressively reduced, according to the following equations:

$$c'_{red} = \frac{c'}{M_{sf}} \quad (13)$$

$$(\tan \varphi')_{red} = \frac{(\tan \varphi')}{M_{sf}} \quad (14)$$

During each $\varphi' - c'$ reduction analysis, the stress-dependent stiffness moduli maintain a constant value, as determined in the last previous step.

3.3.1 Effect of excavation around the block

In the Tender Design of the Calabria Anchor Block the drawings show that the area surrounding the block, after construction, will be refilled with soil such that the anchor block will be entirely surrounded or even covered by soil. Anyway, the extension of this refilling is not shown clearly.

To evaluate the influence of the refilling area on the computed displacement field of the anchor block, a further analysis has been carried out in which, before the application of the external loads, a 4 m excavation was modelled around the anchor block.

The steps of this *comparative* analysis are almost the same as those described in § 3.3. but for the fact that, between the fourth (activation of the block) and fifth step (application of external loads), an intermediate step has been added that consists into a 25 m wide and 4 m deep excavation around the anchor block, from +118 m a.s.l. (top of the block) to +114 m a.s.l. (Figure 27).

As the excavation front is modelled as vertical, soil instability is avoided using a "cohesive" cluster for the soil close to the anchor block ($c' = 40$ kPa); this material is identified by a darker colour in the figure.

		Ponte sullo Stretto di Messina PROGETTO DEFINITIVO		
Calabria Anchor Block – evaluation of block behaviour via 3D FE analyses and of bearing capacity, Annex	<i>Codice documento</i> PF0067_F0_ANX	<i>Rev</i> F0	<i>Data</i> 20-06-2011	

4 RESULTS OF THE 3D ANALYSES

4.1 Application of the design forces

The response of the anchor block to the application of the external loads consists in a translation, directed towards the seashore (z-direction), associated with a downwards rotation in the y-z plane. Figure 28 shows a general view of the deformed mesh at the end of the ULS load condition; Figure 29 shows a detail of the deformed mesh of the anchor block. In both cases, the displacements are scaled up 2000 times outlining the roto-translation of the anchor block.

Figure 30 shows the translation of the central ($x = 254.1$ m) longitudinal sections of the anchor block (North-South; y-z plane). The average values of the z-directed and of the y-directed displacements, calculated on the basis of the whole 12469 nodes of the anchor block model, are assigned to each point of the section. The average displacement is equal to about 8 mm, with an inclination to the horizontal $\alpha = 8$ degrees, directed upwards. In the figure, the displacements are scaled up 1000 times.

Figure 31 shows the roto-translation of the same section of the anchor block. This time the vertical (y) and horizontal (z) components of displacement of the centre of gravity have been assigned to each point of the section; the node coordinates of point G are: $Y = 99.45$ m; $Z = 251$ m. The displacement is still equal to about 8 mm, while the average rotation θ_G around the centre of gravity G is equal to about $3 \cdot 10^{-3}$ degrees, this defining an inclination to the horizontal $\alpha = 13$ degrees. In the figure, the displacements are still scaled up 1000 times.

Table 11 reports the values of displacement applied to the block section in Figure 30 and Figure 31. It is worth noting that the inclination α computed in the 3D analyses are consistent with that obtained in the plane-strain analyses carried out using a simplified soil profile and discussed in the companion report “Calabria anchor block: earthquake-induced displacements and safety against ultimate limit states”.

A general view of the deformed mesh in the *comparative* analysis (4 m deep excavation around the anchor block) is shown in Figure 32.

Table 11: Kinematic mechanism of the anchor block at the application of the ULS external load

kinematics	u_y (mm)	u_z (mm)	u (mm)	θ_G (°)	α (°)
translational	1.1	-7.9	8.0	---	-8.0
roto-translational	1.9	-7.9	8.2	$-3.46 \cdot 10^{-3}$	-13.5

		Ponte sullo Stretto di Messina PROGETTO DEFINITIVO		
Calabria Anchor Block – evaluation of block behaviour via 3D FE analyses and of bearing capacity, Annex	<i>Codice documento</i> PF0067_F0_ANX	<i>Rev</i> F0	<i>Data</i> 20-06-2011	

Ten points were selected to describe the behaviour of the anchor block under the application of the external loads. Five of them (A, B, C, D and E) are located at the top of the block, at the elevation of +118 m a.s.l.: four are located near the corners of the block and the fifth at its centre. Four more points (G, H, I and J) are located at the block base, +76.65 m a.s.l., near its corners. The last point (F) is located in the core of the block, at an elevation of 95.65 m a.s.l. The location of the ten points is shown in Figure 33. The first stages of the analysis (*i.e.* excavation supported by retaining walls and anchors, construction of the block, removal of the provisional retaining anchors, reinstatement of the initial hydraulic conditions) were introduced to reproduce the stress state in the soil at the beginning of the loading process. The displacements computed at the end of these stages were reset to zero and the displacement values discussed in the following refer only to the application of external loads.

Table 12, Table 13 and Table 14 summarize the displacements calculated for each of the ten points at the end of three loading steps, corresponding to SILS, SLS2 and ULS loading conditions considered in the Tender Design. Total displacement u , together with displacement components u_x , u_y , u_z are given in the tables, (y-direction upwards, z-direction towards the sea and x-direction orthogonal to the bridge axis). The average values of displacement are computed for the 10 selected points of the block, with a resulting total average displacement between 6 and 8 mm.

Table 12: Displacements of the selected points at the application of the SILS load ($F = 3142$ MN)

disp.	A	B	C	D	E	F	G	H	I	J	average
u (mm)	7.9	7.4	6.6	6.1	7.2	5.9	4.3	4.0	4.7	4.4	5.9
u_x (mm)	-0.2	0.5	0.0	-0.4	0.0	0.0	0.0	0.0	0.1	-0.3	0.0
u_y (mm)	-1.9	-1.8	2.4	2.2	1.3	1.3	0.8	0.8	1.7	1.7	0.9
u_z (mm)	-7.7	-7.2	-6.2	-5.7	-7.1	-5.8	-4.2	-3.9	-4.4	-4.1	-5.6

Table 13: Displacements of the selected points at the application of the SLS2 load ($F = 3232$ MN)

disp.	A	B	C	D	E	F	G	H	I	J	average
u (mm)	8.2	7.7	6.8	6.3	7.4	6.1	4.4	4.1	4.9	4.6	6.1
u_x (mm)	-0.2	0.5	0.0	-0.4	0.0	0.0	0.0	0.0	0.1	-0.3	0.0
u_y (mm)	-1.9	-1.8	2.4	2.2	1.3	1.3	0.9	0.9	1.8	1.7	0.9
u_z (mm)	-7.9	-7.4	-6.4	-5.9	-7.3	-6.0	-4.4	-4.1	-4.6	-4.3	-5.8

		Ponte sullo Stretto di Messina PROGETTO DEFINITIVO		
Calabria Anchor Block – evaluation of block behaviour via 3D FE analyses and of bearing capacity, Annex		<i>Codice documento</i> PF0067_F0_ANX	<i>Rev</i> F0	<i>Data</i> 20-06-2011

Table 14: Displacements of the selected points at the application of the ULS load (F = 3933 MN)

disp.	A	B	C	D	E	F	G	H	I	J	average
u (mm)	10.3	9.7	8.6	8.0	9.4	7.8	5.7	5.4	6.4	6.0	7.7
u _x (mm)	-0.3	0.6	0.0	-0.5	-0.1	-0.1	0.0	-0.1	0.1	-0.4	-0.1
u _y (mm)	-2.4	-2.3	2.9	2.6	1.7	1.7	1.1	1.1	2.2	2.1	1.1
u _z (mm)	-10.0	-9.4	-8.1	-7.5	-9.2	-7.6	-5.6	-5.3	-6.0	-5.6	-7.4

Table 15 summarises the (total) displacements calculated for each of the ten points in the *comparative* analysis in which, before the application of external loads, a 4 m deep excavation around the block was modelled. The reported values refer to the end of three loading steps, corresponding to SILS, SLS2 and ULS loading conditions, respectively.

Table 15: Displacements of the selected points at the application of the external loads (comparative analysis)

	A	B	C	D	E	F	G	H	I	J	average
load condition	u mm										
SILS	8.5	7.9	7.0	6.4	7.4	6.1	4.4	4.1	4.9	4.5	6.1
SLS2	8.8	8.2	7.2	6.6	7.7	6.3	4.5	4.2	5.0	4.7	6.3
ULS	11.1	10.4	9.1	8.4	9.8	8.1	5.9	5.5	6.6	6.1	8.1

From the data in Table 12 - Table 15 and the curves shown in Figure 34 - Figure 40 (see § 4.2) it is possible to observe that:

- 1) The response of the anchor block to the application of the external loads consists in a translation, directed towards the seashore (z-direction), associated with a downwards rotation in the y-z plane. Figure 28 - Figure 30 show a deformed view of the 3D finite element mesh and of the anchor block, computed under application of the ULS loads.
- 2) The total horizontal displacement of the block, directed towards the seashore (negative z-direction), is smaller than 10 mm, for each of the three loading conditions. The total vertical displacement, directed upwards (positive y-direction) is less than 2 mm, while the horizontal displacement in the x-direction (orthogonal to the force) is substantially equal to zero (see also Figure 34 - Figure 37).
- 3) The differential horizontal displacements of central points E and F of the anchor block permit to evaluate the average angle of rotation of the block in the y-z plane and, if any, in the x-y plane

		Ponte sullo Stretto di Messina PROGETTO DEFINITIVO		
Calabria Anchor Block – evaluation of block behaviour via 3D FE analyses and of bearing capacity, Annex	<i>Codice documento</i> PF0067_F0_ANX	<i>Rev</i> F0	<i>Data</i> 20-06-2011	

(see also Figure 38). The distance between point E (+118 m a.s.l.) and point F (+95.65 m a.s.l.) is equal to 22.35 m. Table 16 summarizes the values of the rotation angle corresponding to SILS, SLS2 and ULS loading conditions. The rotation values in the y-z plane are of the order of the thousandths of degree (positive rotation are directed towards the seashore), while they are substantially equal to zero in the x-y direction.

The rotation in the x-z plane can be determined considering the horizontal displacements in the z-direction of aligned pairs of points (e.g. A-B or C-D at the top of the block, G-H and I-J at its base). Table 16 reports the y-z plane rotation angles obtained for the SILS, SLS2 and ULS loading conditions of the Tender Design, referring to displacements of couple A-B (z-direction - relative distance: 100 m). The values of rotation in the x-z plane are low, demonstrating a negligible effect of the inclination of the soil layers on the response of the block.

Small differences of the computed values of the rotation angles exist considering different couples of points (*i.e.* calculating the y-z rotation using the vertical displacements of couples A-C or B-D). These differences are mainly due to the internal deformation of the anchor block.

Table 16: Average rotation angle at the application of the external loads

	y-z plane	x-y plane	x-z plane
load	θ_{EF} (°)	θ_{EF} (°)	θ_{AB} (°)
SILS	3.3E-03	-2.4E-05	2.8E-04
SLS2	3.3E-03	-2.4E-05	2.9E-04
ULS	4.1E-03	-2.7E-05	3.5E-04

- 4) The *comparative* analysis demonstrates a relatively small influence of the upper 4 m of soil on the anchor block response (see also Figure 39 - Figure 40). Anyway, a full refilling of the area surrounding the anchor block is recommend, at least up to the elevation of the top of the structure (+118 m a.s.l.).
- 5) The average direction of the block movement can be evaluated considering the ratio of the vertical and horizontal displacements, u_y/u_z , of the selected points. Table 17 summarises the obtained values of the inclination angle α (in degrees) of the displacement of each selected point and for the three loading conditions (SILS, SLS2 and ULS). Negative values of α indicate upwards displacements. The average value of α , for each load condition, indicates a global displacement of the anchor block directed upwards, with an inclination of about 10 degrees.

Table 17: Average direction of the block movement at the application of the external loads

		Ponte sullo Stretto di Messina PROGETTO DEFINITIVO		
Calabria Anchor Block – evaluation of block behaviour via 3D FE analyses and of bearing capacity, Annex	<i>Codice documento</i> PF0067_F0_ANX	<i>Rev</i> F0	<i>Data</i> 20-06-2011	

	A	B	C	D	E	F	G	H	I	J	average
load	α (°)										
SILS	13.6	13.9	-20.8	-20.6	-10.3	-12.7	-11.4	-11.9	-21.7	-22.0	-10.4
SLS2	13.6	13.8	-20.6	-20.4	-10.3	-12.6	-11.3	-11.9	-21.5	-21.9	-10.3
ULS	13.2	13.5	-19.4	-19.1	-10.2	-12.4	-11.0	-11.6	-20.4	-20.8	-9.8

4.2 Load-displacement curves: increase of external loads

In the FE analyses described in the previous sections a numerical solution was always found. According to the current Italian Code (Norme Tecniche per le Costruzioni - DM 14.01.2008), which introduces partial safety factors for limit state design, the Design Actions are to be compared with the Design Resistances. If the actions are lower or equal to the resistances, the anchor block performance is satisfactory against the ultimate state ULS. In a FE analysis this comparison is meaningless, as either the numerical analysis converges towards a solution or it doesn't, *i.e.* convergence is not obtained. These two options are strongly dependent on the algorithms built in the software. Therefore, it was decided that, in order to evaluate the actual safety of the anchor block under the applied loads and against the occurrence of a ULS, a load incremental analysis (progressive increase of external loads) or a decreasing soil properties analysis (ϕ' – c' reduction) could be useful. In this manner it was possible to evaluate a "distance" from a general failure condition.

The comments above justify the use of load-displacement curves as a tool to evaluate the safety conditions of the anchor block in terms of ULS. In the following, the load-displacement curves of the 10 selected points of the anchor block (§ 4.1) will be reported and commented, remembering that the displacements calculated in the preliminary stages of the analysis were reset to zero and the load-displacement curves refer only to the application of the external loads.

Further results of the numerical analyses will be reported in the following sections of the report.

The load-displacement curves obtained for the ten points of the anchor block are plotted in Figure 34, while Figure 35 and Figure 36 show the same curves for the load and the displacements in the horizontal (z-direction) and vertical (y-direction) directions; finally Figure 37 shows the curves of horizontal displacements orthogonal to the bridge axis (x-direction); in this last figure, as the x-component of the force is equal to zero, the x-displacements are plotted versus the total external force. In each figure, three continuous lines identify the SILS, SLS2 and ULS loading conditions as obtained in the Tender Design; the dashed lines are for the SILS, SLS2 and ULS loading cases as

		Ponte sullo Stretto di Messina PROGETTO DEFINITIVO		
Calabria Anchor Block – evaluation of block behaviour via 3D FE analyses and of bearing capacity, Annex	<i>Codice documento</i> PF0067_F0_ANX	<i>Rev</i> F0	<i>Data</i> 20-06-2011	

obtained from the global IBDAS model version 3.3b and version 3.3f. The low differences between the cable forces obtained from the Tender Design and those provided by the global IBDAS models result in negligible differences in the displacement field of the anchor block. In the following comments are referred to Tender Design cable forces that provided the higher values for the ULS load conditions.

The evolution of the average angle of rotation of the block in the vertical y-z plane and the horizontal x-z plane (obtained as differential displacement of couples of selected points, see § 4.2) are shown in Figure 38 versus the increasing external loads.

Figure 39 shows the load-displacement curves obtained for the ten selected points of the anchor block in the *comparative* analysis in which, before the application of external loads, a 4 m deep excavation around the whole block was modelled; Figure 40 compares the load-displacement curves of points E and F obtained from the *standard* analysis (without excavation) and the *comparative* analysis (with 4 m deep excavation around the block). The curves show a slight influence of the 4 m deep excavation.

The ultimate failure load for the anchor block can be evaluated using a hyperbolic best fit of the load-displacement curve, as form the following equation:

$$F = \frac{u}{m + n \cdot u} \quad (15)$$

The ultimate load can be estimated using the conservative relationship:

$$F_{\text{lim}} = \frac{0.9}{n} \quad (16)$$

Figure 41 shows the load-displacement curves data of points E and F in a $u-u/F$ diagram. The inclination of the interpolating straight lines provides the ultimate load that, in both cases, results equal to about 11000 MN. This provides a global safety factor of about 2.75 for the ULS loading conditions and of about 3.5 for the SILS loading condition.

4.3 Msf-displacement curves: ϕ' – c' reduction analyses

In the ϕ' – c' reduction analyses, the strength properties of the soils were progressively reduced by increasing the factor Msf (see § 3.3). The ϕ' – c' reduction procedure starts from the block configuration corresponding to the SILS, SLS2 and ULS loading conditions, i.e. three different ϕ' – c' reduction analyses were carried out.

		Ponte sullo Stretto di Messina PROGETTO DEFINITIVO		
Calabria Anchor Block – evaluation of block behaviour via 3D FE analyses and of bearing capacity, Annex	<i>Codice documento</i> PF0067_F0_ANX	<i>Rev</i> F0	<i>Data</i> 20-06-2011	

Msf-displacement curves for the $\varphi' - c'$ reduction analyses show that the displacements increase with increasing Msf factor, whose physical meaning is comparable to a safety factor. The displacements start from zero since their previous values have been reset. As expected, the highest the initial external load value in the $\varphi' - c'$ reduction analysis, the lowest is the Msf final factor.

The load-displacement curves obtained from the three $\varphi' - c'$ reduction analyses for point E (top of the block, central position) and point F (block core) are plotted in Figure 42 up to displacements of 45 mm. A dashed line identifies the value of Msf corresponding to a sharp change of slope of the curves; a conservative value of Msf, valid for all three analyses, may be equal to 3. Figure 43 shows the results of the $\varphi' - c'$ reduction analyses over the whole range of computed displacements.

Figure 44 shows the Msf-displacement curves obtained from the *comparative* analysis, with a 4 m deep excavation around the block. In this case a conservative Msf value corresponding to a sharp change of slope of the curves may be equal to 2.5 (slightly less than from the *standard* analysis). This confirms the importance of refilling the area surrounding the anchor block with soil, after construction.

4.4 Plaxis 3D foundation output

In the following section, a selection of the output is presented for relevant steps of the analyses. According to PLAXIS sign conventions, compressive stresses are negative.

4.4.1 Soil stress state

The state of stress in the soil during the main steps of the analysis is shown in terms of contours of relative shear stress τ_{rel} :

$$\tau_{rel} = \frac{\tau_{mob}}{\tau_{max}} \quad (17)$$

where τ_{mob} is the mobilised shear strength (*i.e.* the radius of the Mohr stress circle) and τ_{max} is the maximum value of the shear stress, obtained expanding the Mohr's circle until it is tangent to the Mohr-Coulomb failure envelope, while keeping its centre constant.

Figure 45 to Figure 48 show the contours of relative shear stress on two sections through the centre of the block, one longitudinal (North-South direction or y-z plane) and one transversal

		Ponte sullo Stretto di Messina PROGETTO DEFINITIVO		
Calabria Anchor Block – evaluation of block behaviour via 3D FE analyses and of bearing capacity, Annex	<i>Codice documento</i> PF0067_F0_ANX	<i>Rev</i> F0	<i>Data</i> 20-06-2011	

(West-East direction or x-y plane), respectively. Figure 45 shows the initial conditions; Figure 46 shows the situation at the end of excavation; a moderate reduction of the values of τ_{rel} can be seen in Figure 47, at the end of the block construction. Finally, Figure 48 shows the τ_{rel} distribution at the end of the ULS load application. While the active earth pressure is fully mobilised on the south side, the passive earth pressure is still far from being completely activated on the north side. Figure 49 and Figure 50 show the vertical total stresses σ_y and the horizontal total stresses (σ_z or σ_x) induced by ULS load condition, with reference to two central, longitudinal and transversal, sections, as in the previous figures. Figure 51 and Figure 52 show the vertical total stresses σ_y and the horizontal total stresses σ_z on a horizontal section at an elevation of 105.05 m a.s.l. Figure 52 also shows the soil layer position at the same elevation, justifying the discontinuities of the horizontal total stress.

4.4.2 Mesh displacements

The contours of computed displacements discussed in the following are those corresponding to the ULS loading condition, that is the highest value of the three applied external loads.

Figure 53 shows the contours of total displacements contours of the whole mesh, while Figure 54 details the displacements of the anchor block. In this last figure the local deformation of the anchor block due to the application of the external loads can be appreciated (corresponding to a maximum displacement in the loaded nodes of the mesh of about 15 mm)

Figure 55 shows the total displacements along two sections through the centre of gravity, North-South and West-East oriented, respectively. As discussed in the previous sections (§ 4.1), the maximum anchor block displacement is equal to about 11 mm (top of the block), while the core block displacement is equal to about 8 mm. The North-South section shows clearly the roto-translational movement of the anchor block, discussed in section § 4.1.

Figure 56 and Figure 57 show the z-direction and the y-direction components of the displacements in the same along the same sections presented in Figure 55.

4.4.3 Water pressure distribution

During excavation, a seepage process is induced from the outside of the pit towards the excavated area (§ 3.3). Due to limitation of Plaxis 3D, the 3D seepage process cannot be resolved numerically. However, it is possible to change the water pressure distribution of the soil clusters where seepage takes place, interpolating the pore pressures between those corresponding to the

		Ponte sullo Stretto di Messina PROGETTO DEFINITIVO		
Calabria Anchor Block – evaluation of block behaviour via 3D FE analyses and of bearing capacity, Annex	<i>Codice documento</i> PF0067_F0_ANX		<i>Rev</i> F0	<i>Data</i> 20-06-2011

external general groundwater level (+102 m a.s.l.) and the groundwater level corresponding to the elevation of the current dredge line. The general groundwater conditions are then restored at the end of block construction.

Figure 58 shows the pore water pressure distribution assigned to the soil clusters at the end of the last excavation step (maximum excavation depth: +76.65 m a.s.l.), again along two central sections, oriented North-South and West-East, respectively; the corresponding groundwater head profile is shown in Figure 59. For comparison, Figure 60 shows the groundwater distribution, corresponding to the initial conditions, at the end of block construction.

		Ponte sullo Stretto di Messina PROGETTO DEFINITIVO		
Calabria Anchor Block – evaluation of block behaviour via 3D FE analyses and of bearing capacity, Annex	<i>Codice documento</i> PF0067_F0_ANX		<i>Rev</i> F0	<i>Data</i> 20-06-2011

5 CONCLUSIONS

In this report, the behaviour of Calabria Anchor Block under SILS, SLS2 and ULS loading conditions has been studied through static 3D analyses carried out using the finite element code Plaxis 3D Foundation. The calculations are based on both drawings and cable forces provided in the Tender Design; account is also given for the influence of the cable forces computed from the global IBDAS model version 3.3b and version 3.3f.

The evaluation of earthquake-induced block displacements and of safety against ultimate limit states are discussed in the companion report “Calabria anchor block: earthquake-induced displacements and safety against ultimate limit states”.

The Calabria Anchor Block consists of a massive block, with the shape of a trapezoid-based prism. The dimensions of the upper rectangle, in plane, are 98 x 87.5 m²; the maximum height of the construction is 41 m. The excavation is supported by diaphragm walls, with a thickness of 1.0 m and a width of 2.5 m, whose length varies according to the shape of the block. The excavation is supported also by several levels of retaining anchors, varying in number along the different sides of the pit.

The present level of the ground surface at the location of the Calabria Anchor Block lies between +114 m and +127 m a.s.l.; the sea shore is located at a distance of about 900 m from the anchor block. The groundwater level results from steady state seepage between a head of about +107 m a.s.l. in the south-east corner of the anchor block to a head of +95 m a.s.l. in the opposite corner, in the north-west position.

The geotechnical profile of the area is characterised by the following units: 1. Coastal Deposits (sand and gravel); 2. Messina Gravel (gravel and sand); 3. Pezzo Conglomerate (clasts of granitic nature in a sandy-silty matrix and sandstone, comparable to a soft rock); it is generally possible to distinguish an upper layer of weathered conglomerate and a lower layer of in situ conglomerate. The geotechnical profile is characterised by significant variations of the level of the soil layers in the direction parallel to the coastline and, to a lesser extent, in the direction orthogonal to the coastline. The geotechnical characterisation is based on the site investigations carried out in 1988 and 1992.

The behaviour of the Anchor Block was studied through finite element analyses performed using the Plaxis 3D Foundation code; the 3D model used for the analyses, extending 500 x 500 m² in plan and 200 m below ground level, consists of about 60 thousands elements. The mechanical behaviour of the soil was described using the Hardening Soil model, capable of reproducing soil

		Ponte sullo Stretto di Messina PROGETTO DEFINITIVO		
Calabria Anchor Block – evaluation of block behaviour via 3D FE analyses and of bearing capacity, Annex	<i>Codice documento</i> PF0067_F0_ANX	<i>Rev</i> F0	<i>Data</i> 20-06-2011	

non-linearity due to the occurrence of plastic strains from the beginning of the loading process. The mechanical behaviour of the anchor block concrete and of the ballast material were described as linear elastic. The diaphragm walls were modelled as WALL shell elements, while the retaining anchors were modelled as SPRING elements, which simulate anchors in a simplified way, without taking into account anchor – soil interaction.

3D finite element analyses were carried out adopting the following sequence of main steps: 1. computation of the initial stress state; 2. activation of diaphragm walls; 3. progressive excavation of the soil to reach the anchor block base and simultaneous activation of the retaining anchors levels; 4. progressive activation of the anchor block from the bottom up; 5. application of the external loads; 6a. increase of external loads; 6b. reduction of soil properties (φ' – c' reduction).

To evaluate the effect of the uppermost layer of soil on the displacements of the block, a further *comparative* analysis was carried out in which, before application of the external loads, a 4 m deep excavation around the block was simulated.

Forces in the main cables at Calabria Anchor Block were provided by the structural analyses of the tender design, for three different loading conditions (SILS, SLS2 and ULS). The direction of the forces is inclined of 15 degrees on the horizontal and directed upwards, towards the sea. The influence of the cable forces computed using the global IBDAS model version 3.3b and 3.3f are also discussed.

The results of the finite element analyses are examined in terms of load-displacement curves; ten representative points of the anchor block were selected to this purpose. The preliminary stages of the analyses (*i.e.* excavation of the pit supported by retaining walls and anchors, construction of the block, removal of the provisional retaining anchors, reinstatement of the initial hydraulic conditions) were simulated to reproduce fully the stress state in the soil at the beginning of the loading process. The displacements calculated in these stages were reset to zero and the load-displacement curves refer to the application of external loads only.

The results obtained from the finite element analyses demonstrate that:

1. the anchor block response to the external loads consists in a translation towards the seashore (z-direction), associated with a downwards rotation in the y-z plane;
2. for all three loading conditions, the horizontal displacement of the block towards the seashore is smaller than 10 mm;
3. the total vertical displacement, directed upwards, is less than 2 mm, while the horizontal displacement in x-direction (*i.e.* orthogonal to the bridge axis) is practically equal to zero;
4. the rotation in the vertical plane (y-z) are of the order of some thousandth of degree (directed

		Ponte sullo Stretto di Messina PROGETTO DEFINITIVO		
Calabria Anchor Block – evaluation of block behaviour via 3D FE analyses and of bearing capacity, Annex	<i>Codice documento</i> PF0067_F0_ANX	<i>Rev</i> F0	<i>Data</i> 20-06-2011	

towards the seashore), while they are practically equal to zero in the x-y direction. The values of rotation in the x-z plane are low, showing only a slight influence of the inclination of the foundation soil layers on the response of the block;

5. the *comparative* analysis indicates a relatively small influence of the uppermost 4 m of soil on the response of the block;
6. the average direction of the block movement, for all three loading conditions, is directed upwards, with an inclination to the horizontal of about 10 degrees;
7. the ultimate failure load for the anchor block, evaluated using an hyperbolic best-fit of the load-displacement data, is equal to about 11000 MN. This results in a safety factor against increasing external forces of about 2.75 for ULS loads and of about 3.5 for SILS load;
8. In the $\phi' - c'$ reduction analyses the strength of the soils was progressively reduced by increasing the factor M_{sf} , whose physical meaning is comparable to a safety factor. A conservative value of factor M_{sf} , valid for all three loading conditions, is about 3. The *comparative* analysis, with a 4 m deep excavation around the block, yielded a conservative value of $M_{sf} = 2.5$, thus confirming the importance of refilling the area around the block with soil, after construction.

		<p align="center">Ponte sullo Stretto di Messina PROGETTO DEFINITIVO</p>		
<p>Calabria Anchor Block – evaluation of block behaviour via 3D FE analyses and of bearing capacity, Annex</p>	<p><i>Codice documento</i> PF0067_F0_ANX</p>		<p><i>Rev</i> F0</p>	<p><i>Data</i> 20-06-2011</p>

6 FIGURES

		Ponte sullo Stretto di Messina PROGETTO DEFINITIVO		
Calabria Anchor Block – evaluation of block behaviour via 3D FE analyses and of bearing capacity, Annex	<i>Codice documento</i> PF0067_F0_ANX	<i>Rev</i> F0	<i>Data</i> 20-06-2011	

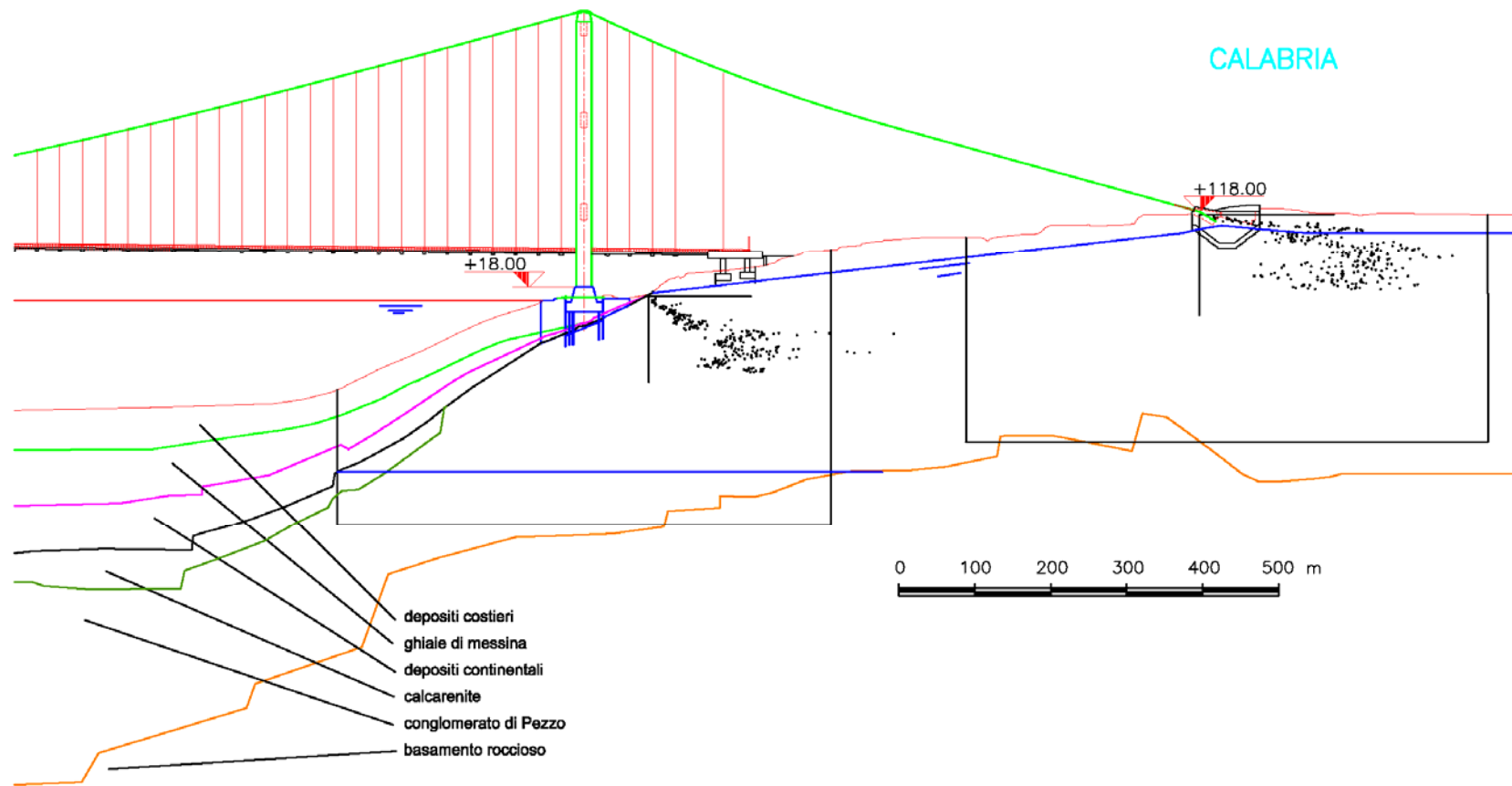


Figure 1: Soil profile on the Calabria shore

 Stretto di Messina		Ponte sullo Stretto di Messina PROGETTO DEFINITIVO		
Calabria Anchor Block – evaluation of block behaviour via 3D FE analyses and of bearing capacity, Annex	Codice documento PF0067_F0_ANX	Rev F0	Data 20-06-2011	

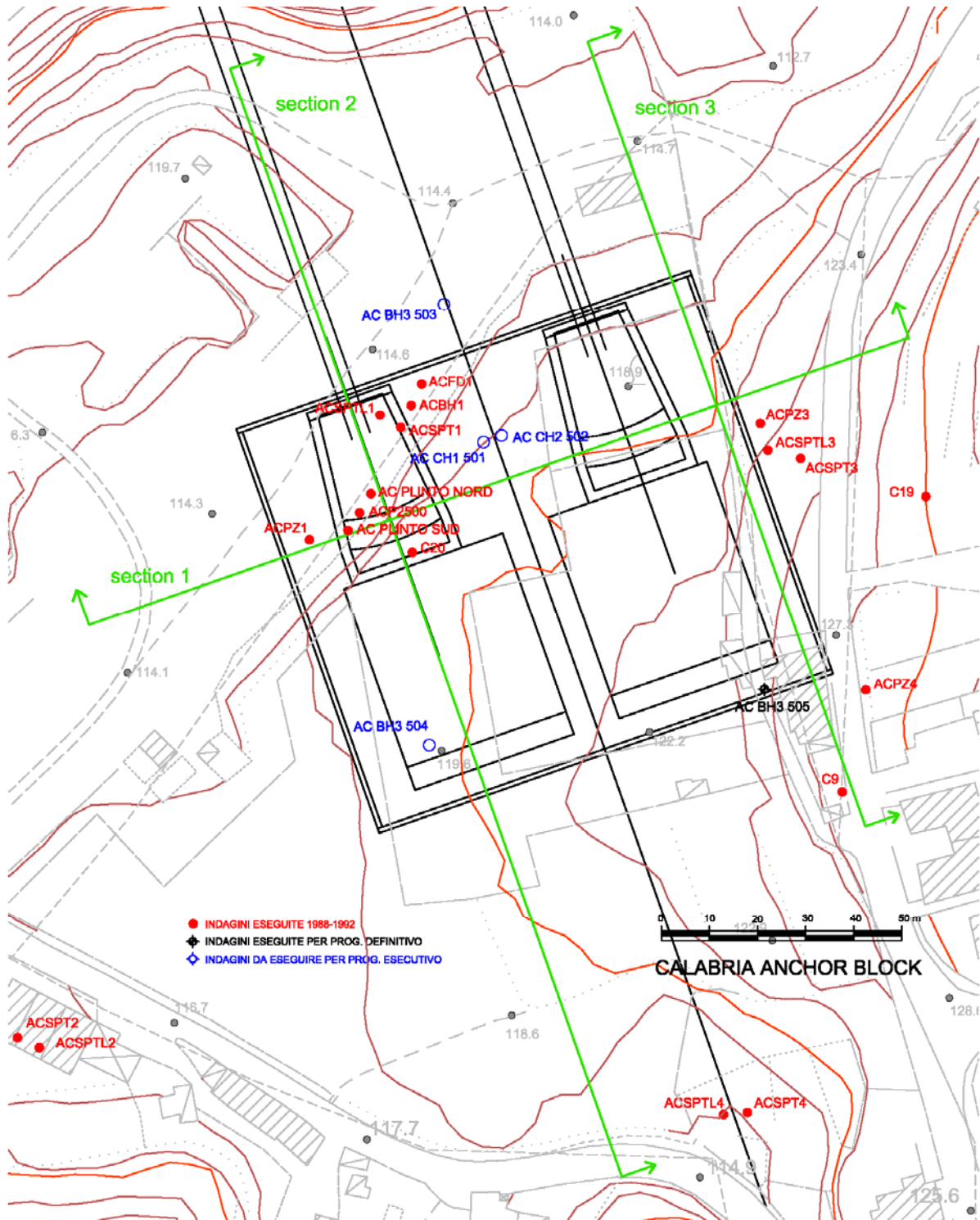


Figure 2: Plan view at the location of Calabria Anchor Block

		<p align="center">Ponte sullo Stretto di Messina PROGETTO DEFINITIVO</p>		
<p>Calabria Anchor Block – evaluation of block behaviour via 3D FE analyses and of bearing capacity, Annex</p>	<p><i>Codice documento</i> PF0067_F0_ANX</p>		<p><i>Rev</i> F0</p>	<p><i>Data</i> 20-06-2011</p>

		Ponte sullo Stretto di Messina PROGETTO DEFINITIVO		
		Calabria Anchor Block – evaluation of block behaviour via 3D FE analyses and of bearing capacity, Annex	Codice documento PF0067_F0_ANX	Rev F0

SECTION N. 1

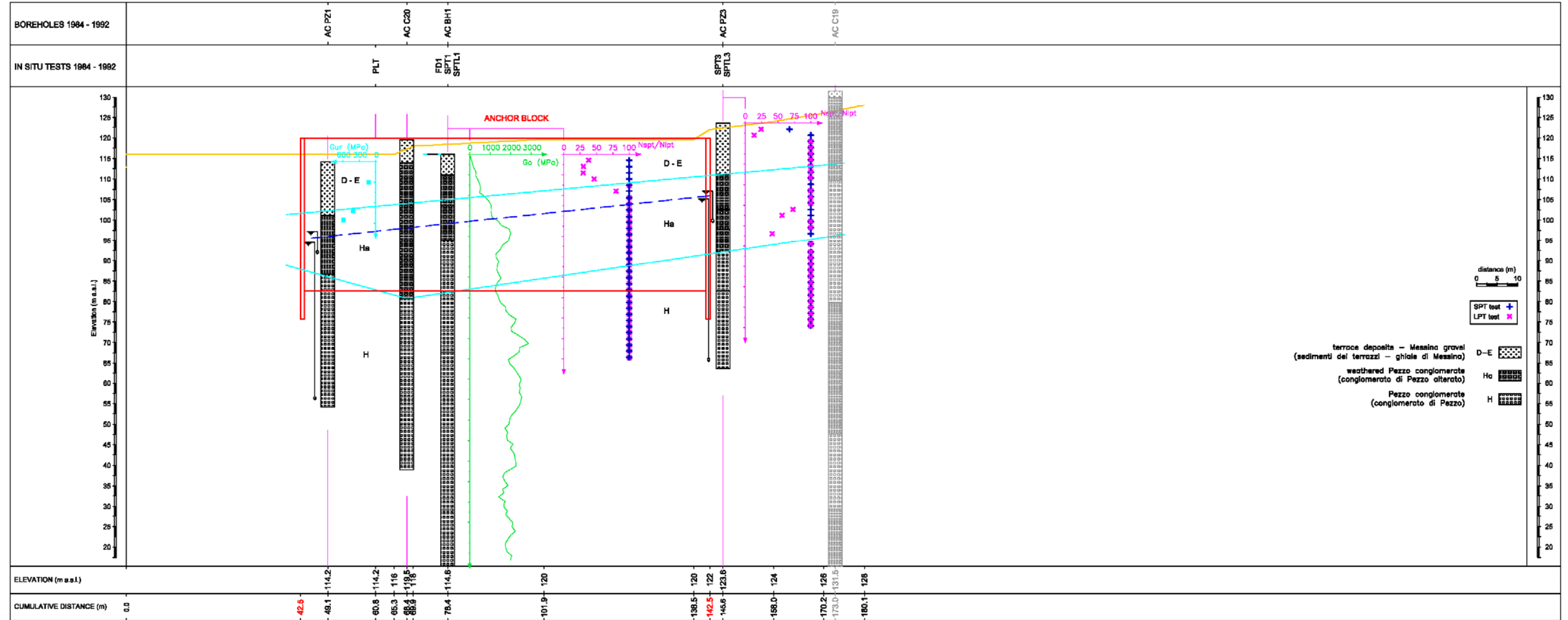


Figure 3: Calabria Anchor Block, cross section No. 1

		Ponte sullo Stretto di Messina PROGETTO DEFINITIVO		
Calabria Anchor Block – evaluation of block behaviour via 3D FE analyses and of bearing capacity, Annex	<i>Codice documento</i> PF0067_F0_ANX	<i>Rev</i> F0	<i>Data</i> 20-06-2011	

SECTION N. 2

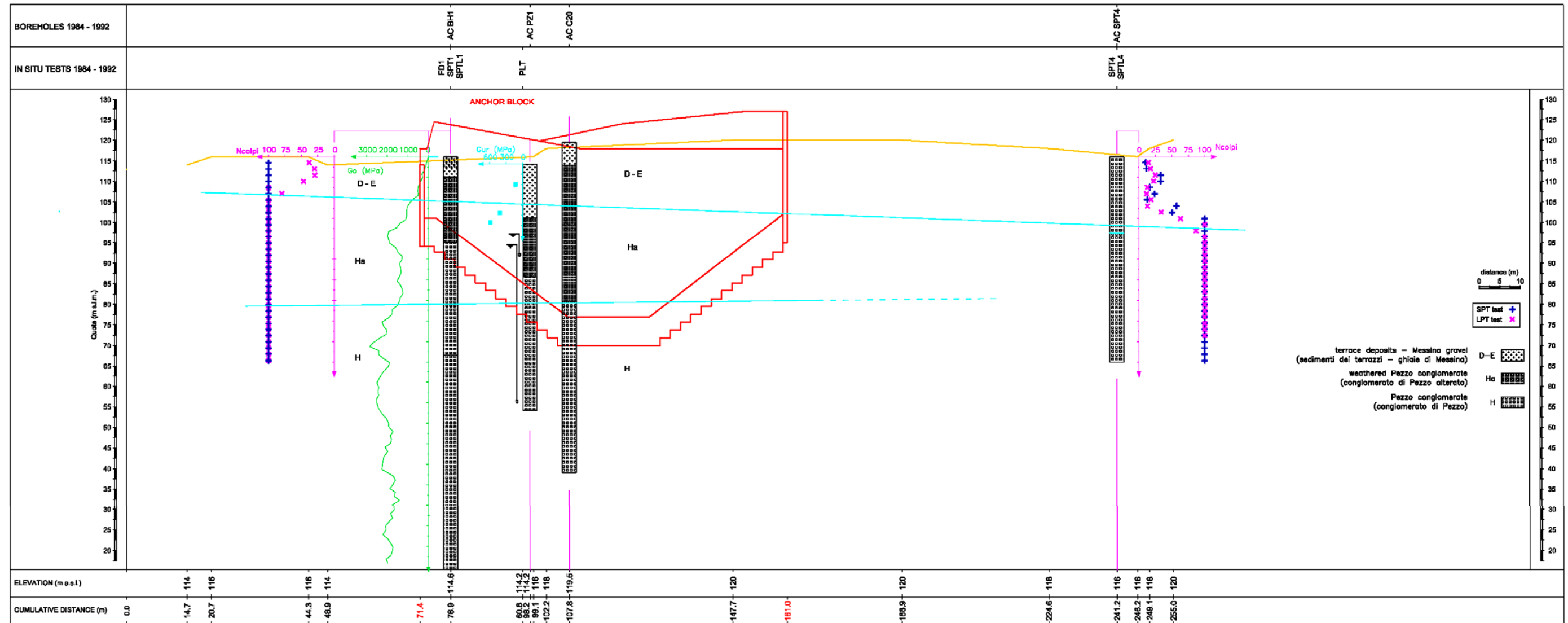


Figure 4: Calabria Anchor Block, cross section No. 2

		<p align="center">Ponte sullo Stretto di Messina PROGETTO DEFINITIVO</p>		
Calabria Anchor Block – evaluation of block behaviour via 3D FE analyses and of bearing capacity, Annex	<i>Codice documento</i> PF0067_F0_ANX	<i>Rev</i> F0	<i>Data</i> 20-06-2011	

SECTION N. 3

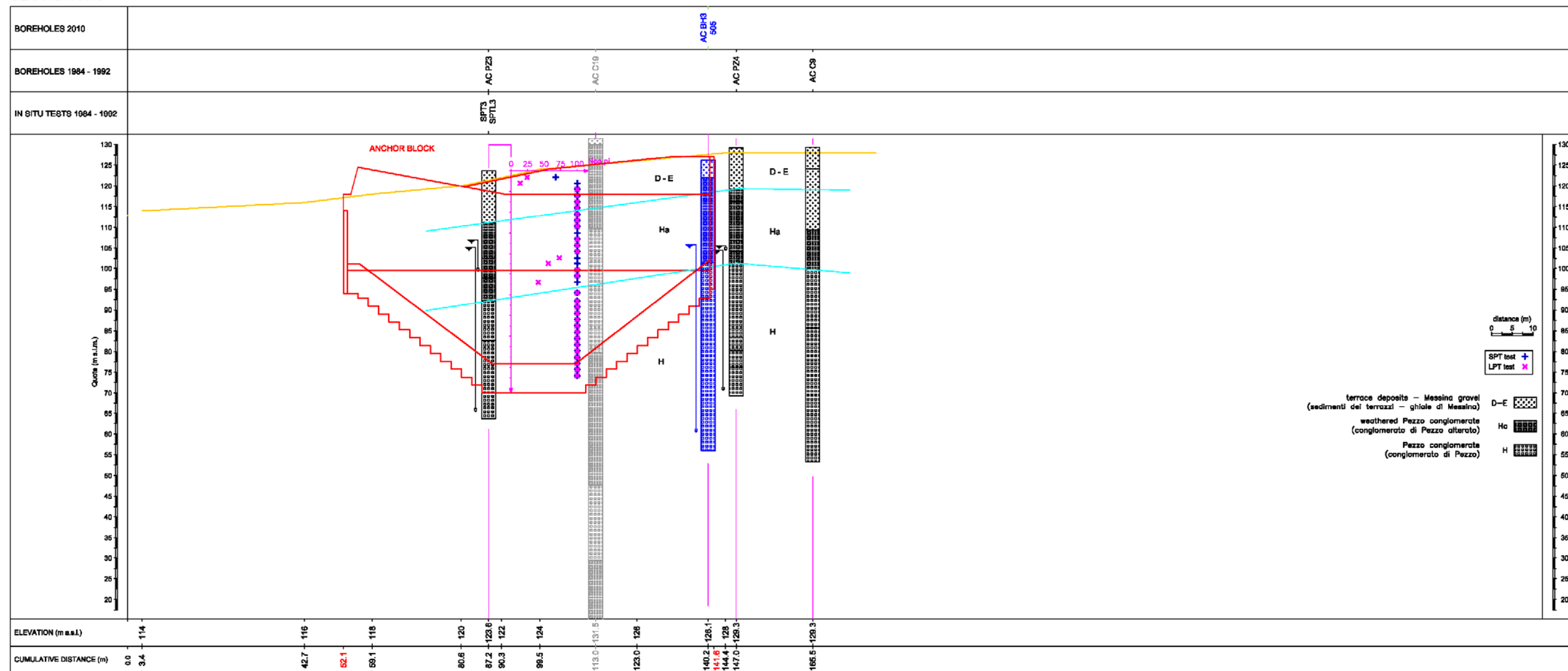


Figure 5: Calabria Anchor Block, cross section No. 3

		Ponte sullo Stretto di Messina PROGETTO DEFINITIVO	
Calabria Anchor Block – evaluation of block behaviour via 3D FE analyses and of bearing capacity, Annex	<i>Codice documento</i> PF0067_F0_ANX	<i>Rev</i> F0	<i>Data</i> 20-06-2011

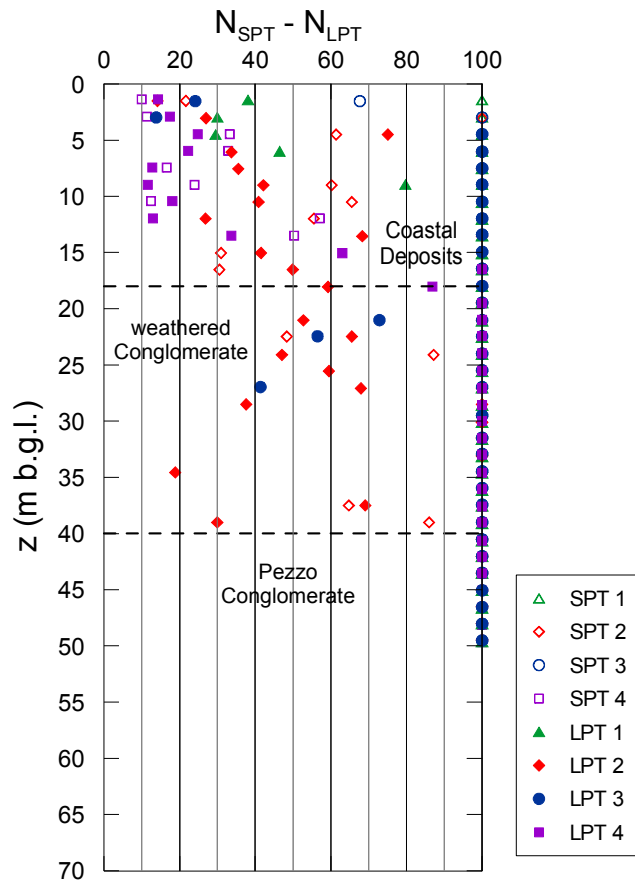


Figure 6: Calabria Anchor Block – SPT and LPT test results

		Ponte sullo Stretto di Messina PROGETTO DEFINITIVO	
Calabria Anchor Block – evaluation of block behaviour via 3D FE analyses and of bearing capacity, Annex	<i>Codice documento</i> PF0067_F0_ANX	<i>Rev</i> F0	<i>Data</i> 20-06-2011

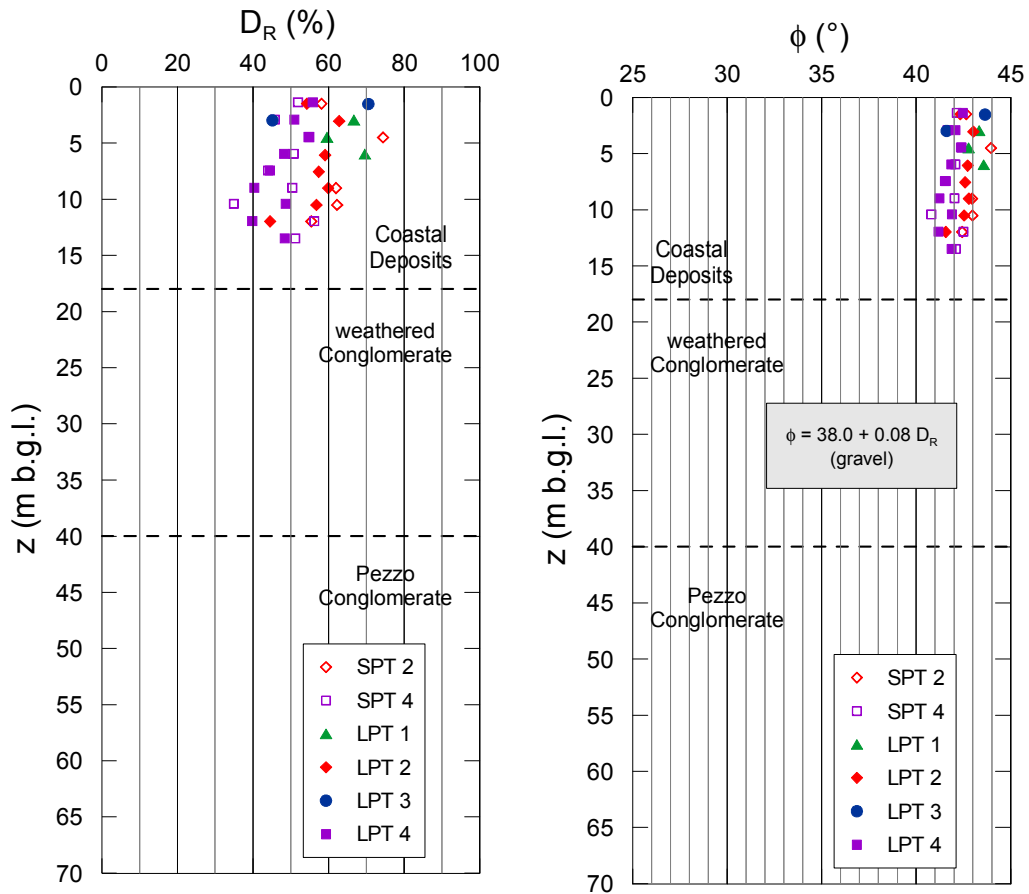


Figure 7: Calabria Anchor Block – relative density and angle of shearing resistance

		Ponte sullo Stretto di Messina PROGETTO DEFINITIVO	
Calabria Anchor Block – evaluation of block behaviour via 3D FE analyses and of bearing capacity, Annex	<i>Codice documento</i> PF0067_F0_ANX	<i>Rev</i> F0	<i>Data</i> 20-06-2011

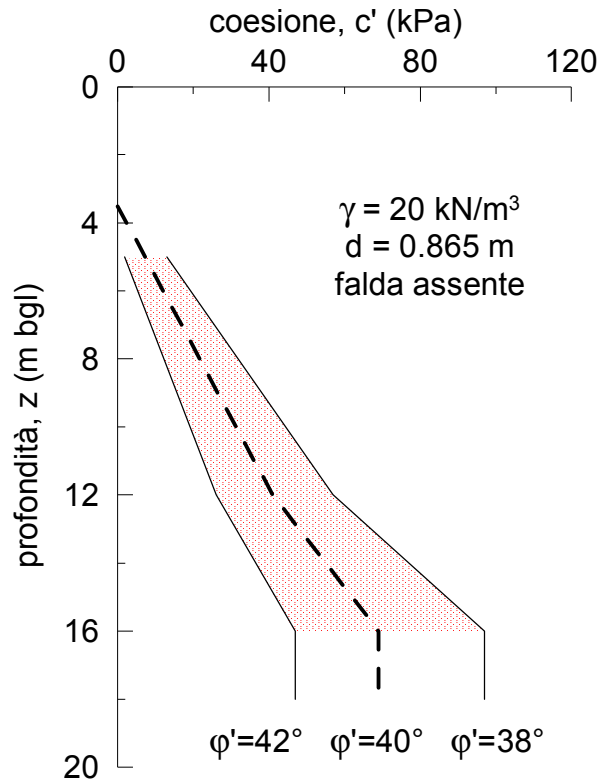


Figure 8: Calabria Anchor Block – c' profile from large diameter plate loading test

		Ponte sullo Stretto di Messina PROGETTO DEFINITIVO	
Calabria Anchor Block – evaluation of block behaviour via 3D FE analyses and of bearing capacity, Annex	<i>Codice documento</i> PF0067_F0_ANX	<i>Rev</i> F0	<i>Data</i> 20-06-2011

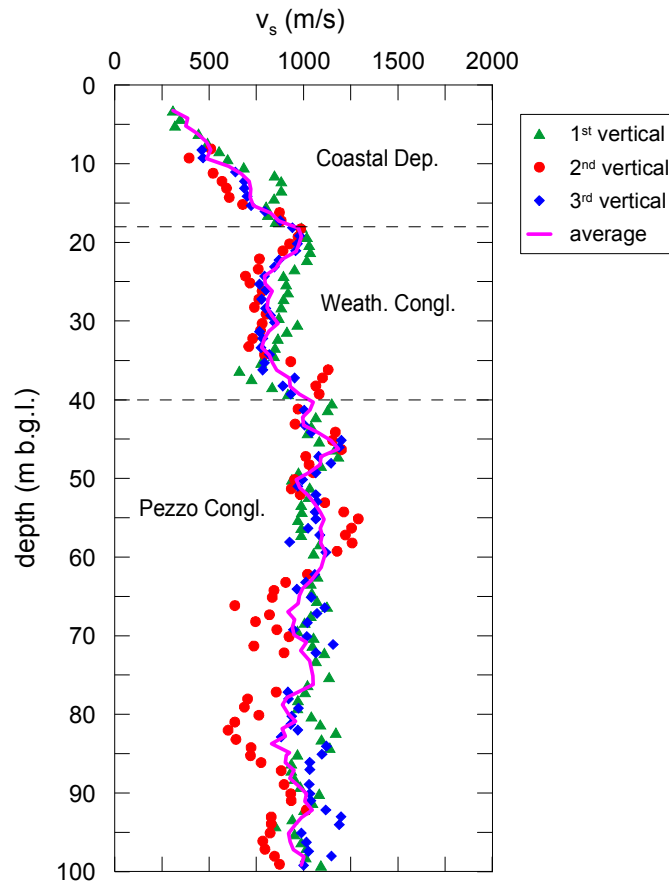


Figure 9: Calabria Anchor Block, v_s profile from cross-hole test

		Ponte sullo Stretto di Messina PROGETTO DEFINITIVO	
Calabria Anchor Block – evaluation of block behaviour via 3D FE analyses and of bearing capacity, Annex	<i>Codice documento</i> PF0067_F0_ANX	<i>Rev</i> F0	<i>Data</i> 20-06-2011

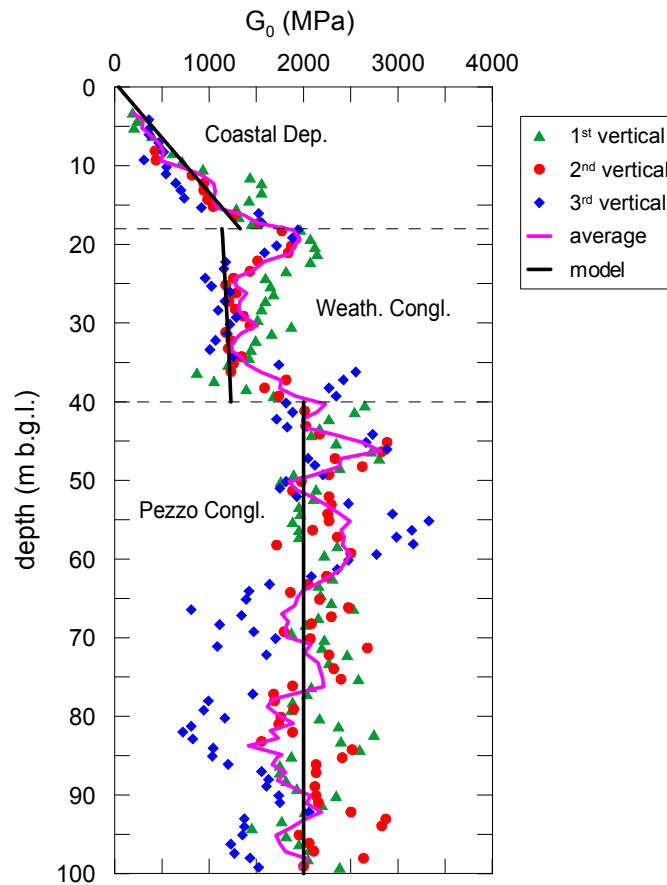


Figure 10: Calabria Anchor Block, G_0 profile from cross-hole test and HS model prediction

 Stretto di Messina		Ponte sullo Stretto di Messina PROGETTO DEFINITIVO		
Calabria Anchor Block – evaluation of block behaviour via 3D FE analyses and of bearing capacity, Annex	<i>Codice documento</i> PF0067_F0_ANX	<i>Rev</i> F0	<i>Data</i> 20-06-2011	

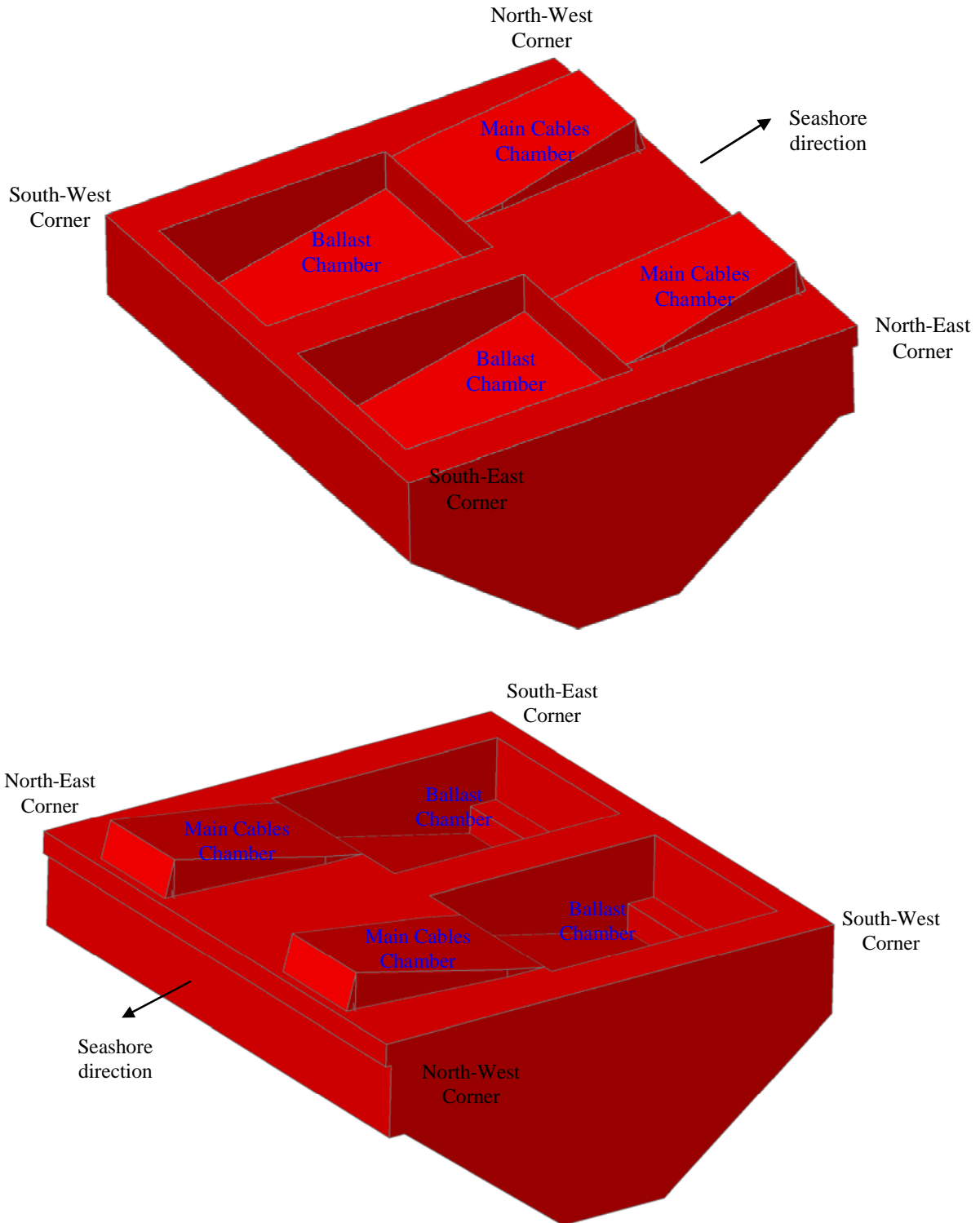


Figure 11: two axonometric views of the Calabria Anchor Block

Calabria Anchor Block – evaluation of block behaviour via 3D FE analyses and of bearing capacity, Annex

Codice documento
PF0067_F0_ANX

Rev	Data
F0	20-06-2011

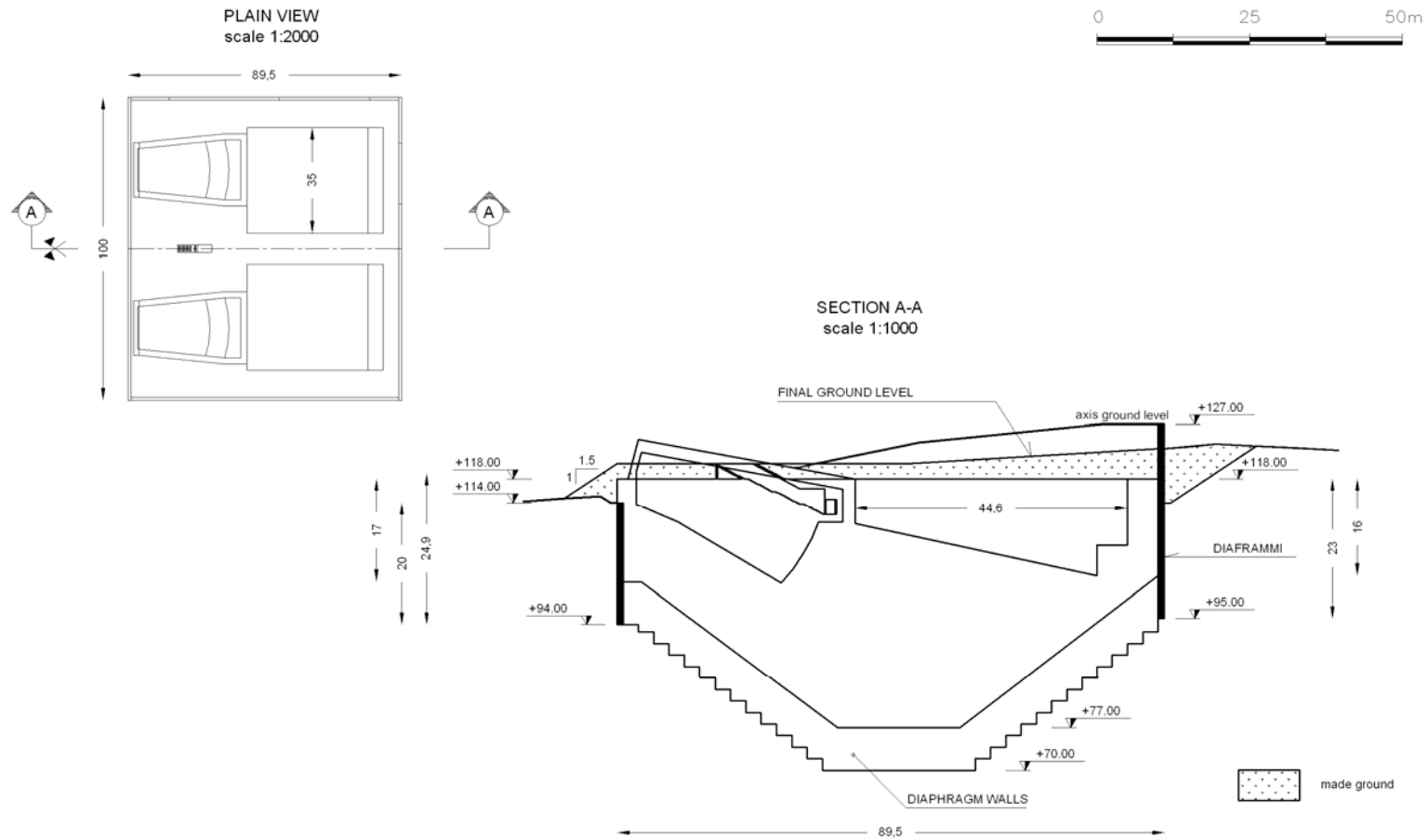


Figure 12: Plan view and cross section of Calabria Anchor Block

 Stretto di Messina		Ponte sullo Stretto di Messina PROGETTO DEFINITIVO	
Calabria Anchor Block – evaluation of block behaviour via 3D FE analyses and of bearing capacity, Annex	<i>Codice documento</i> PF0067_F0_ANX	<i>Rev</i> F0	<i>Data</i> 20-06-2011

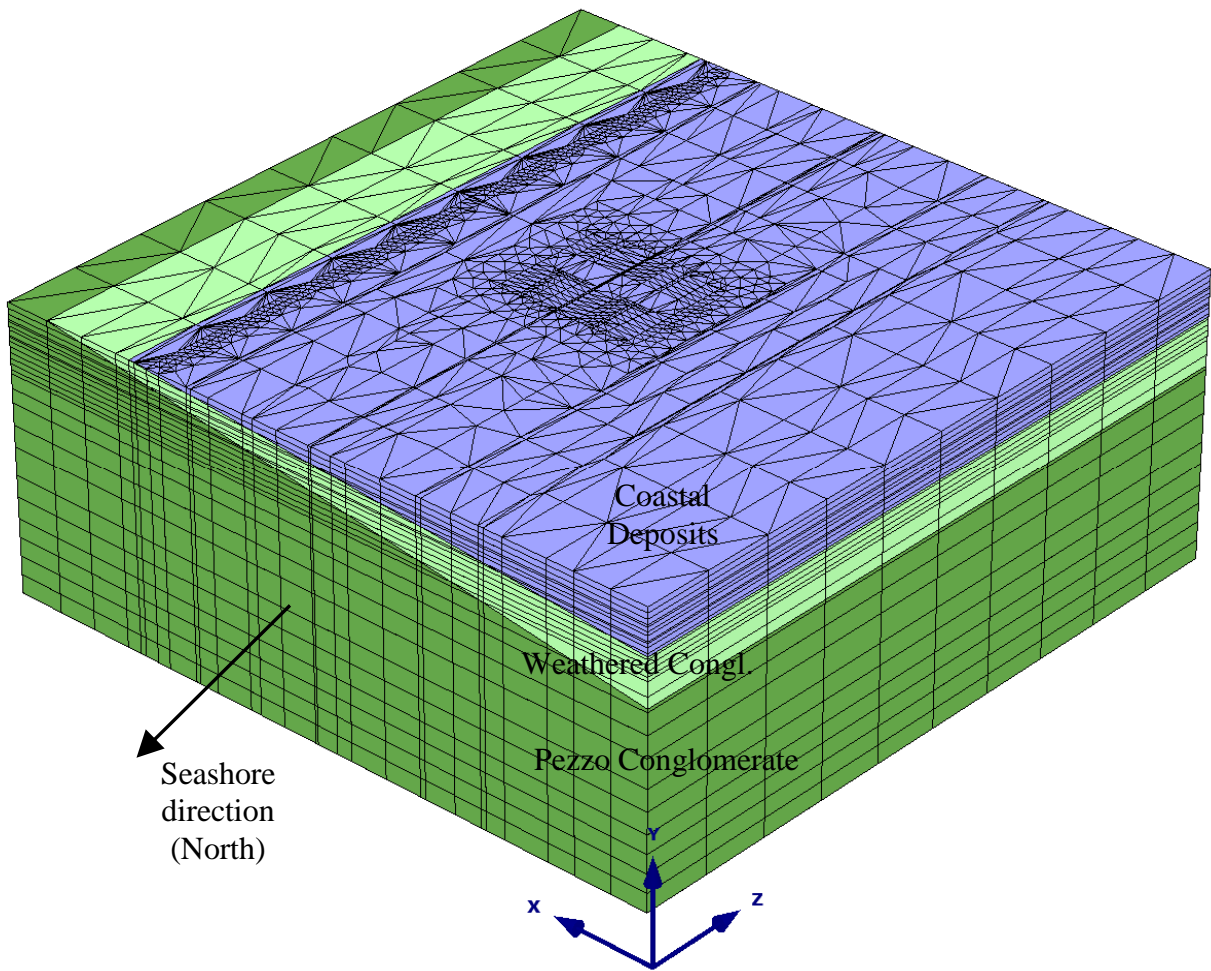


Figure 13: FEM model in the initial steps: axonometric view

		Ponte sullo Stretto di Messina PROGETTO DEFINITIVO	
Calabria Anchor Block – evaluation of block behaviour via 3D FE analyses and of bearing capacity, Annex	<i>Codice documento</i> PF0067_F0_ANX	<i>Rev</i> F0	<i>Data</i> 20-06-2011

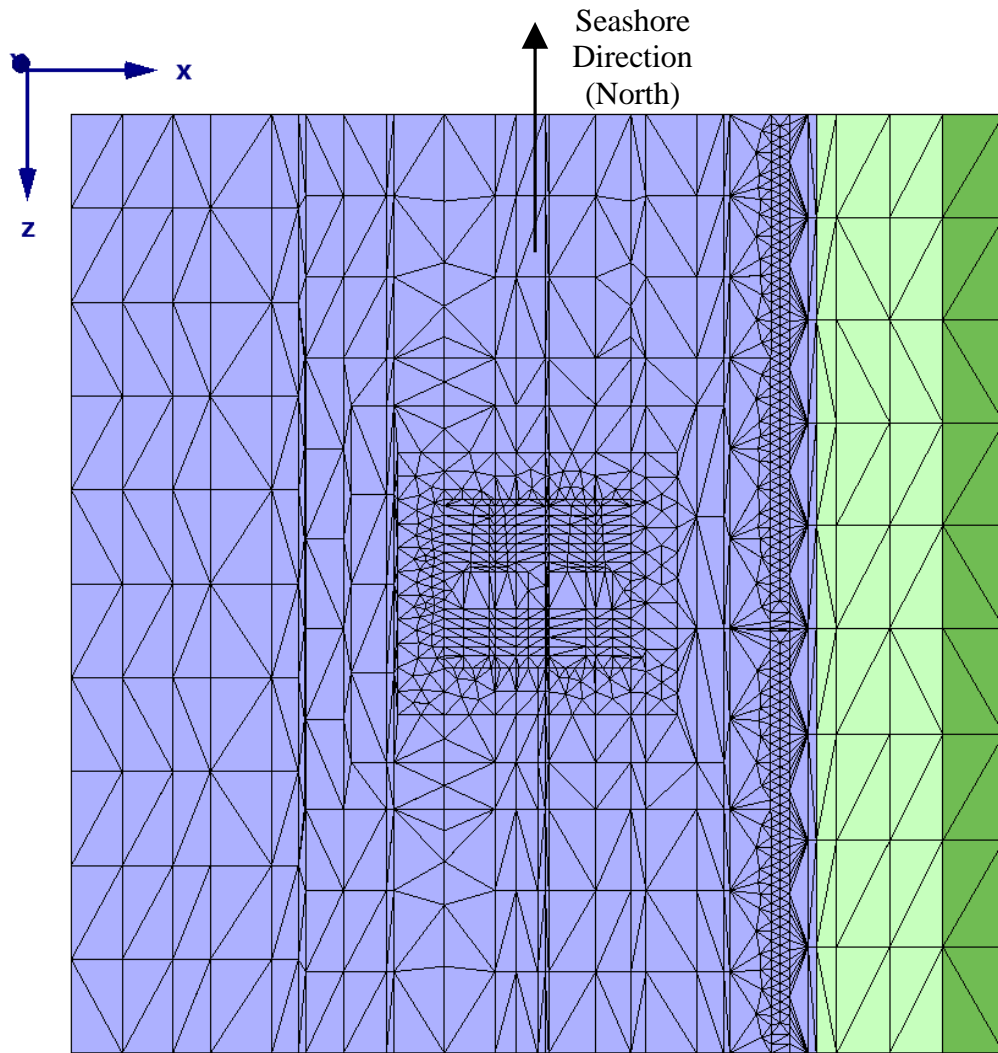


Figure 14: FEM model: top-view of the initial mesh

		Ponte sullo Stretto di Messina PROGETTO DEFINITIVO		
Calabria Anchor Block – evaluation of block behaviour via 3D FE analyses and of bearing capacity, Annex	<i>Codice documento</i> PF0067_F0_ANX	<i>Rev</i> F0	<i>Data</i> 20-06-2011	

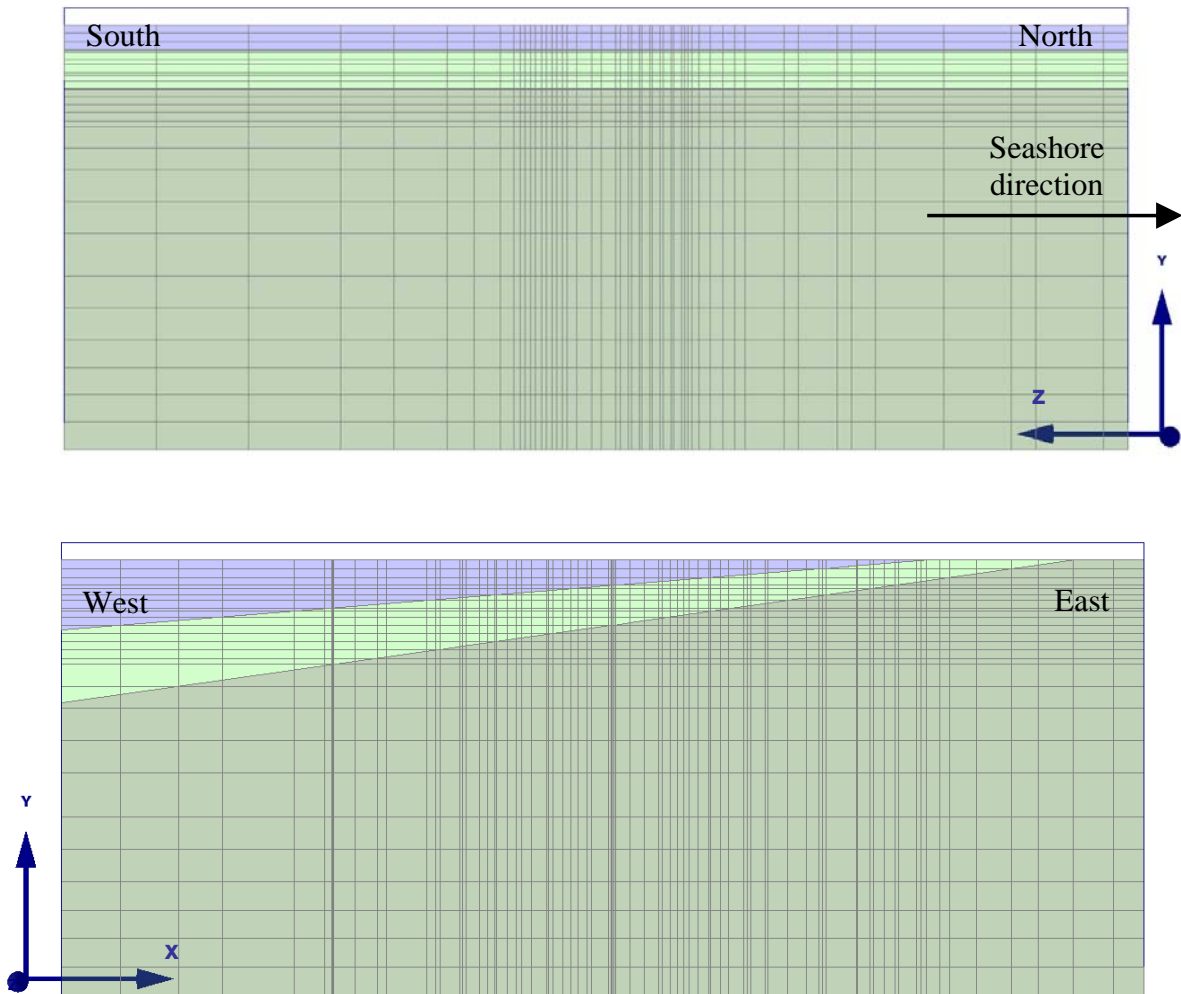


Figure 15: FEM model: longitudinal and transversal sections of the initial mesh: North-South direction (above) and East-West direction (below)

		Ponte sullo Stretto di Messina PROGETTO DEFINITIVO	
Calabria Anchor Block – evaluation of block behaviour via 3D FE analyses and of bearing capacity, Annex	Codice documento PF0067_F0_ANX	Rev F0	Data 20-06-2011

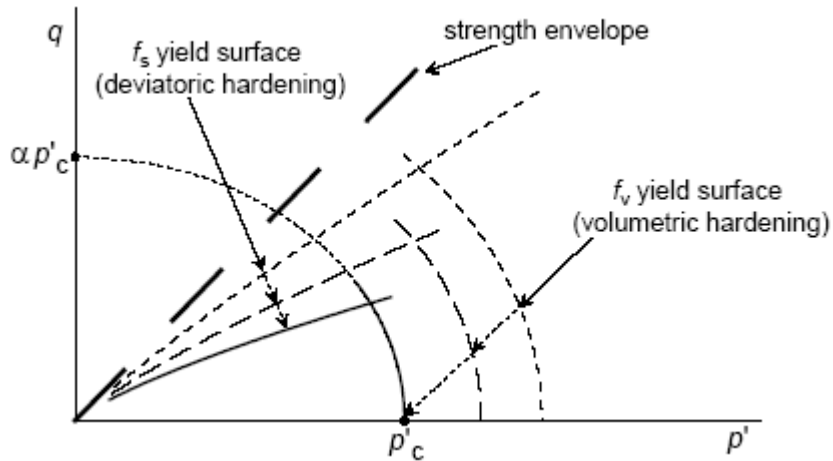


Figure 16: Yield surfaces of the Hardening Soil model and their evolution

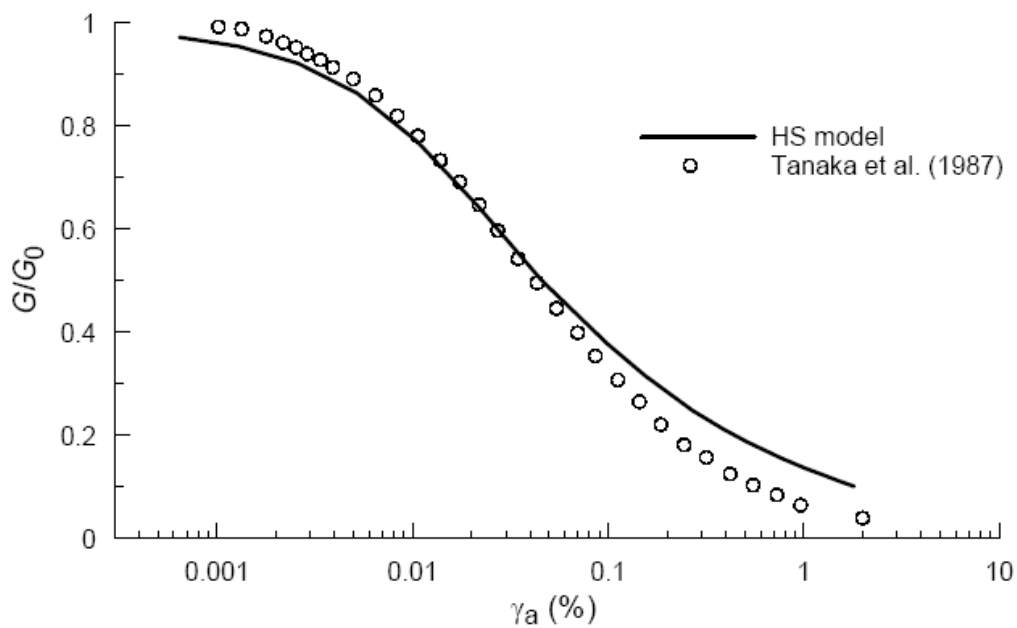


Figure 17: Comparison between the stiffness decay observed by Tanaka et al (1987) and computed by HS model

		Ponte sullo Stretto di Messina PROGETTO DEFINITIVO	
Calabria Anchor Block – evaluation of block behaviour via 3D FE analyses and of bearing capacity, Annex	<i>Codice documento</i> PF0067_F0_ANX	<i>Rev</i> F0	<i>Data</i> 20-06-2011

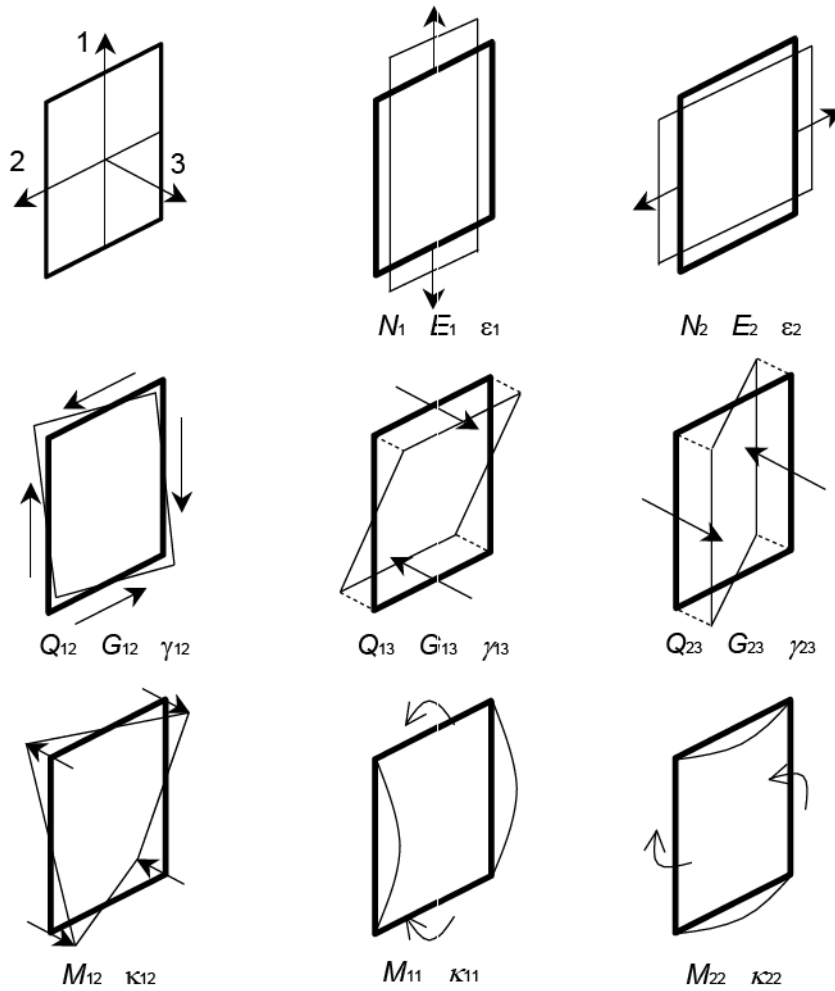


Figure 18: WALL elements in Plaxis 3D Foundation

		Ponte sullo Stretto di Messina PROGETTO DEFINITIVO	
Calabria Anchor Block – evaluation of block behaviour via 3D FE analyses and of bearing capacity, Annex	<i>Codice documento</i> PF0067_F0_ANX	<i>Rev</i> F0	<i>Data</i> 20-06-2011

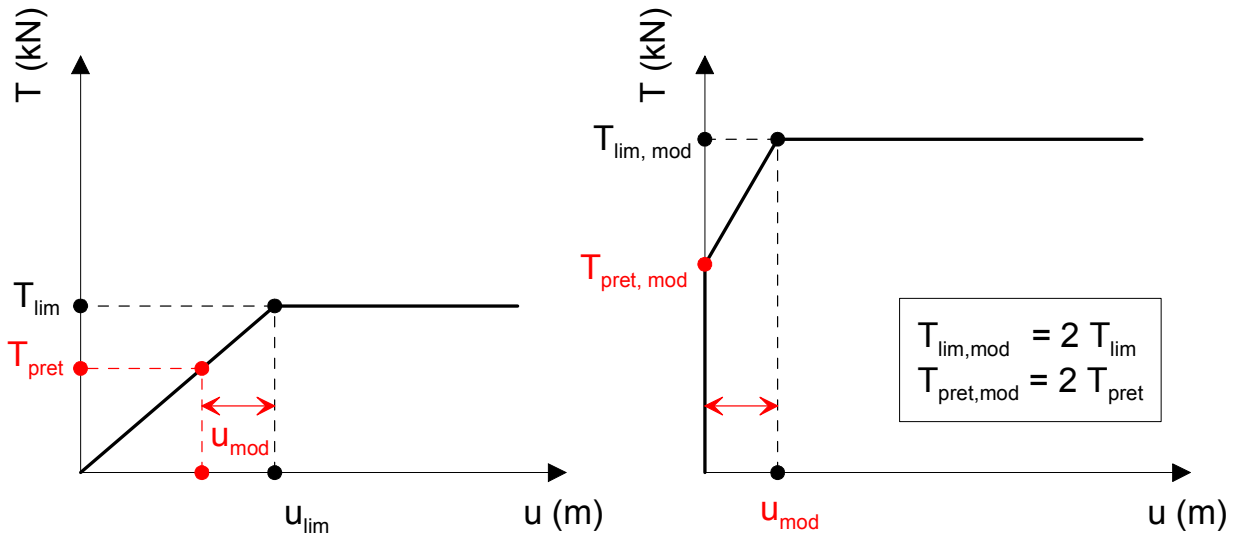


Figure 19: SPRINGS elements: non linear stiffness and (T-u) relation for the pre-tensioned springs in the model

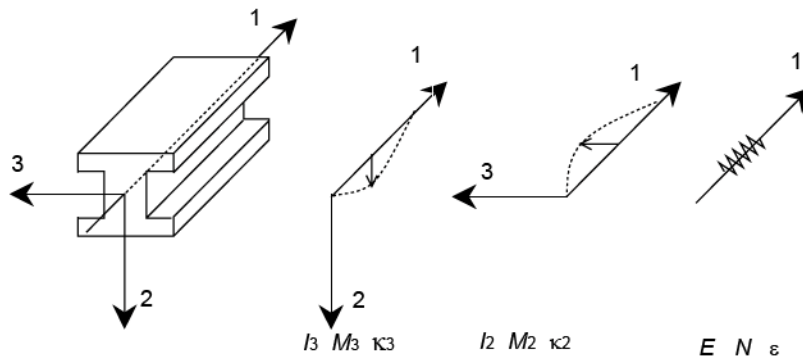


Figure 20: Horizontal BEAM elements in Plaxis 3D Foundation

		<p align="center">Ponte sullo Stretto di Messina PROGETTO DEFINITIVO</p>	
Calabria Anchor Block – evaluation of block behaviour via 3D FE analyses and of bearing capacity, Annex	Codice documento PF0067_F0_ANX	Rev F0	Data 20-06-2011

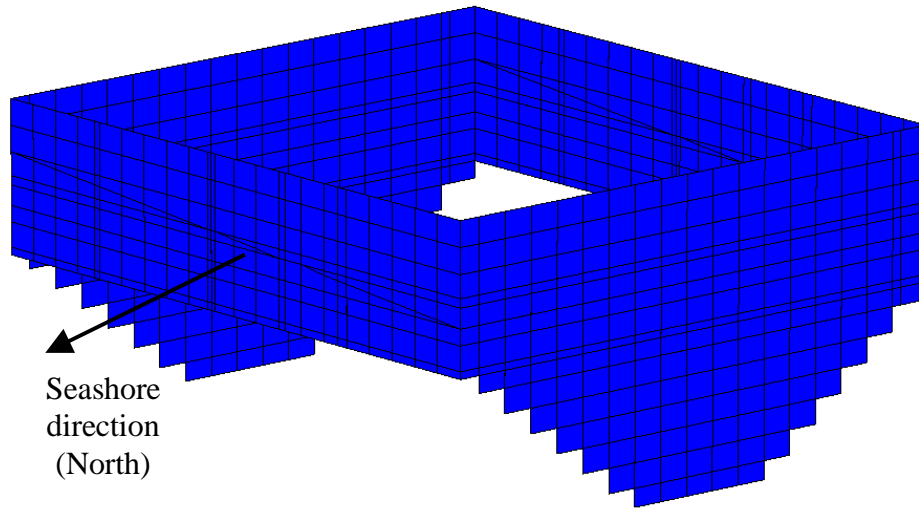


Figure 21: retaining walls: axonometric view

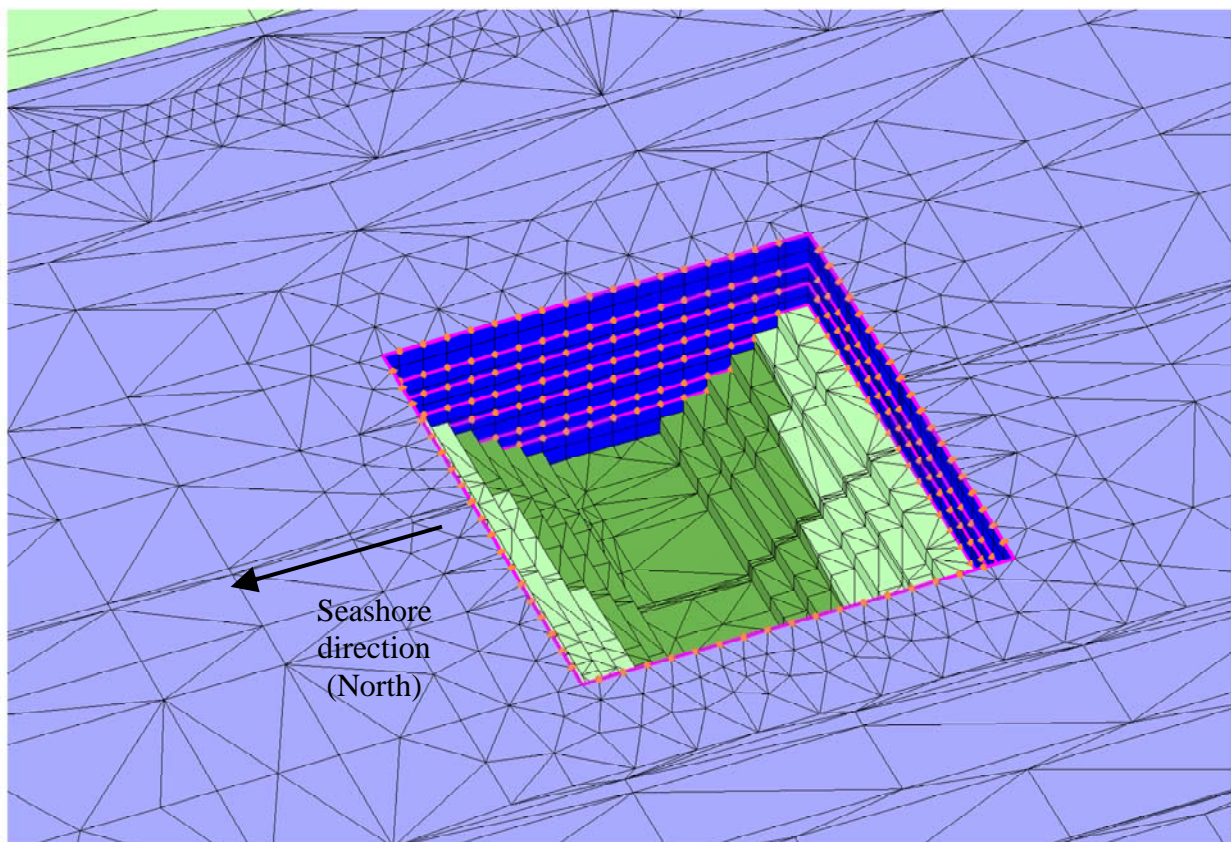


Figure 22: fully completed excavation step: axonometric view

		Ponte sullo Stretto di Messina PROGETTO DEFINITIVO		
Calabria Anchor Block – evaluation of block behaviour via 3D FE analyses and of bearing capacity, Annex	<i>Codice documento</i> PF0067_F0_ANX	<i>Rev</i> F0	<i>Data</i> 20-06-2011	

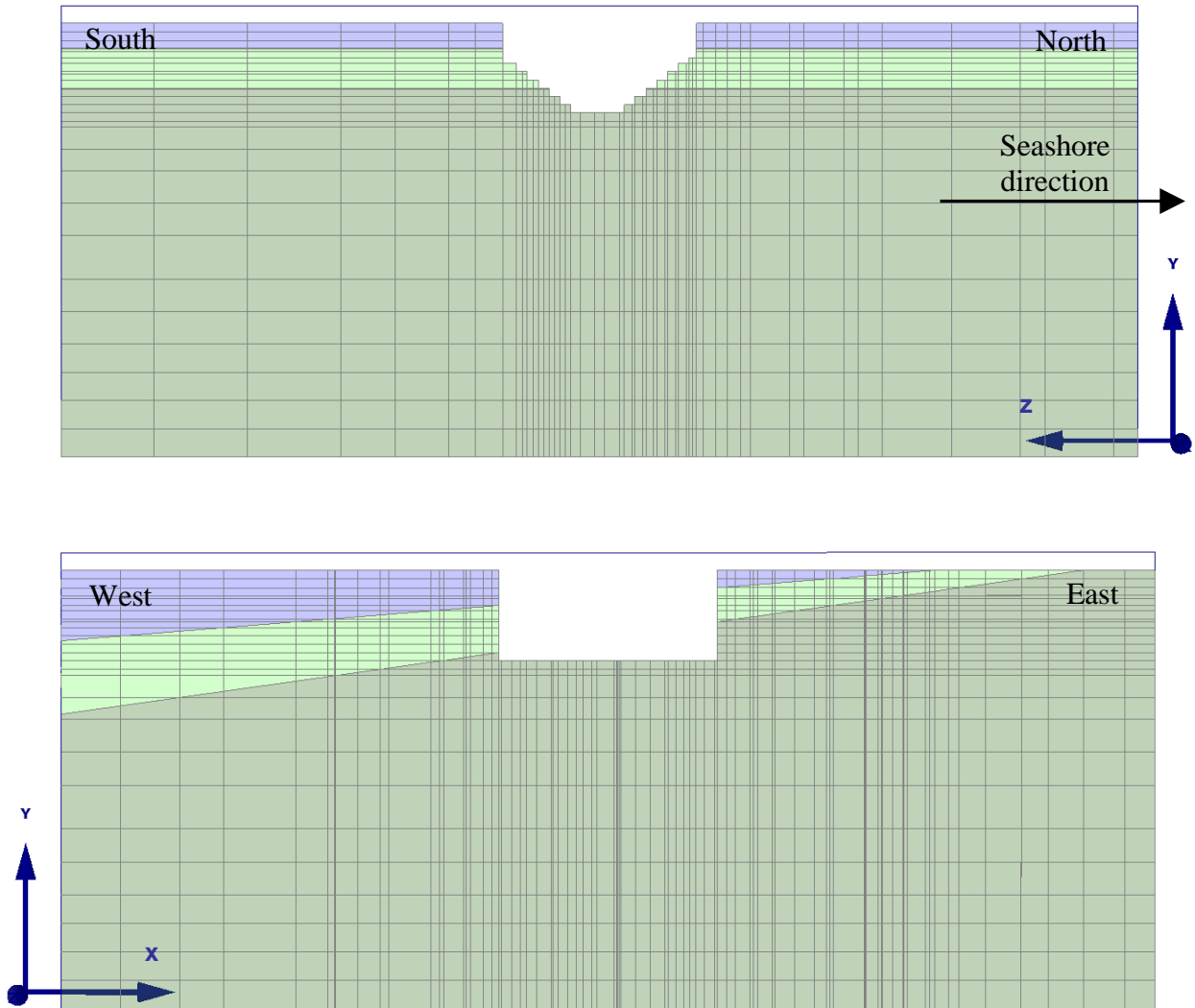


Figure 23: fully completed excavation: sections in the North-South direction (above) and in the East-West direction (below)

		Ponte sullo Stretto di Messina PROGETTO DEFINITIVO		
Calabria Anchor Block – evaluation of block behaviour via 3D FE analyses and of bearing capacity, Annex	<i>Codice documento</i> PF0067_F0_ANX	<i>Rev</i> F0	<i>Data</i> 20-06-2011	

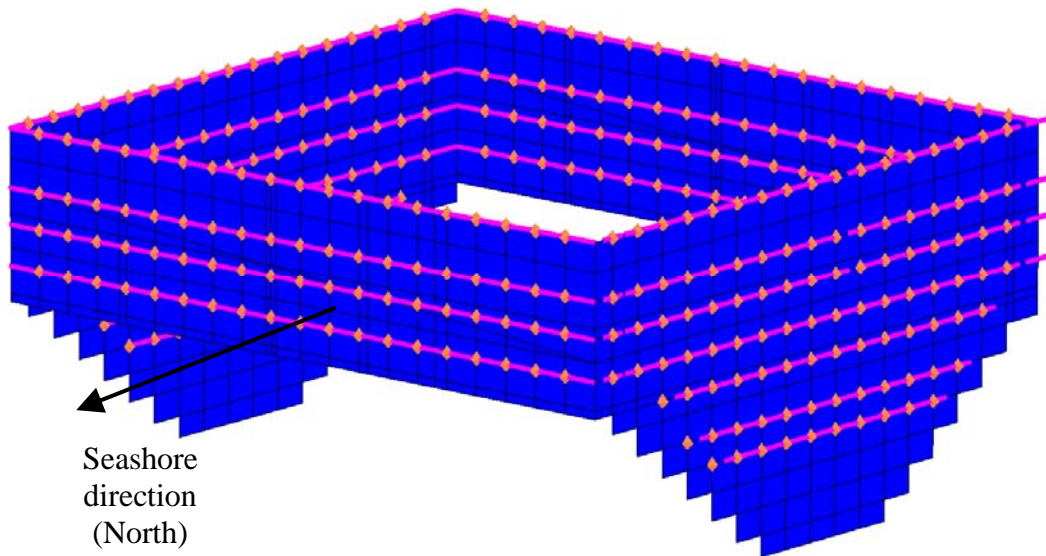


Figure 24: fully completed excavation: axonometric view of the retaining walls, retaining anchors and connection beams

		<p align="center">Ponte sullo Stretto di Messina PROGETTO DEFINITIVO</p>	
Calabria Anchor Block – evaluation of block behaviour via 3D FE analyses and of bearing capacity, Annex	<i>Codice documento</i> PF0067_F0_ANX	<i>Rev</i> F0	<i>Data</i> 20-06-2011

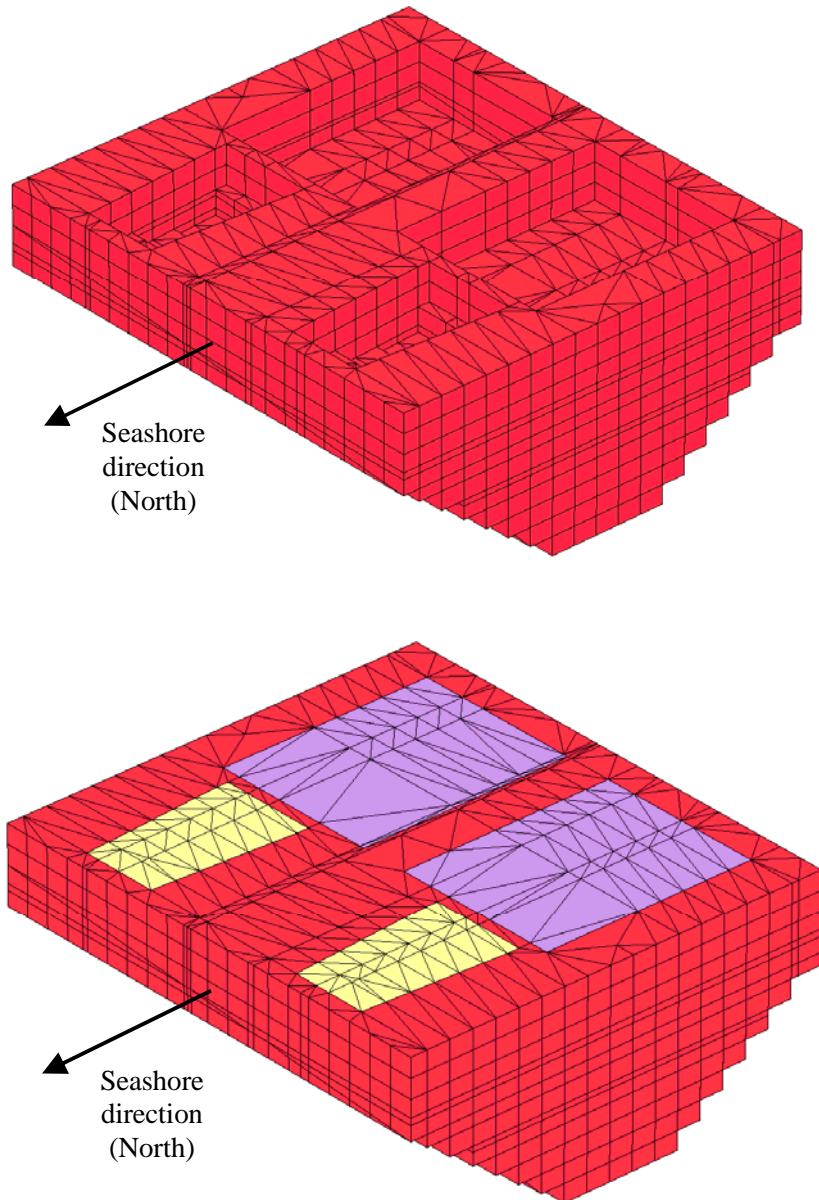


Figure 25: Anchor block model: axonometric view before chambers filling (above) and after chambers filling (below)

		Ponte sullo Stretto di Messina PROGETTO DEFINITIVO		
Calabria Anchor Block – evaluation of block behaviour via 3D FE analyses and of bearing capacity, Annex	<i>Codice documento</i> PF0067_F0_ANX	<i>Rev</i> F0	<i>Data</i> 20-06-2011	

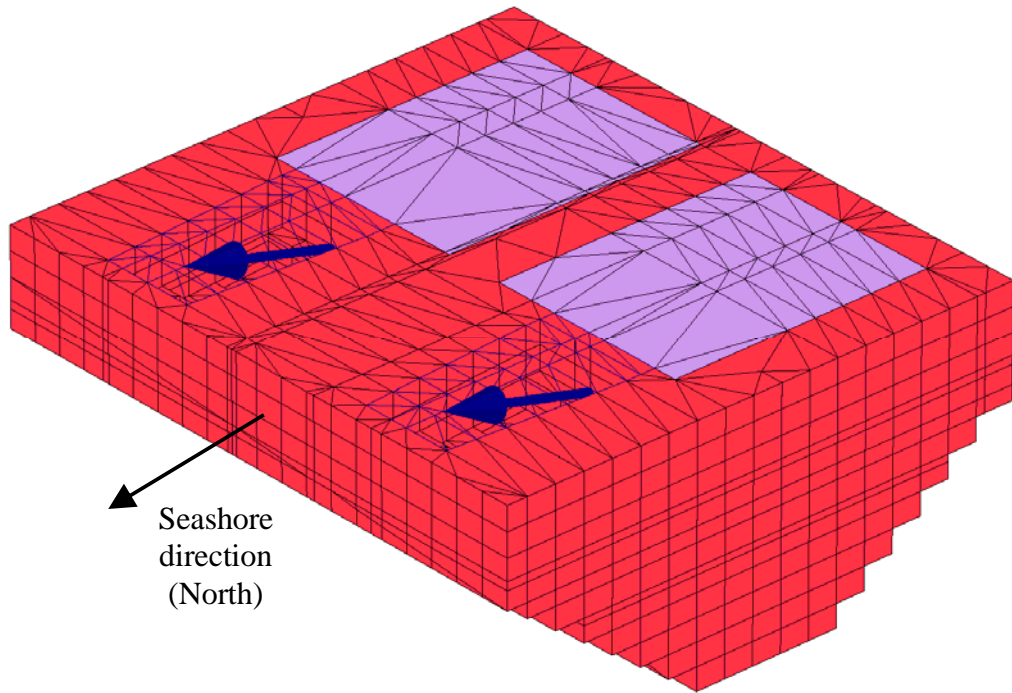


Figure 26: Anchor block model: axonometric view of the external force application

		Ponte sullo Stretto di Messina PROGETTO DEFINITIVO		
Calabria Anchor Block – evaluation of block behaviour via 3D FE analyses and of bearing capacity, Annex	<i>Codice documento</i> PF0067_F0_ANX	<i>Rev</i> F0	<i>Data</i> 20-06-2011	

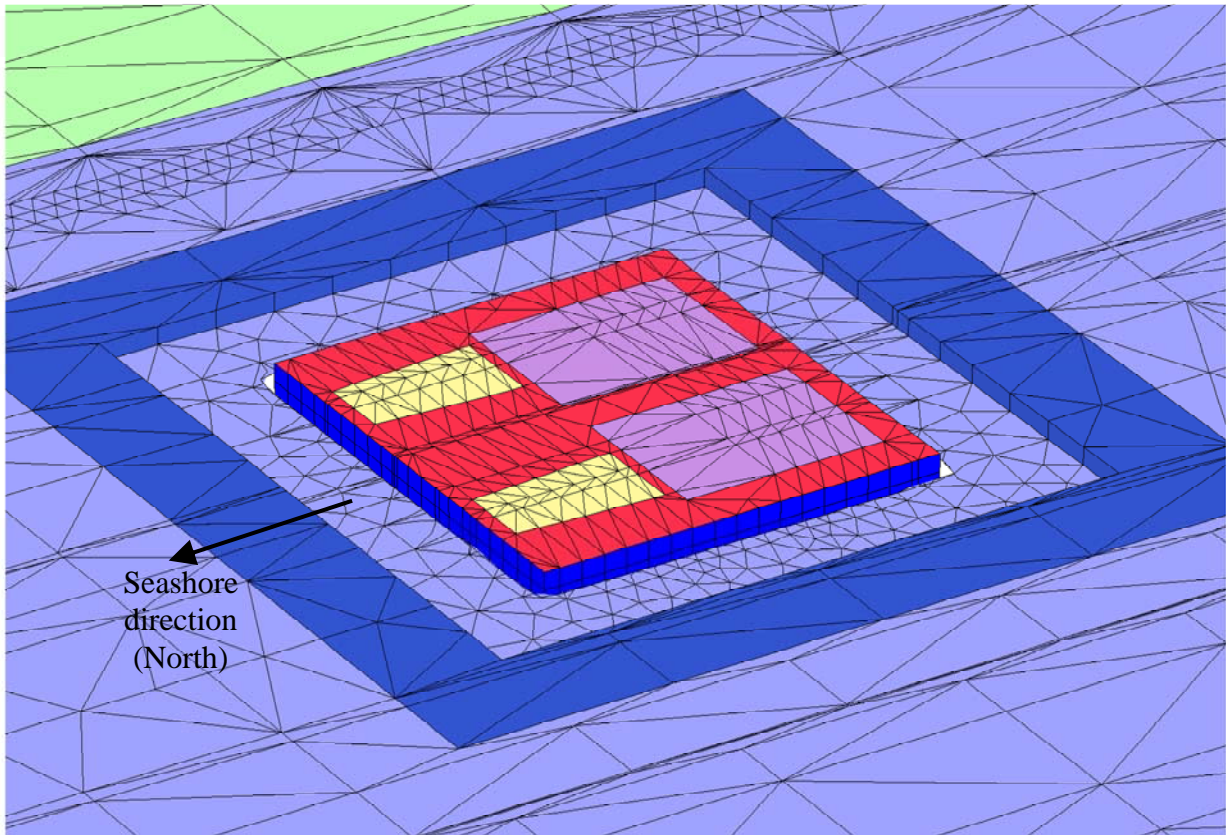


Figure 27: Comparative analysis: axonometric view of the 4 m deep excavation around the block

		<p align="center">Ponte sullo Stretto di Messina PROGETTO DEFINITIVO</p>	
Calabria Anchor Block – evaluation of block behaviour via 3D FE analyses and of bearing capacity, Annex	Codice documento PF0067_F0_ANX	Rev F0	Data 20-06-2011

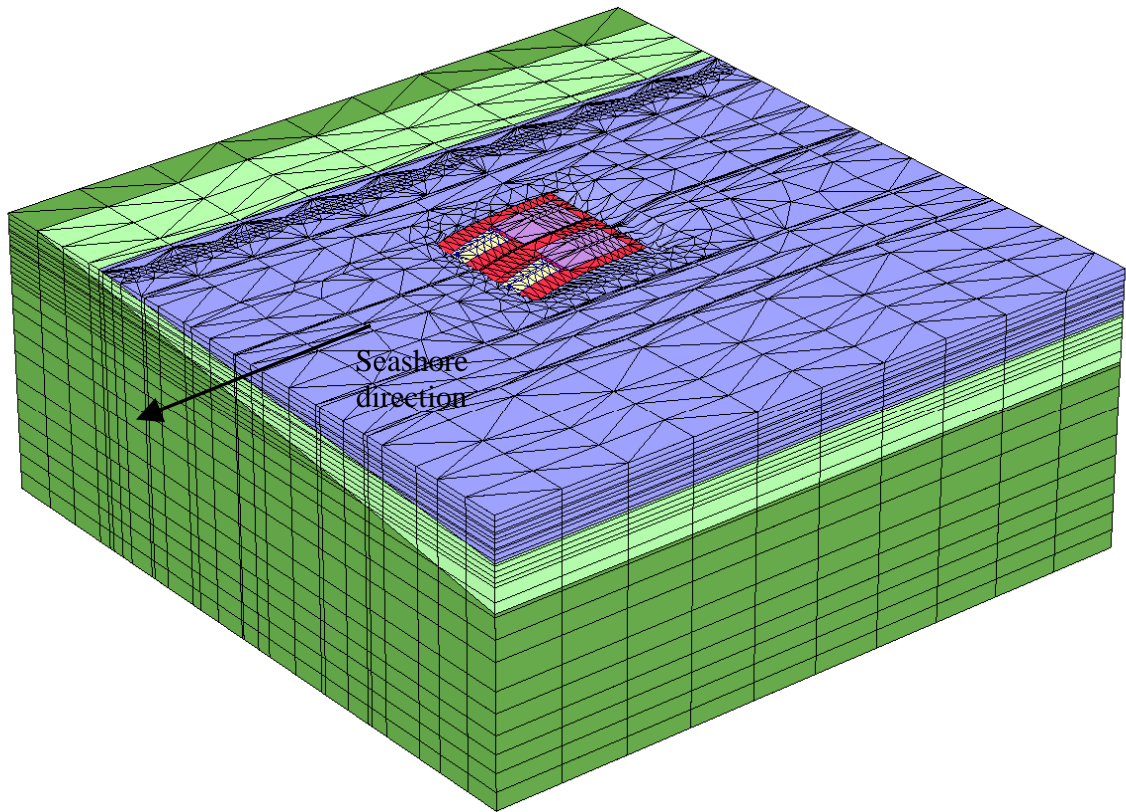


Figure 28: deformed mesh at the application of the ULS load (displacements scaled up 2000 times)

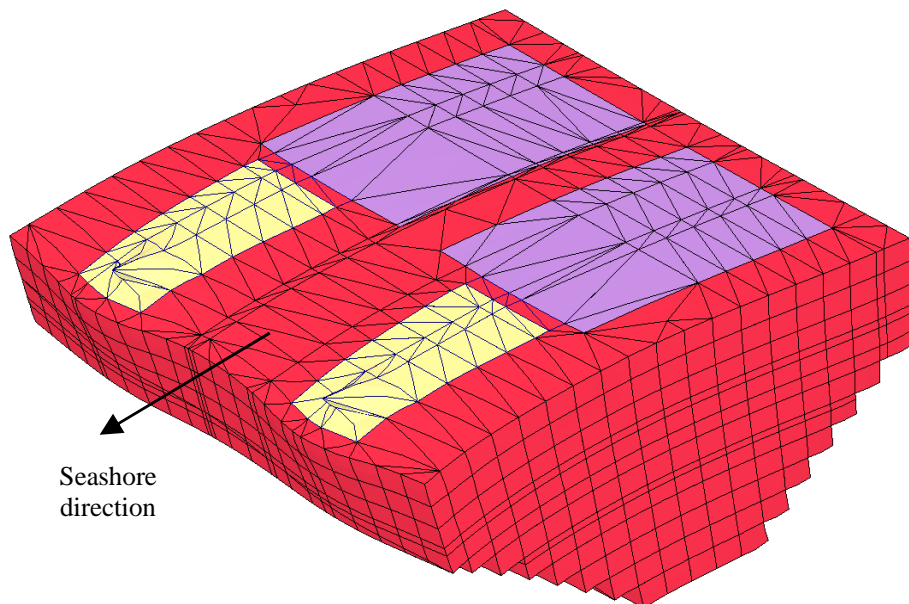


Figure 29: anchor block deformed mesh at the application of the ULS load (displacements scaled up 2000 times)

 Stretto di Messina		Ponte sullo Stretto di Messina PROGETTO DEFINITIVO		
Calabria Anchor Block – evaluation of block behaviour via 3D FE analyses and of bearing capacity, Annex		Codice documento PF0067_F0_ANX	Rev F0	Data 20-06-2011

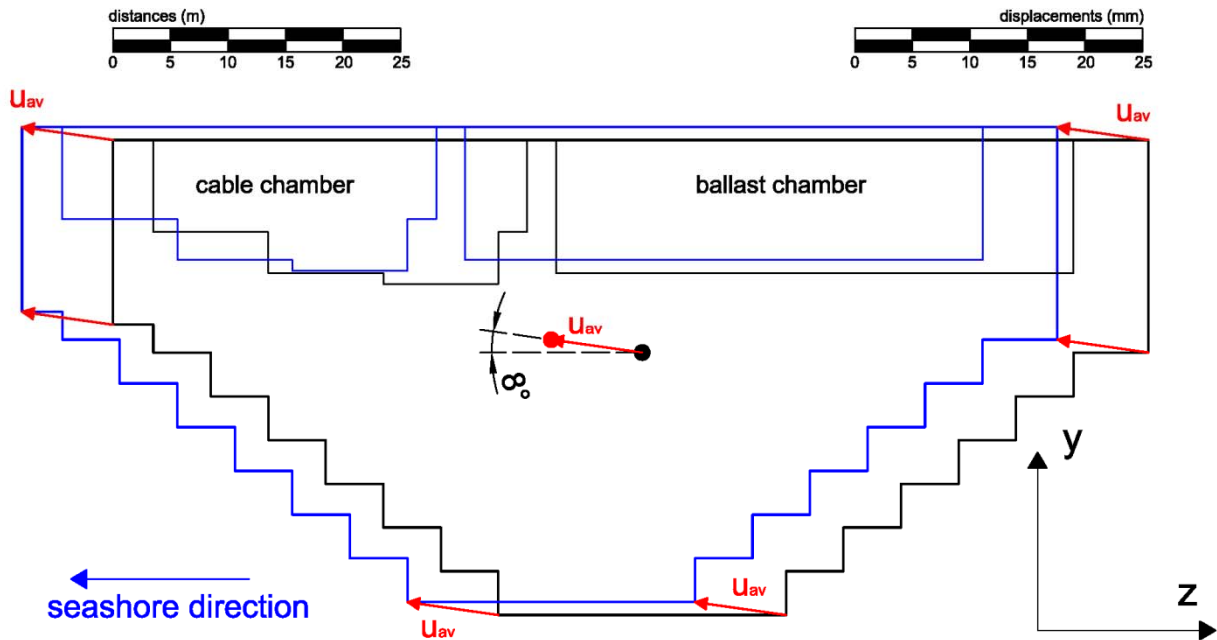


Figure 30: anchor block section: translational mechanism at the application of the ULS load (displacements scaled up 1000 times)

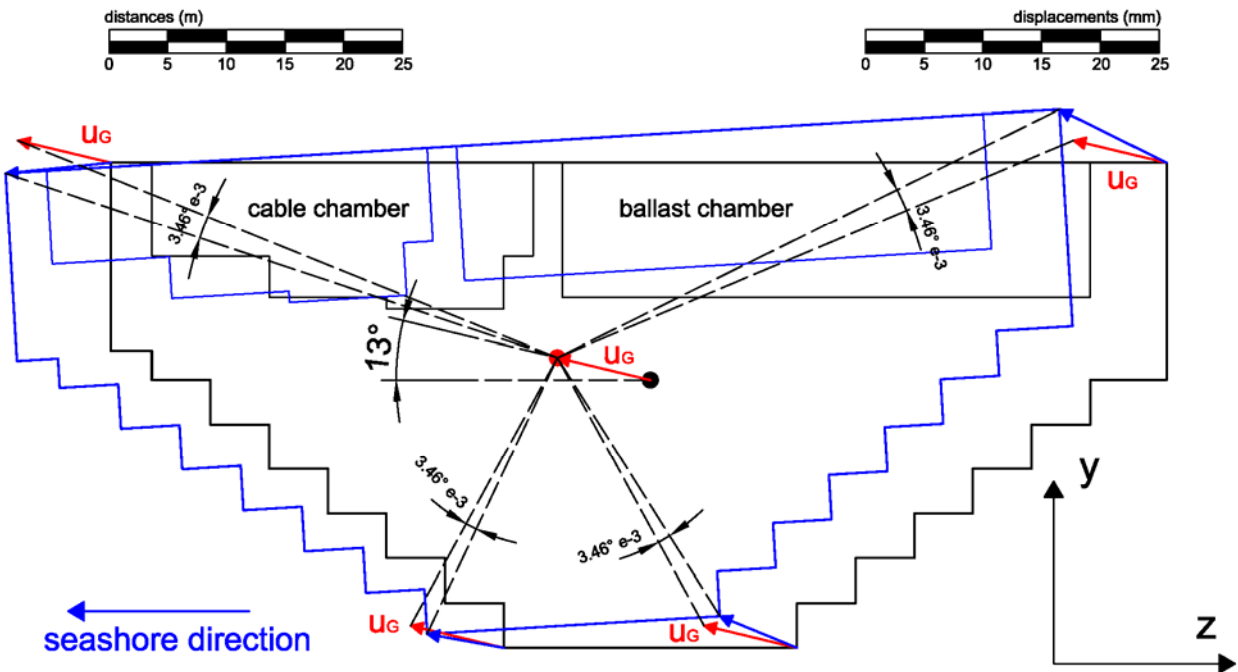


Figure 31: anchor block section: roto-translational mechanism at the application of the ULS load

		Ponte sullo Stretto di Messina PROGETTO DEFINITIVO	
Calabria Anchor Block – evaluation of block behaviour via 3D FE analyses and of bearing capacity, Annex	<i>Codice documento</i> PF0067_F0_ANX	<i>Rev</i> F0	<i>Data</i> 20-06-2011

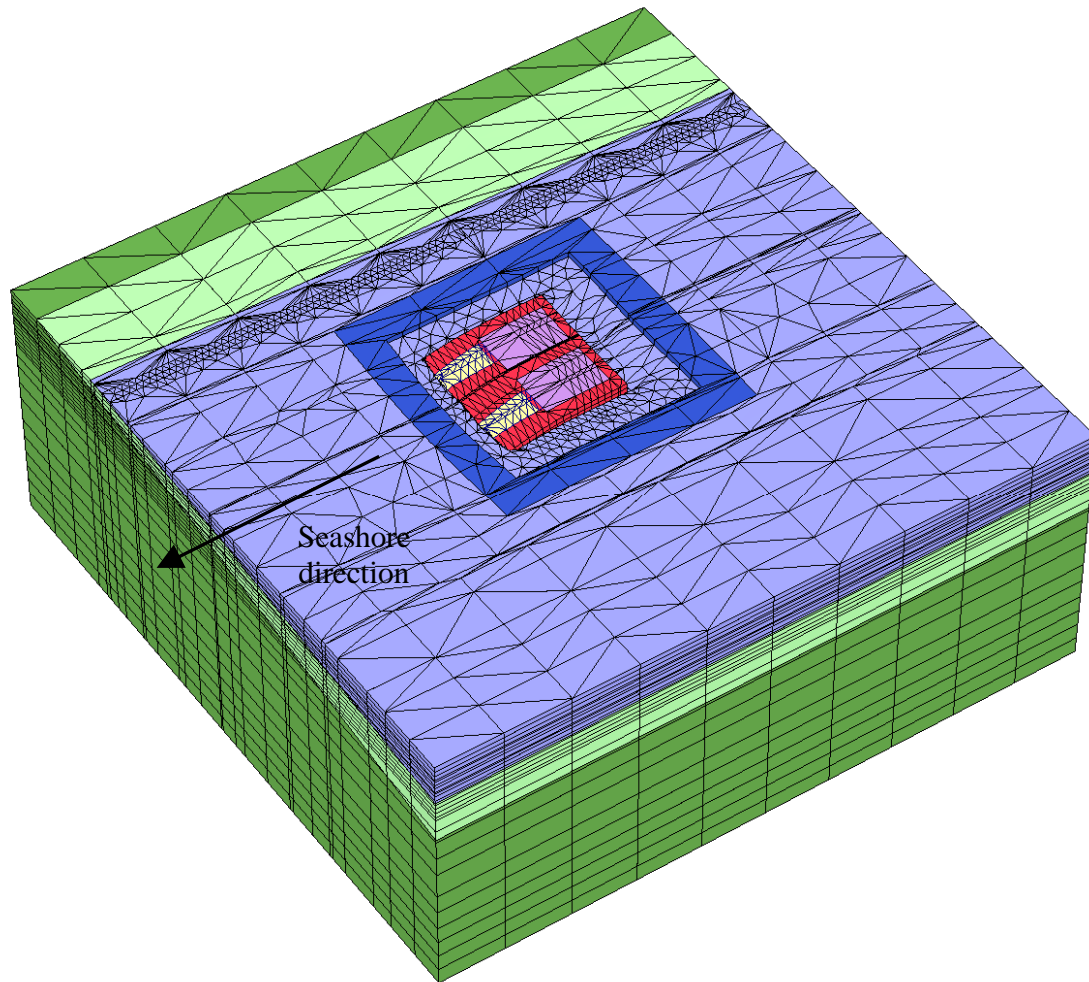


Figure 32: comparison analysis - deformed mesh at the application of the ULS load (displacements scaled up 2000 times)

		Ponte sullo Stretto di Messina PROGETTO DEFINITIVO	
Calabria Anchor Block – evaluation of block behaviour via 3D FE analyses and of bearing capacity, Annex	Codice documento PF0067_F0_ANX	Rev F0	Data 20-06-2011

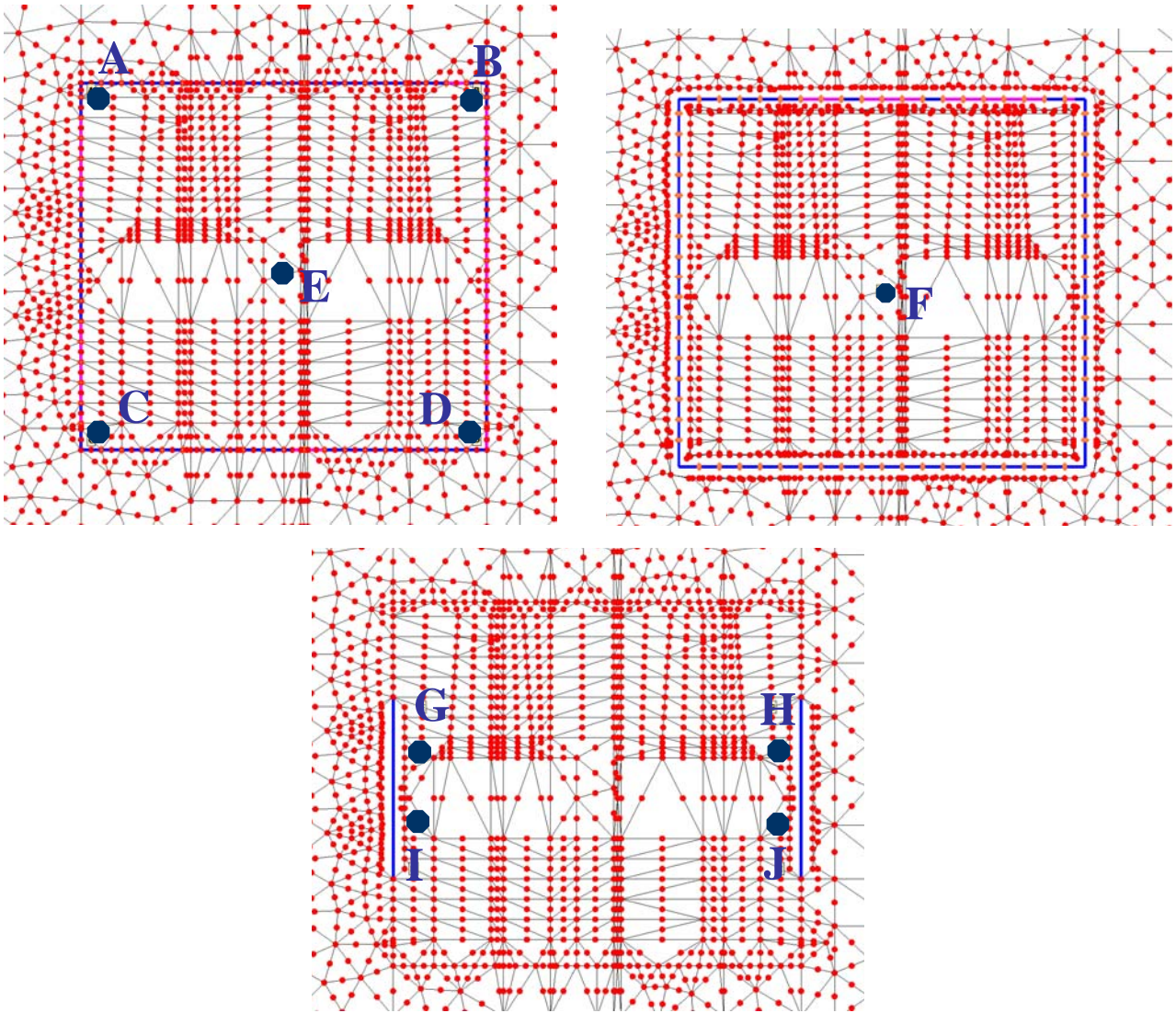


Figure 33: Position of selected nodes at elevation +118 m a.s.l. (above on the left), +95.65 m a.s.l. (above on the right) and +76.65 m a.s.l (below)

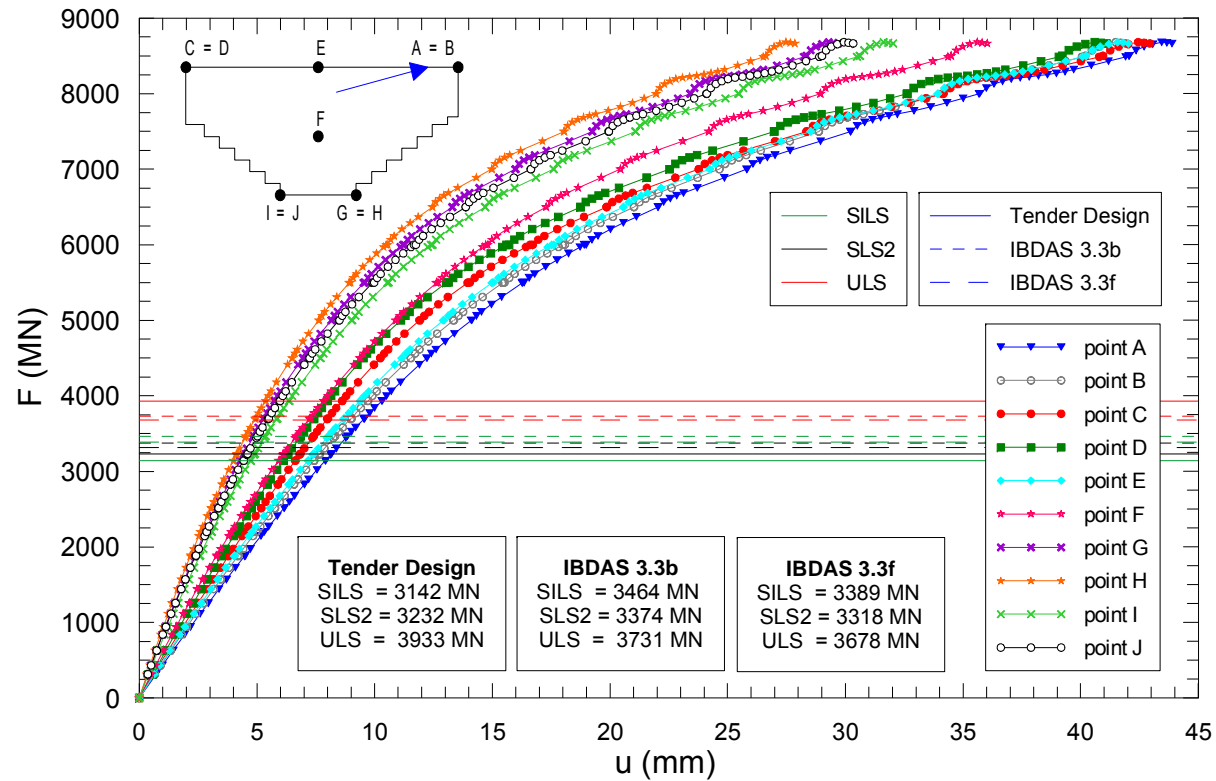


Figure 34: Analyses results: load-displacement curves for the selected points of the block

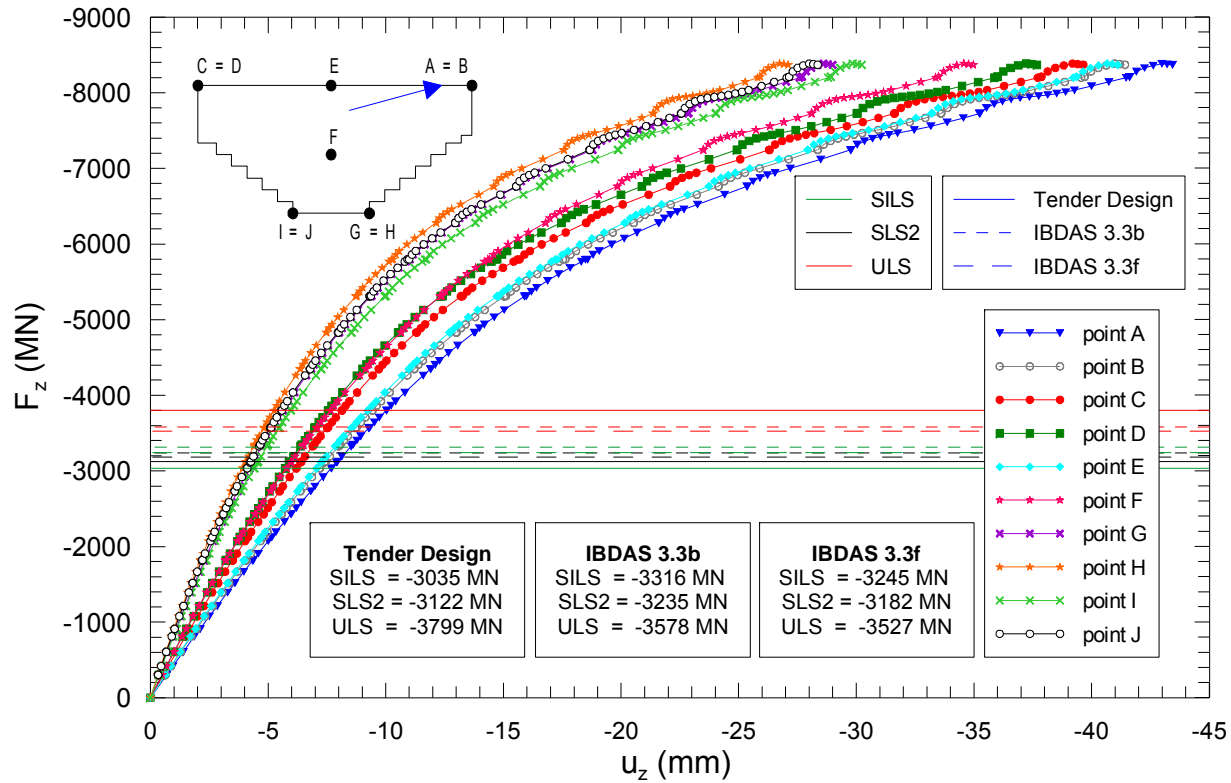


Figure 35: Analyses results: horizontal load-horizontal displacement curves for the selected points of the block (z-direction)

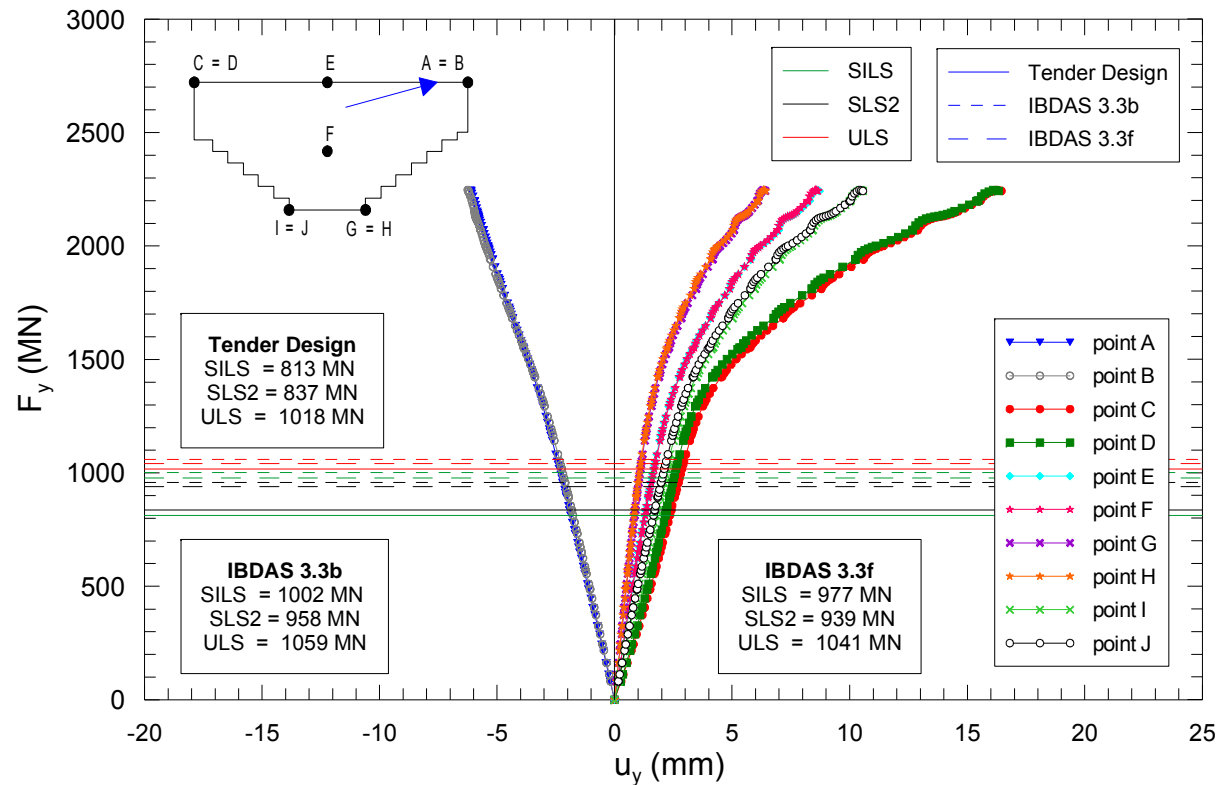


Figure 36: Analyses results: vertical load-horizontal displacement curves for the selected points of the block (y-direction)

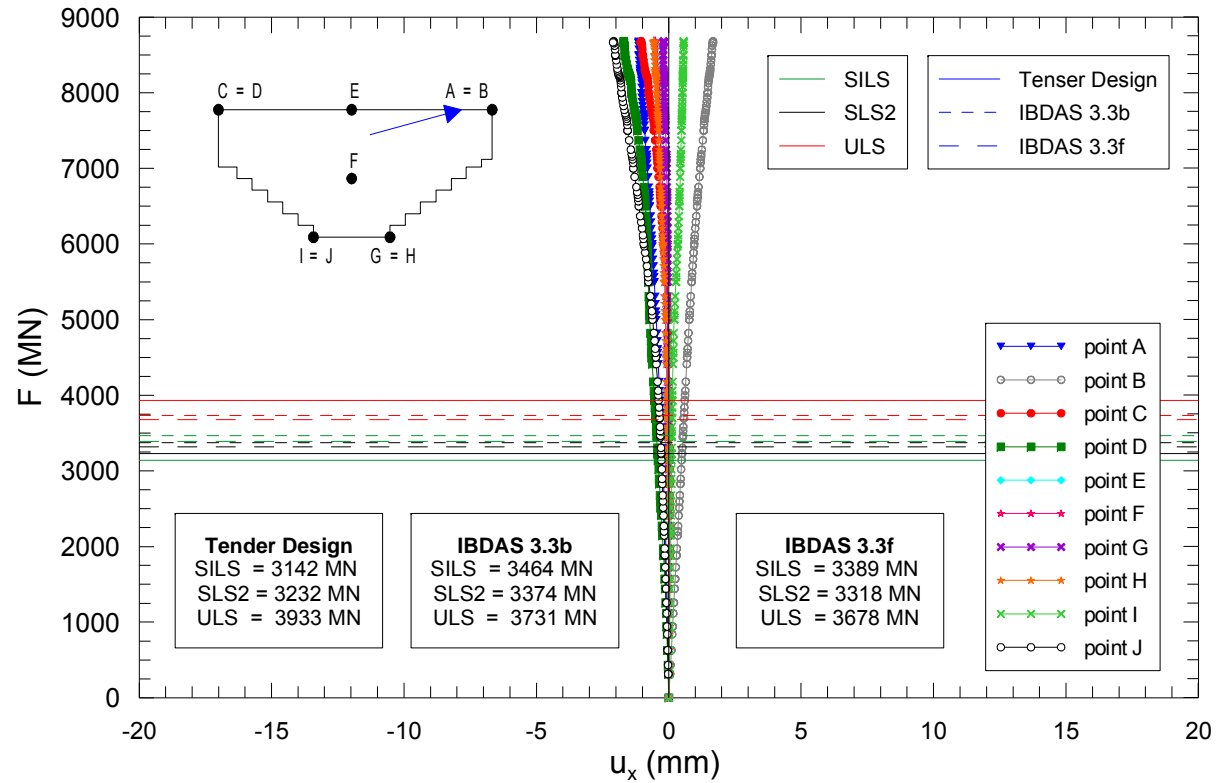


Figure 37: Analysis results: load-horizontal displacement curves for the selected points of the block (x-direction, orthogonal to the force)

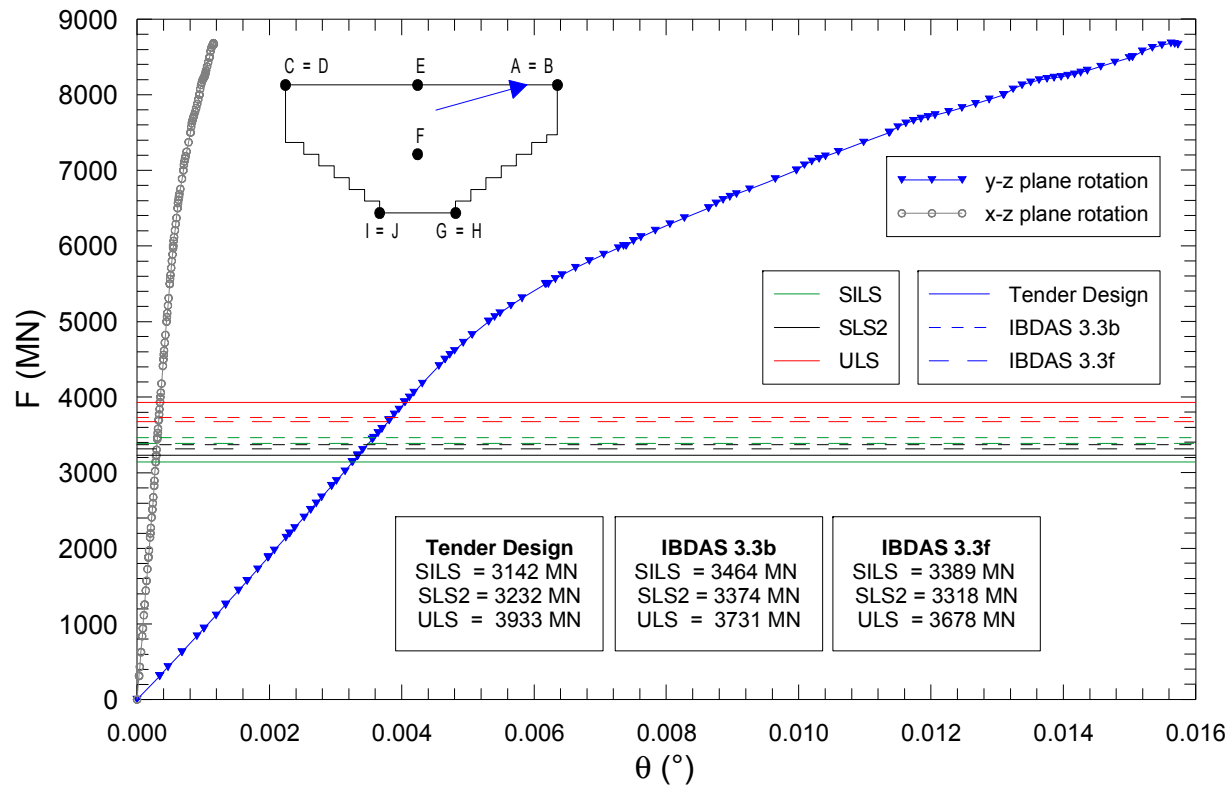


Figure 38: load-rotation angle curves in the y-z plane and in the x-z plane

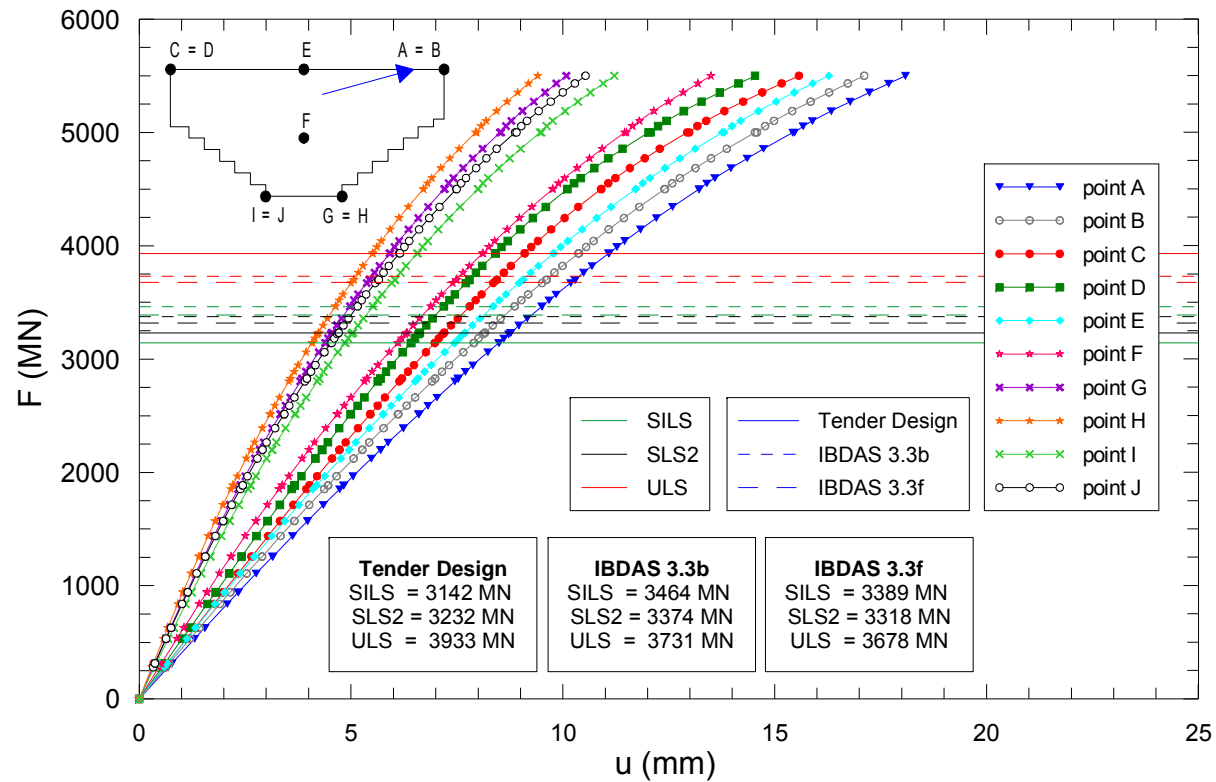


Figure 39: Comparison Analyses results: load-displacement curves for the selected points of the block

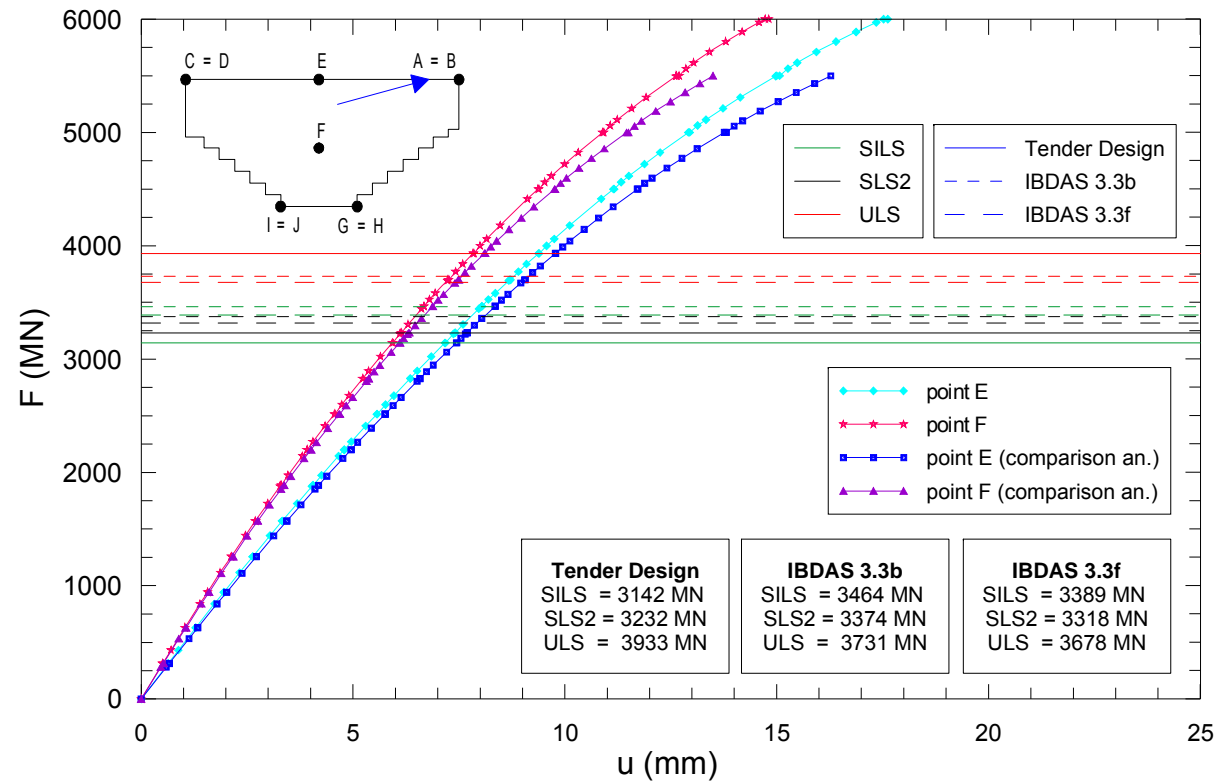


Figure 40: Points E and F: matching of the load-displacement curves for standard and comparison analyses (4 m deep excavation around the block)

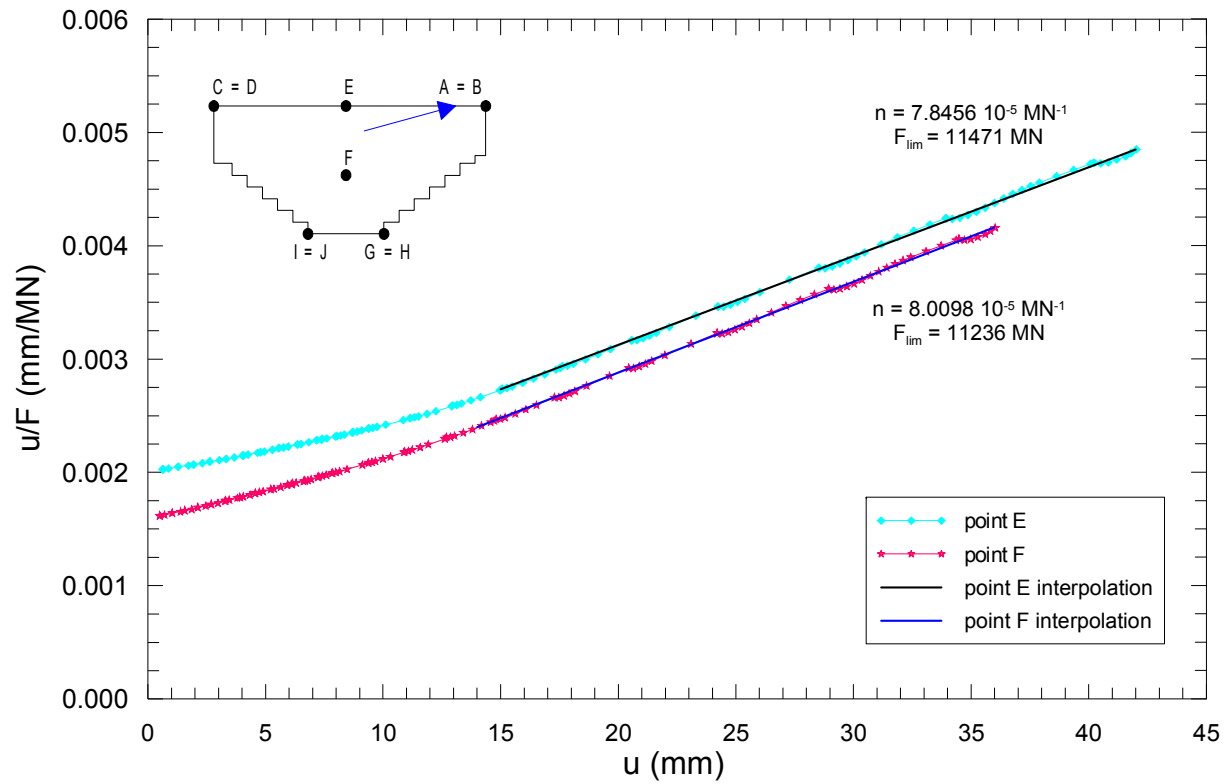


Figure 41: hyperbolic best-fitting of load-displacement data: ultimate load

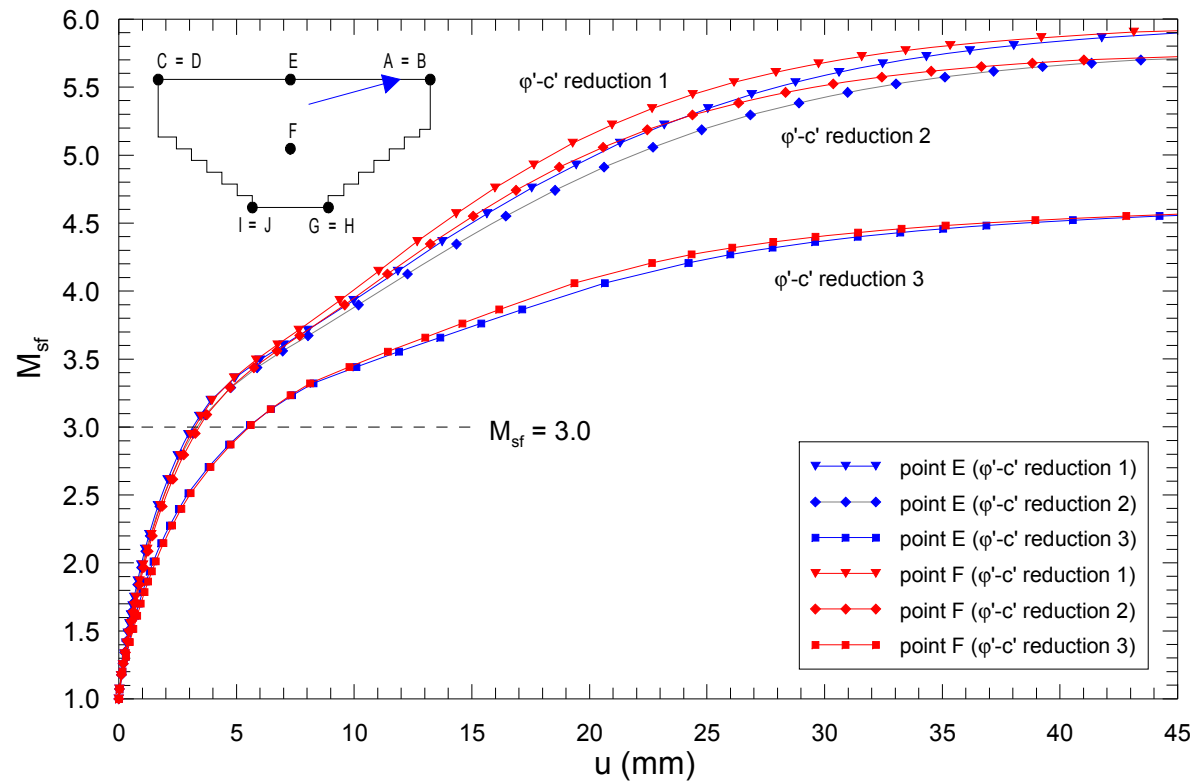


Figure 42: $\phi' - c'$ reduction analyses: M_{sf} -displacement curves (points E and F)

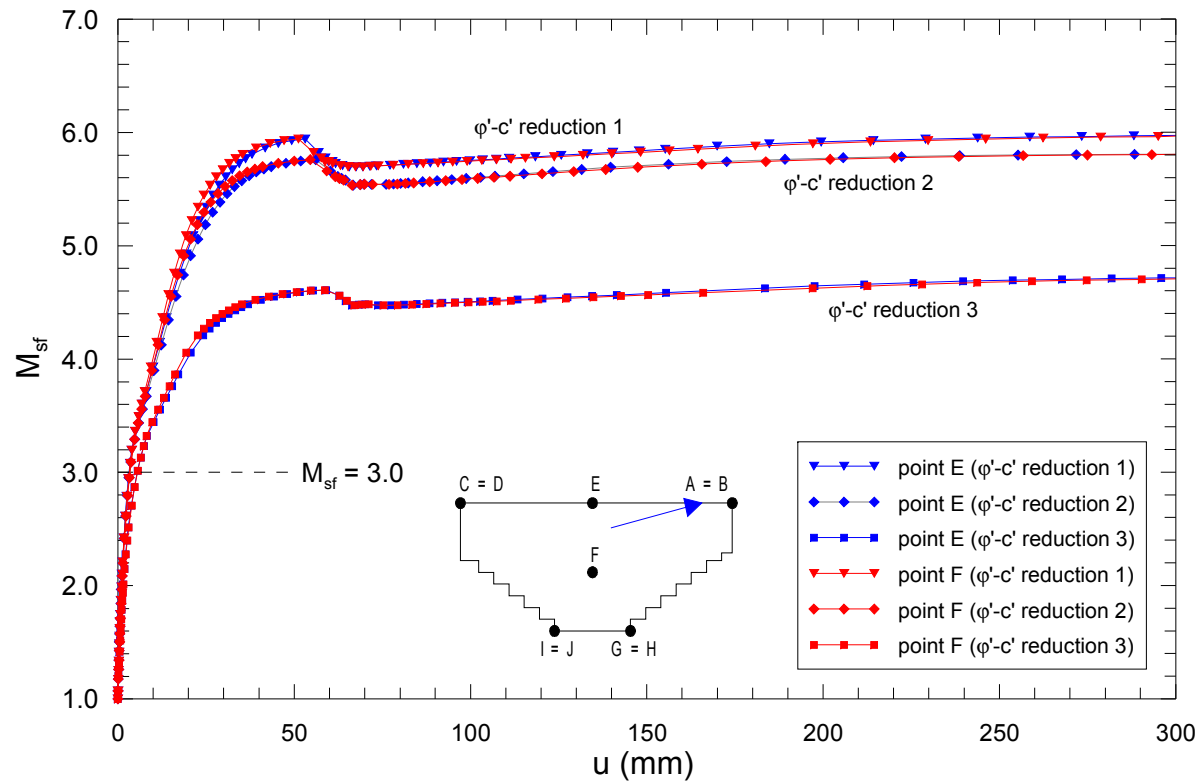


Figure 43: $\phi' - c'$ reduction analyses: M_{sf} -displacement curves (points E and F; larger view)

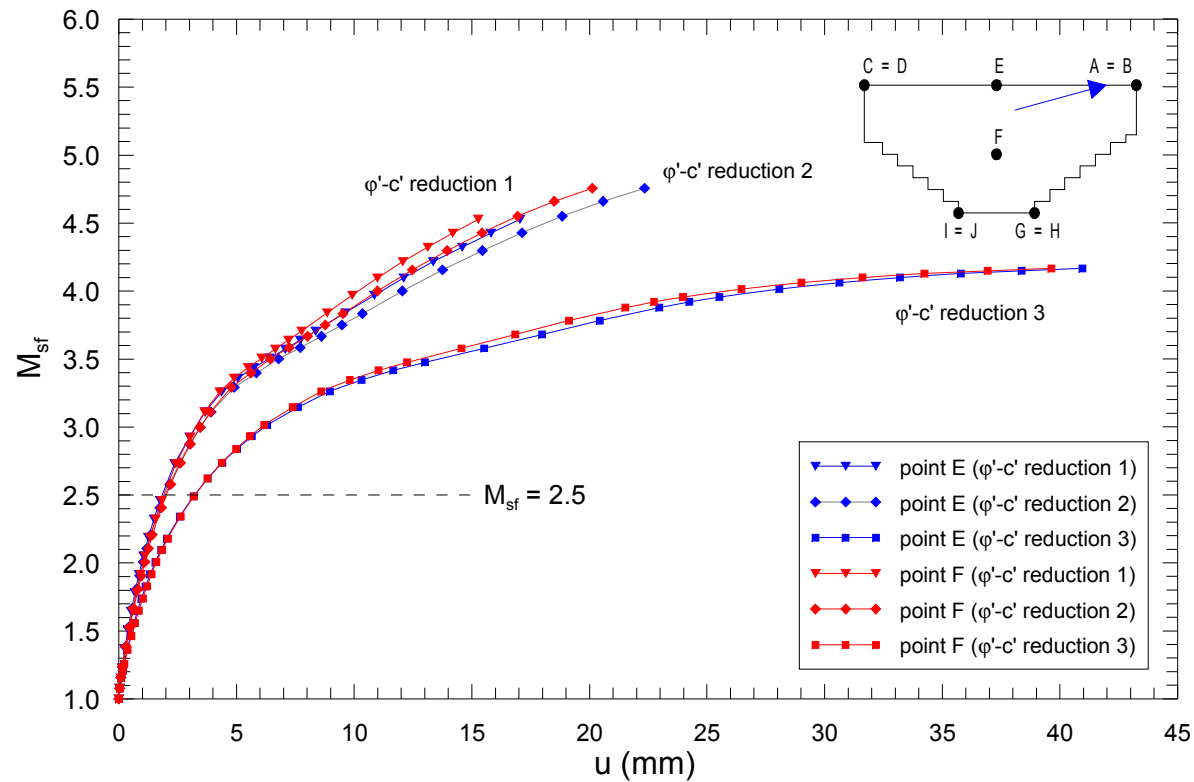


Figure 44: $\phi' - c'$ reduction analyses (4 m deep excavation around the block): M_{sf} -displacement curves (points E and F)

 Stretto di Messina		Ponte sullo Stretto di Messina PROGETTO DEFINITIVO		
Calabria Anchor Block – evaluation of block behaviour via 3D FE analyses and of bearing capacity, Annex	<i>Codice documento</i> PF0067_F0_ANX	<i>Rev</i> F0	<i>Data</i> 20-06-2011	

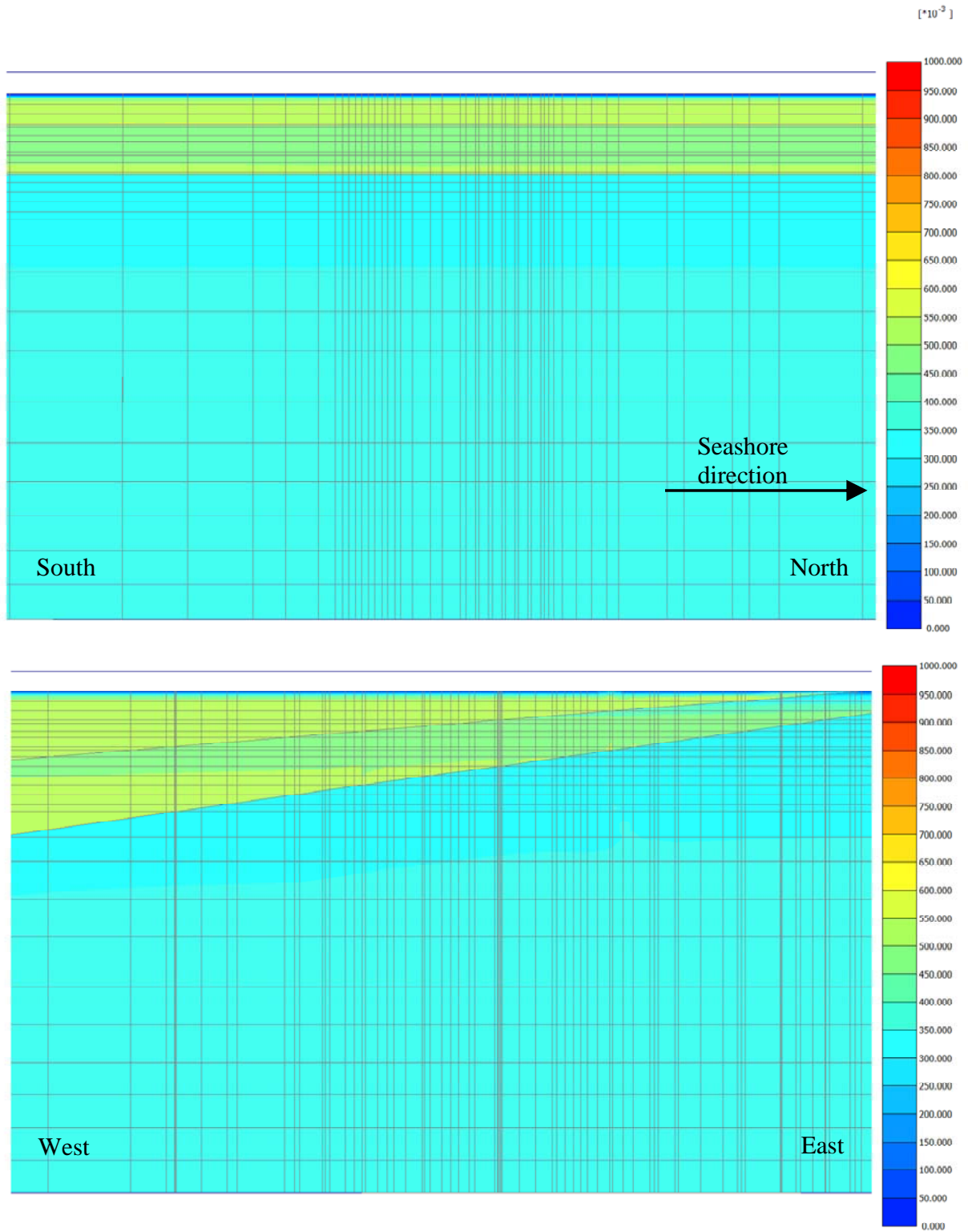


Figure 45: relative shear stress in the initial conditions along longitudinal and transversal sections

 Stretto di Messina		Ponte sullo Stretto di Messina PROGETTO DEFINITIVO		
Calabria Anchor Block – evaluation of block behaviour via 3D FE analyses and of bearing capacity, Annex	<i>Codice documento</i> PF0067_F0_ANX	<i>Rev</i> F0	<i>Data</i> 20-06-2011	

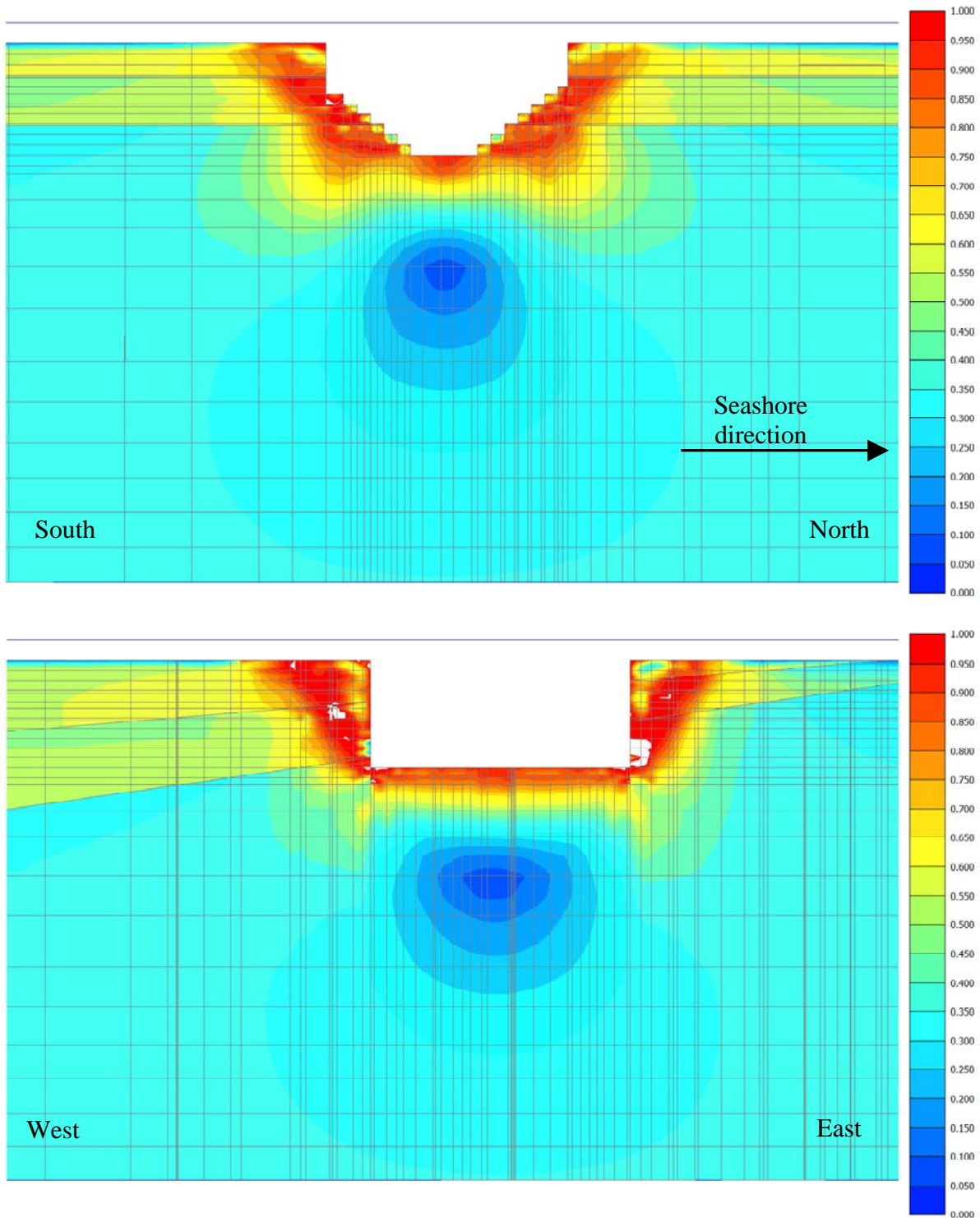


Figure 46: relative shear stress after full excavation along longitudinal and transversal sections

 Stretto di Messina		Ponte sullo Stretto di Messina PROGETTO DEFINITIVO		
Calabria Anchor Block – evaluation of block behaviour via 3D FE analyses and of bearing capacity, Annex	<i>Codice documento</i> PF0067_F0_ANX	<i>Rev</i> F0	<i>Data</i> 20-06-2011	

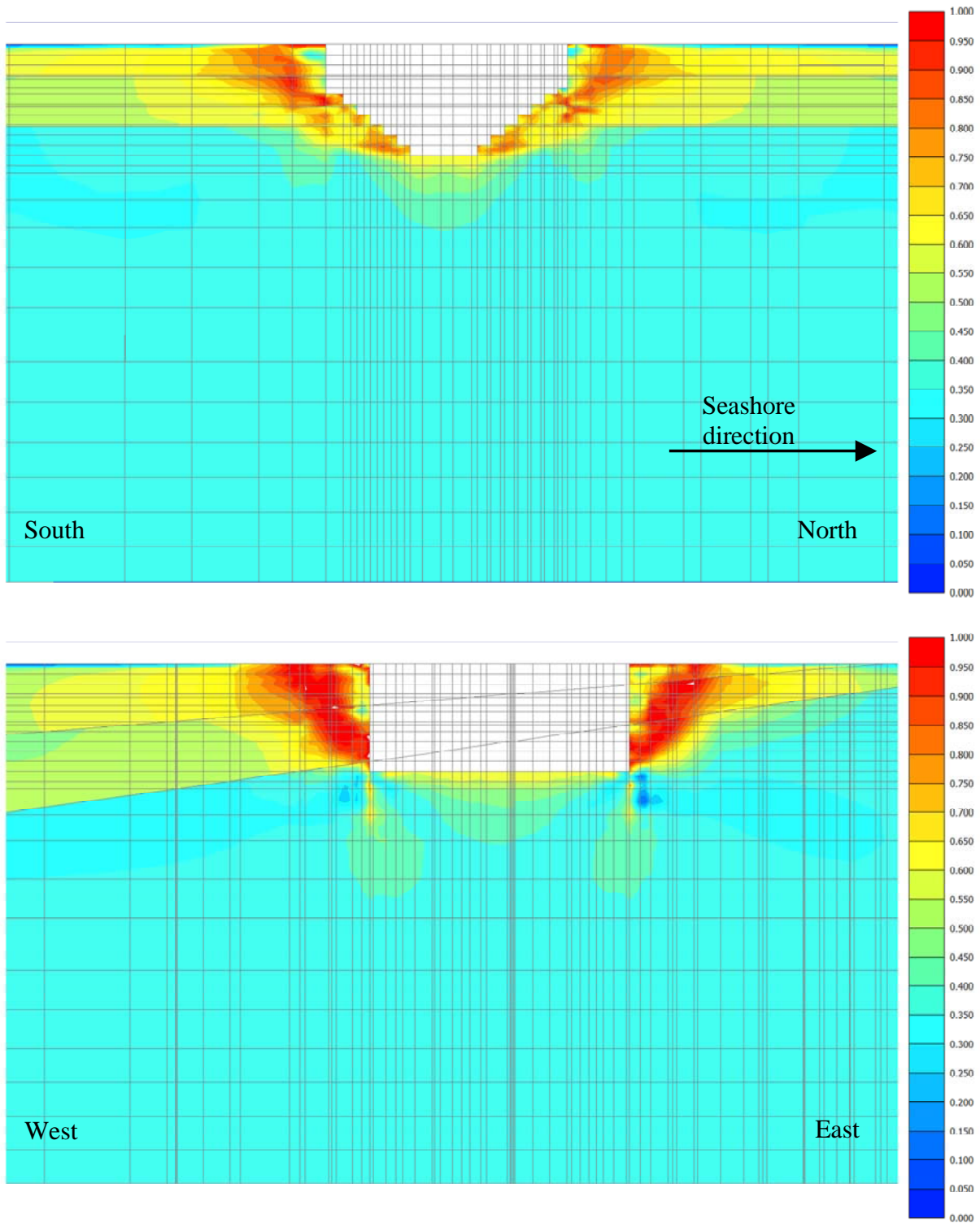


Figure 47: relative shear stress after block construction along longitudinal and transversal sections

 Stretto di Messina		Ponte sullo Stretto di Messina PROGETTO DEFINITIVO		
Calabria Anchor Block – evaluation of block behaviour via 3D FE analyses and of bearing capacity, Annex	<i>Codice documento</i> PF0067_F0_ANX	<i>Rev</i> F0	<i>Data</i> 20-06-2011	

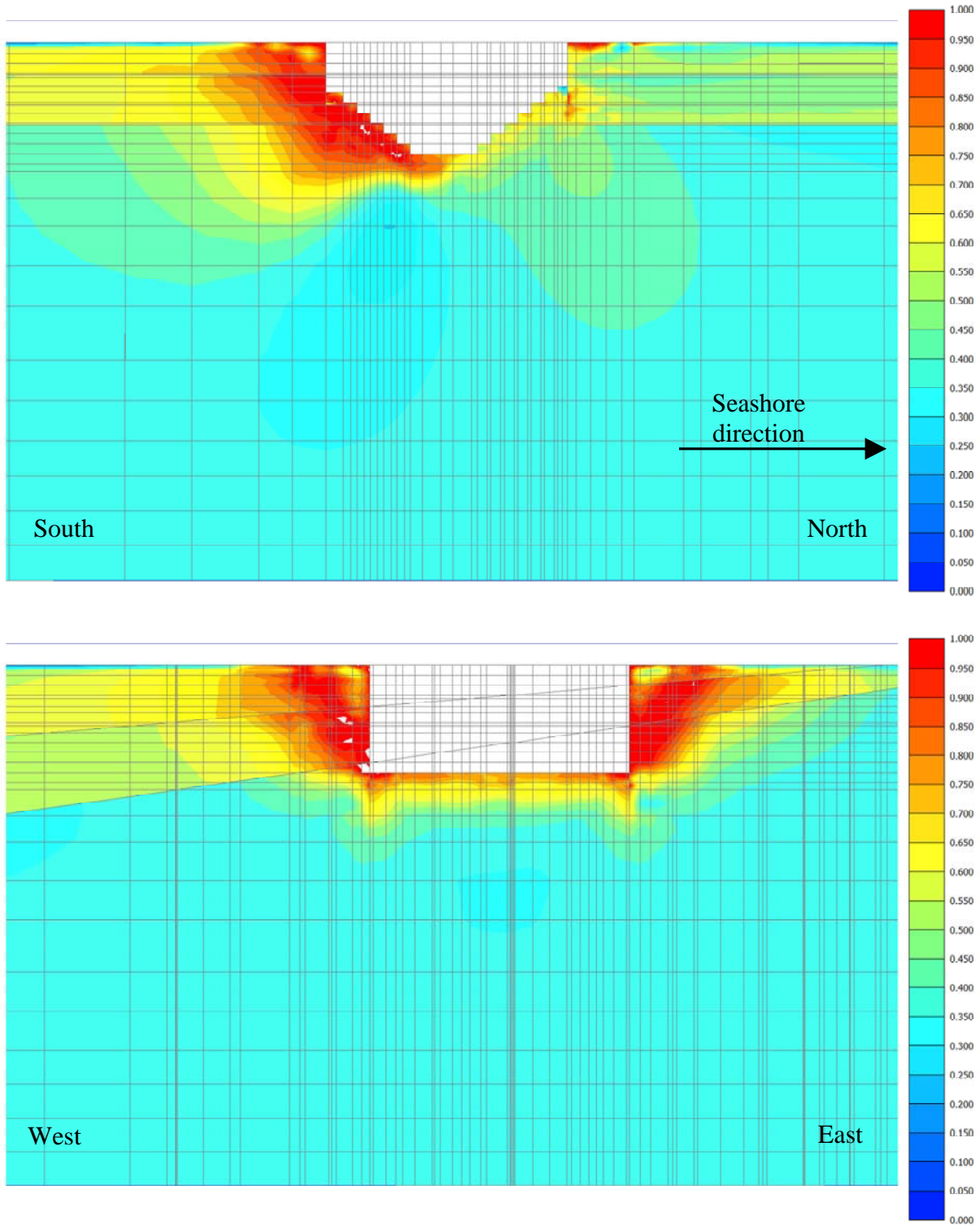


Figure 48: relative shear stress for ULS loads along longitudinal and transversal sections

 Stretto di Messina		Ponte sullo Stretto di Messina PROGETTO DEFINITIVO	
Calabria Anchor Block – evaluation of block behaviour via 3D FE analyses and of bearing capacity, Annex	<i>Codice documento</i> PF0067_F0_ANX	<i>Rev</i> F0	<i>Data</i> 20-06-2011

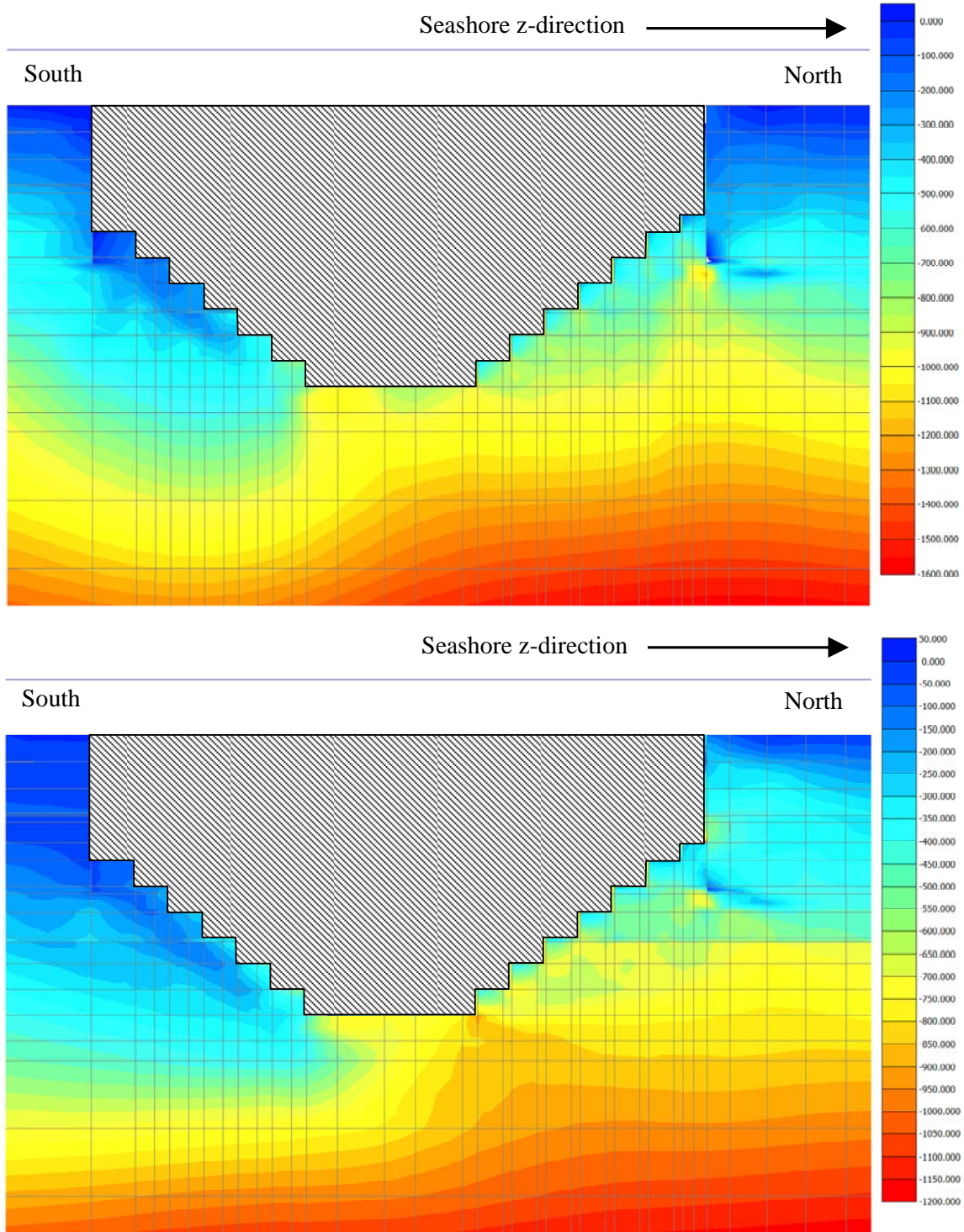


Figure 49: vertical total stresses σ_y and horizontal total stresses σ_z (in kPa) for ULS loads along the longitudinal central section

		Ponte sullo Stretto di Messina PROGETTO DEFINITIVO	
Calabria Anchor Block – evaluation of block behaviour via 3D FE analyses and of bearing capacity, Annex	<i>Codice documento</i> PF0067_F0_ANX	<i>Rev</i> F0	<i>Data</i> 20-06-2011

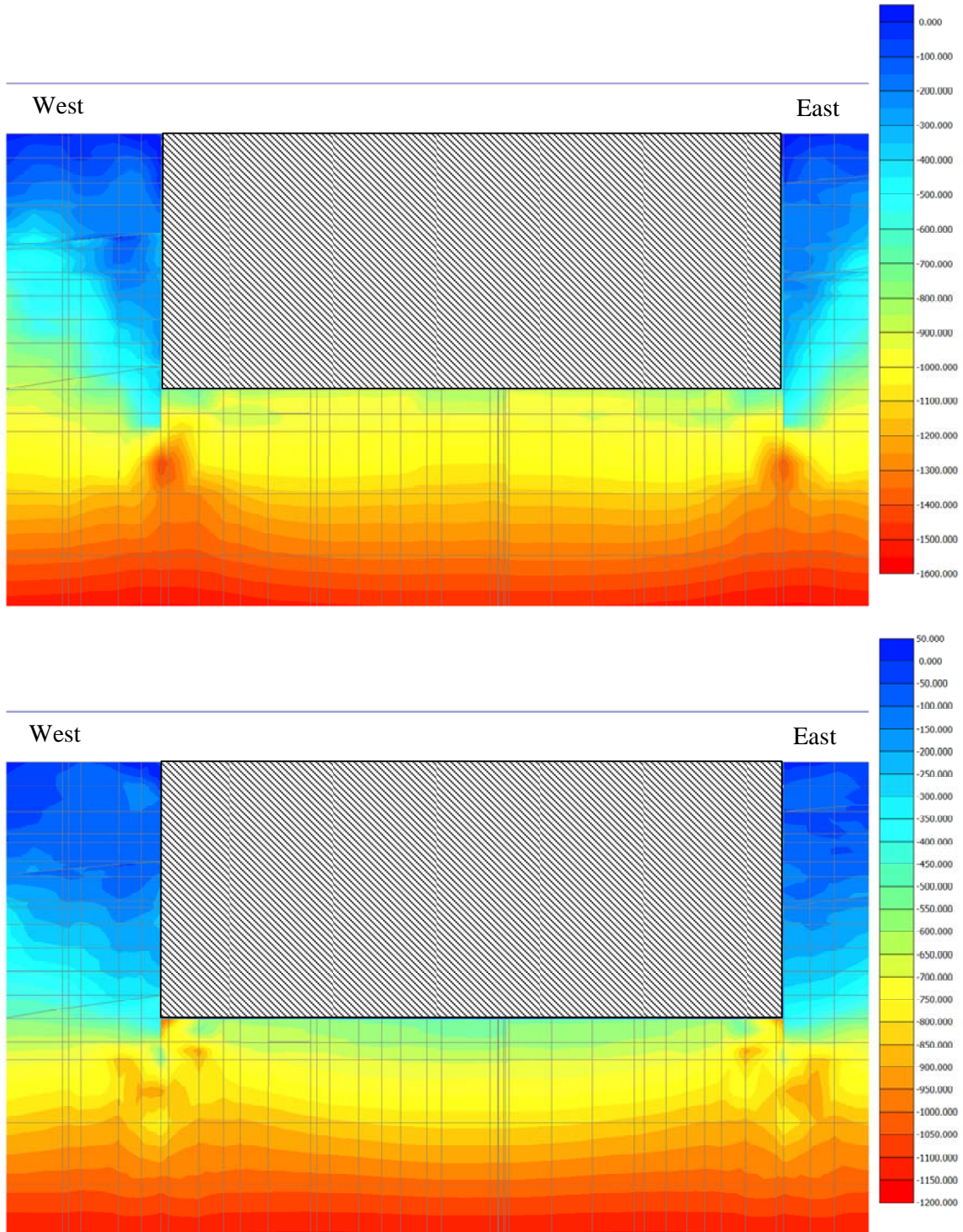


Figure 50: vertical total stresses σ_y and horizontal total stresses σ_x (in kPa) for ULS loads along the transversal central section

 Stretto di Messina		Ponte sullo Stretto di Messina PROGETTO DEFINITIVO	
Calabria Anchor Block – evaluation of block behaviour via 3D FE analyses and of bearing capacity, Annex	<i>Codice documento</i> PF0067_F0_ANX	<i>Rev</i> F0	<i>Data</i> 20-06-2011

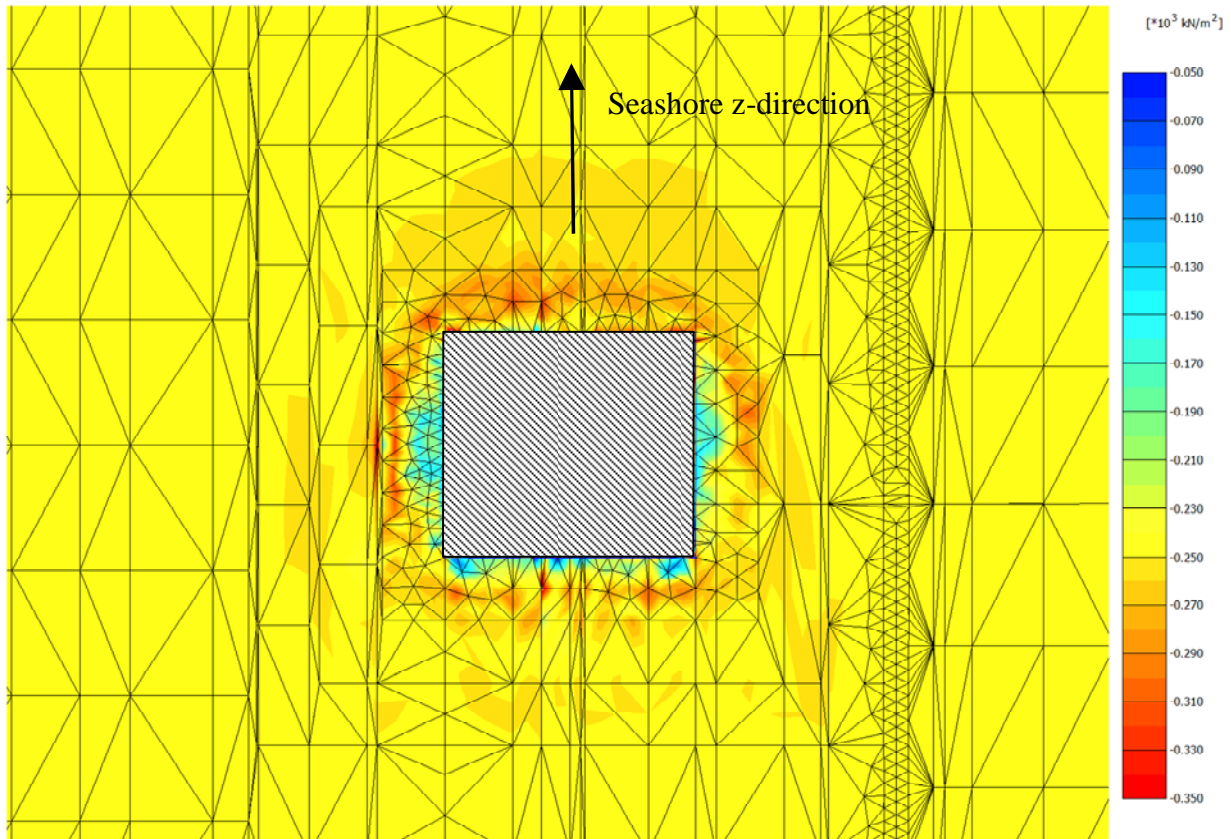


Figure 51: vertical total stresses σ_y (in kPa) for ULS loads along the horizontal section at 105.05 m a.s.l.

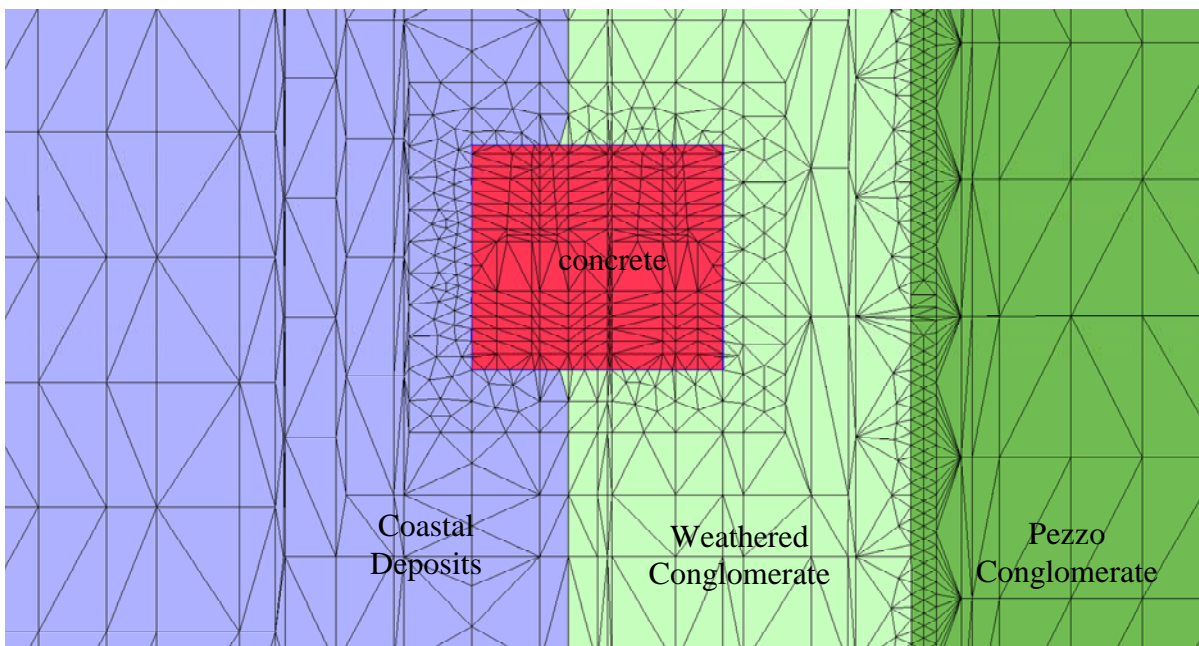
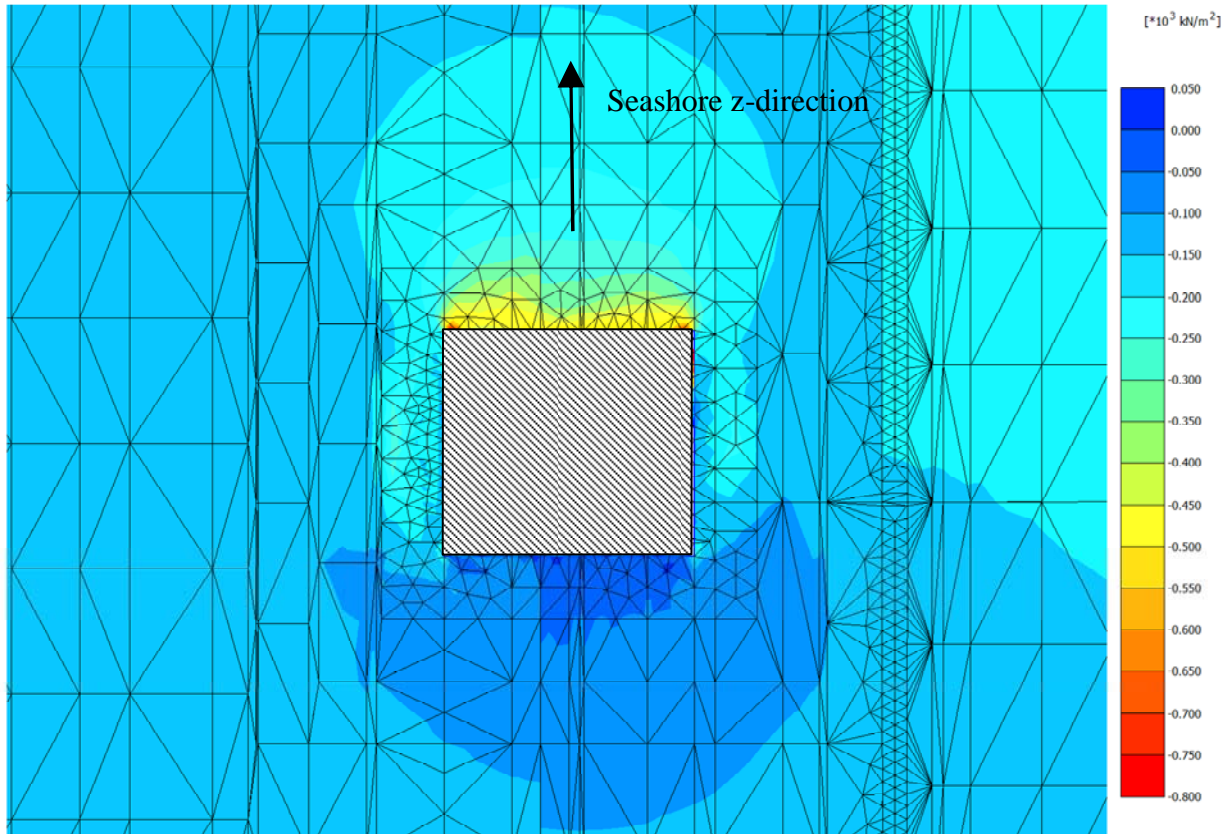


Figure 52: horizontal total stresses σ_z (in kPa) for ULS loads along the horizontal section at 105.05 m a.s.l. and soil layer position at the same elevation

 Stretto di Messina		Ponte sullo Stretto di Messina PROGETTO DEFINITIVO		
Calabria Anchor Block – evaluation of block behaviour via 3D FE analyses and of bearing capacity, Annex	<i>Codice documento</i> PF0067_F0_ANX	<i>Rev</i> F0	<i>Data</i> 20-06-2011	

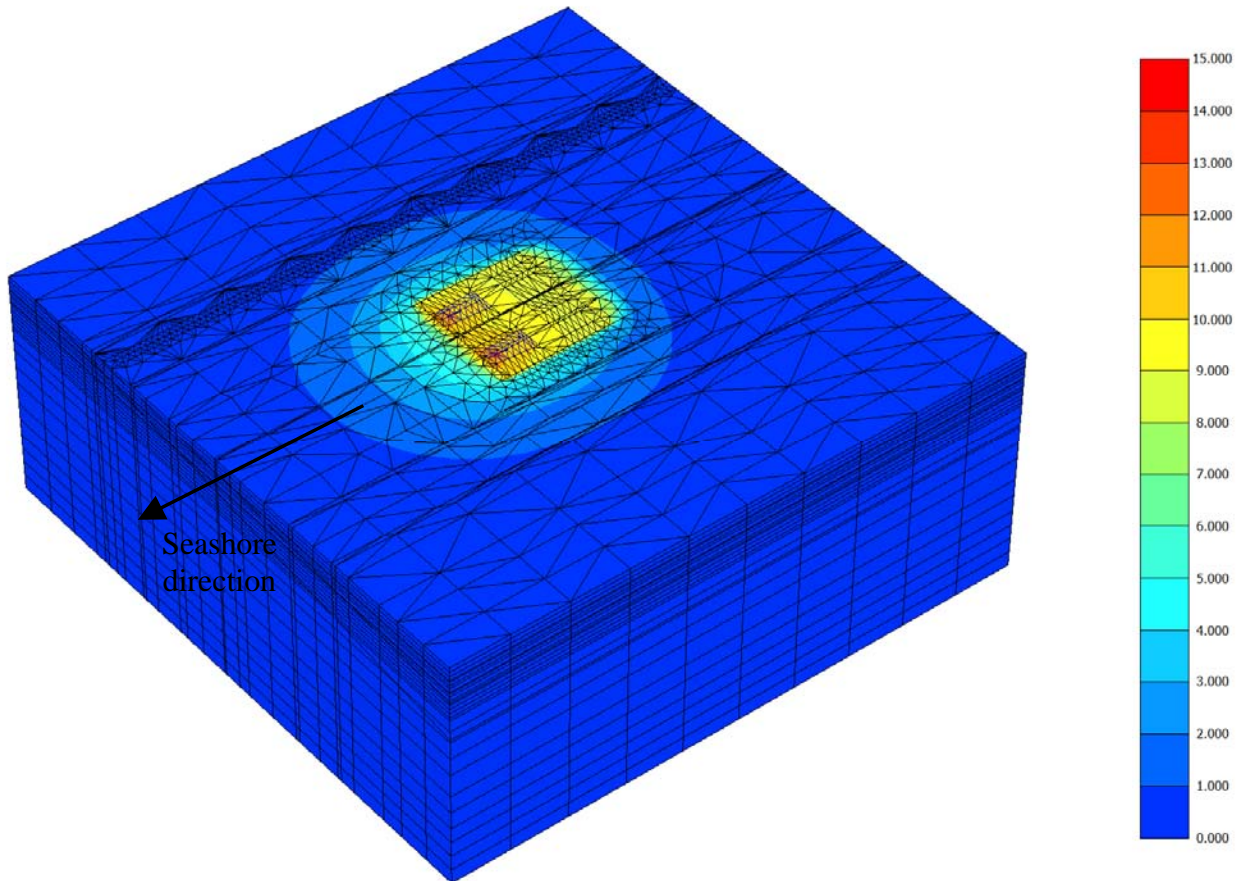


Figure 53: ULS load step: total mesh displacements (in mm)

		<p align="center">Ponte sullo Stretto di Messina PROGETTO DEFINITIVO</p>		
Calabria Anchor Block – evaluation of block behaviour via 3D FE analyses and of bearing capacity, Annex	<i>Codice documento</i> PF0067_F0_ANX	<i>Rev</i> F0	<i>Data</i> 20-06-2011	

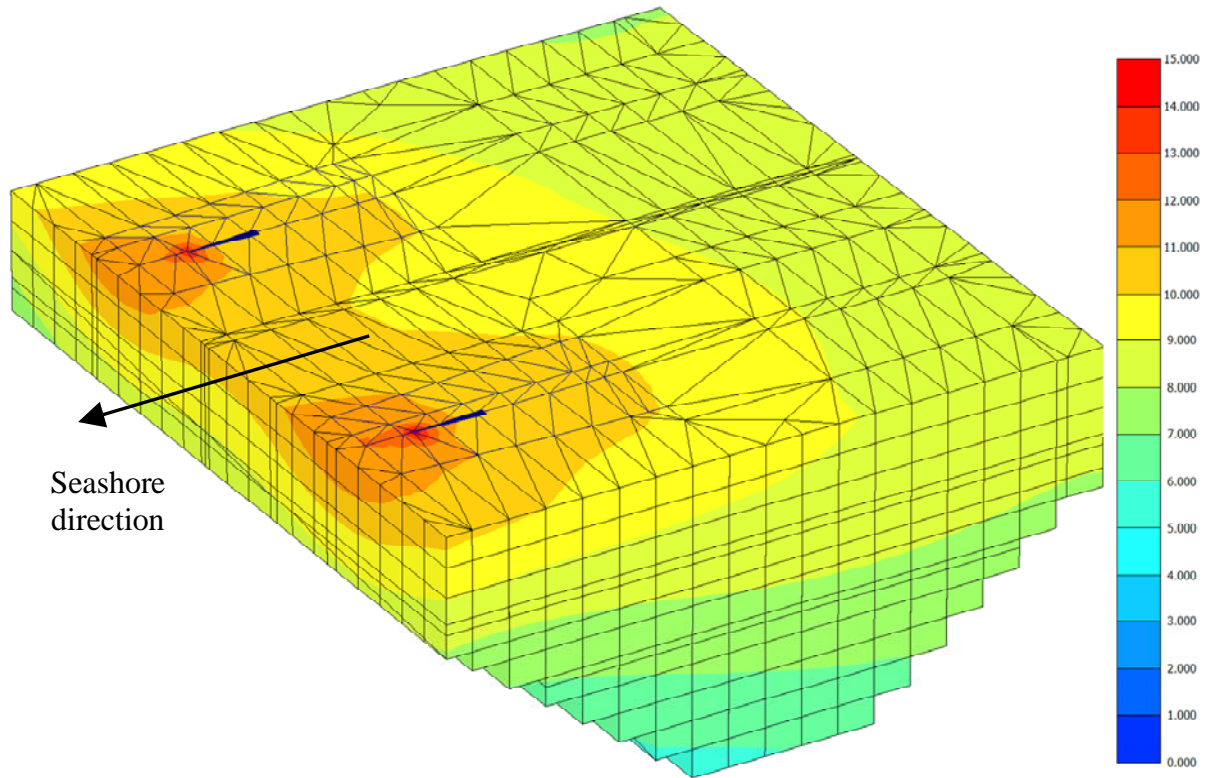


Figure 54: ULS load step: total mesh and anchor block mesh displacements (in mm)

		Ponte sullo Stretto di Messina PROGETTO DEFINITIVO		
Calabria Anchor Block – evaluation of block behaviour via 3D FE analyses and of bearing capacity, Annex	<i>Codice documento</i> PF0067_F0_ANX	<i>Rev</i> F0	<i>Data</i> 20-06-2011	

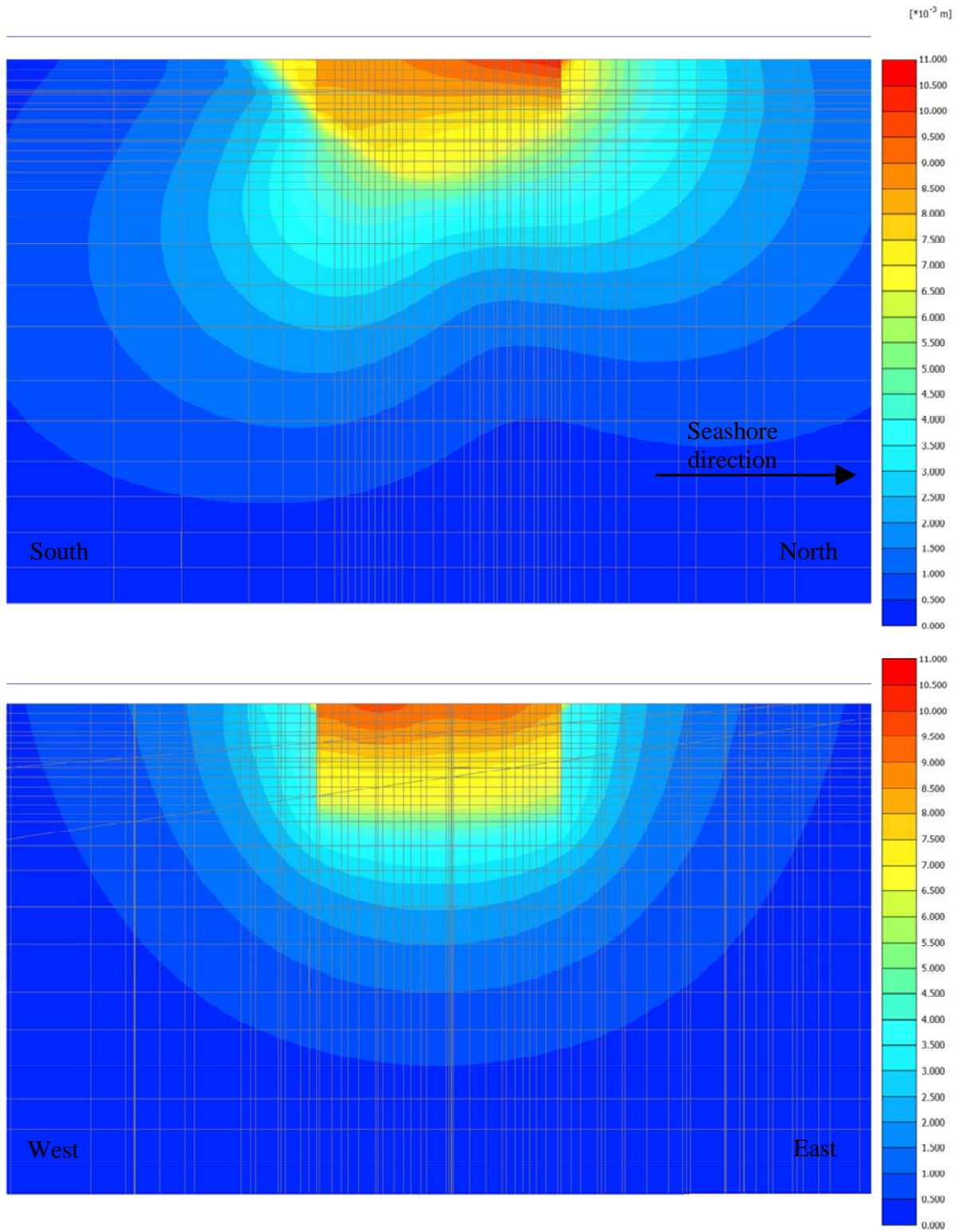


Figure 55: ULS load step: total displacements along longitudinal and transversal sections

		Ponte sullo Stretto di Messina PROGETTO DEFINITIVO		
Calabria Anchor Block – evaluation of block behaviour via 3D FE analyses and of bearing capacity, Annex	<i>Codice documento</i> PF0067_F0_ANX	<i>Rev</i> F0	<i>Data</i> 20-06-2011	

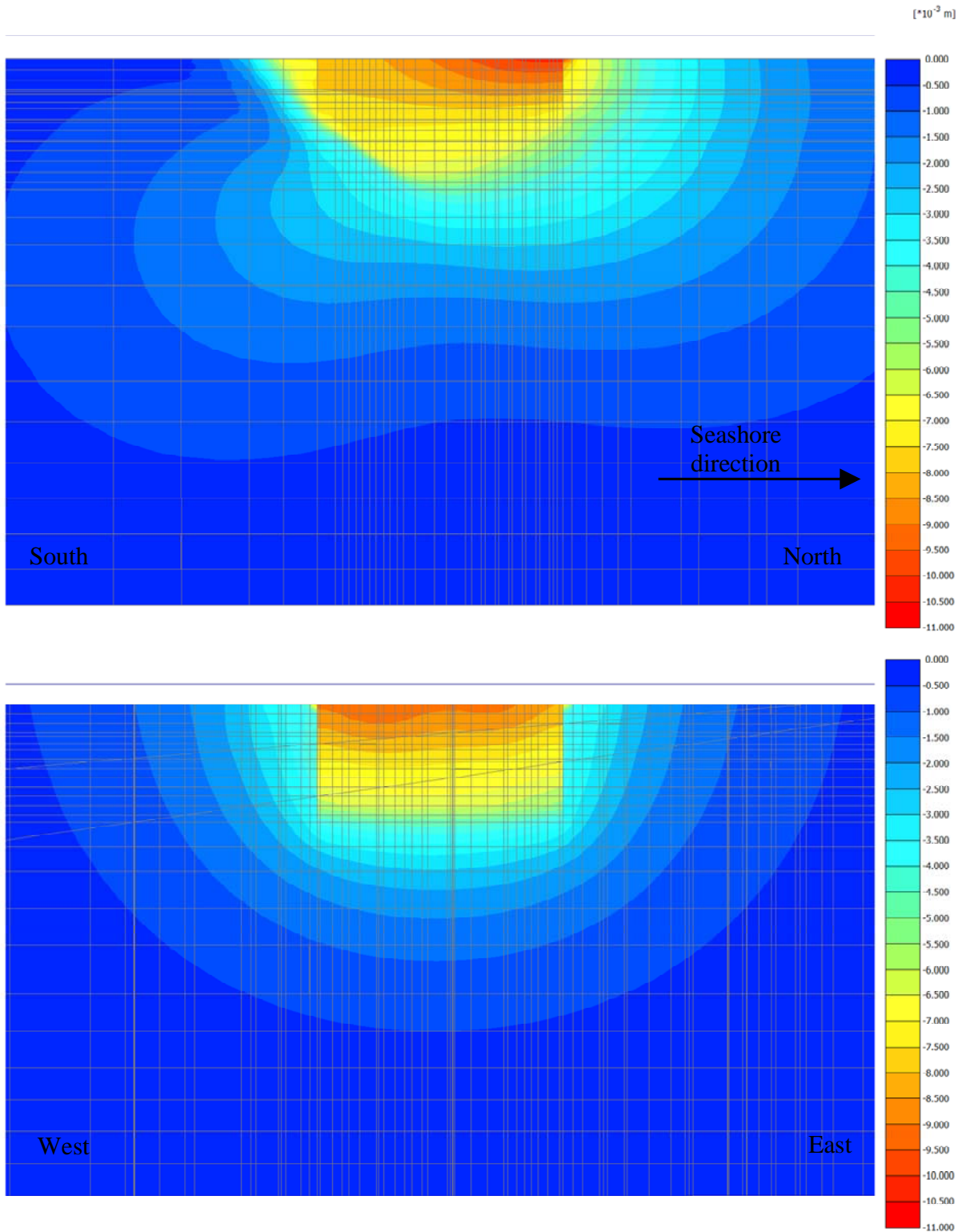


Figure 56: ULS load step: z-direction displacements along longitudinal and transversal sections

 Stretto di Messina		Ponte sullo Stretto di Messina PROGETTO DEFINITIVO		
Calabria Anchor Block – evaluation of block behaviour via 3D FE analyses and of bearing capacity, Annex	<i>Codice documento</i> PF0067_F0_ANX	<i>Rev</i> F0	<i>Data</i> 20-06-2011	

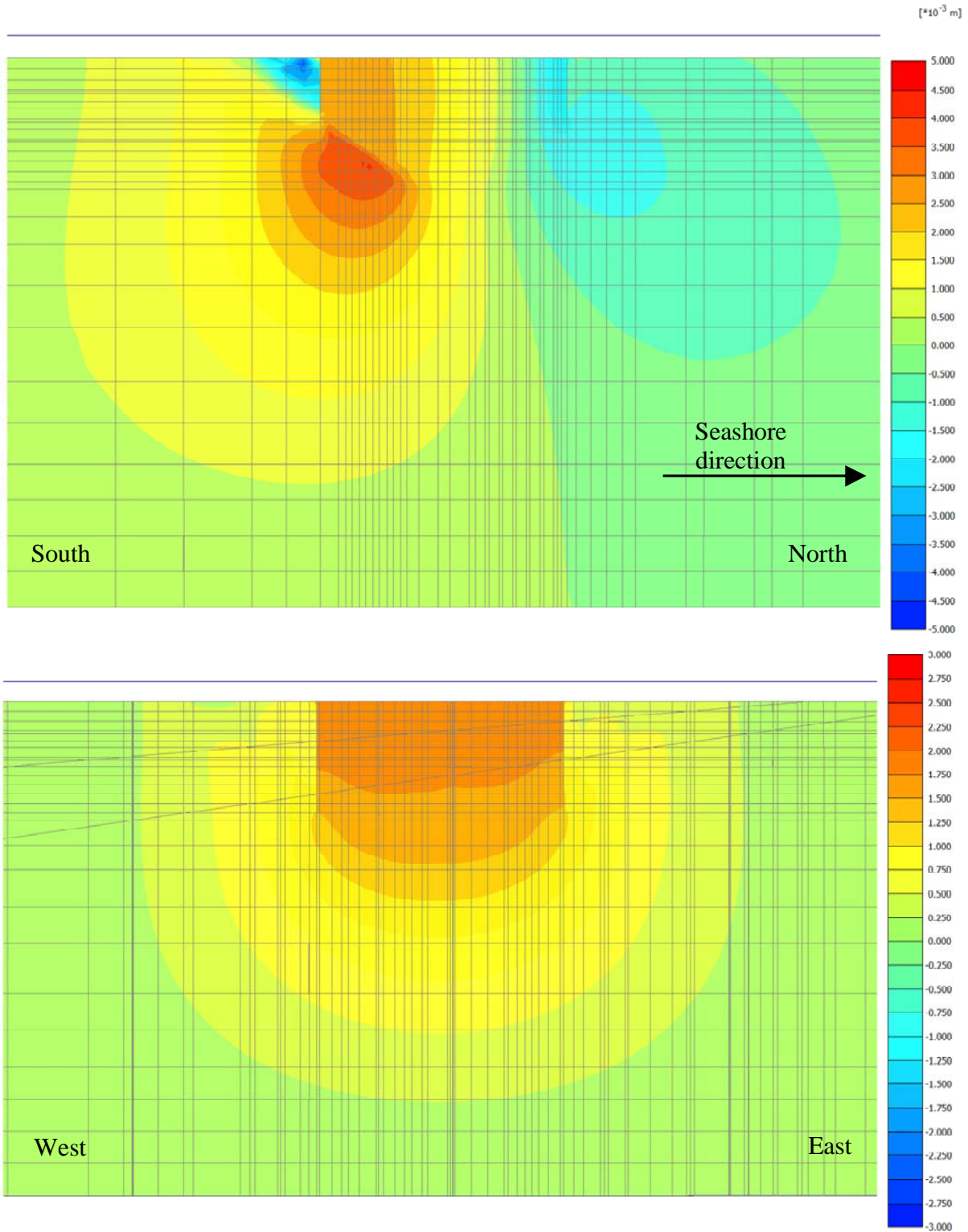


Figure 57: ULS load step: y-direction displacements along longitudinal and transversal sections

 Stretto di Messina		Ponte sullo Stretto di Messina PROGETTO DEFINITIVO		
Calabria Anchor Block – evaluation of block behaviour via 3D FE analyses and of bearing capacity, Annex	<i>Codice documento</i> PF0067_F0_ANX	<i>Rev</i> F0	<i>Data</i> 20-06-2011	

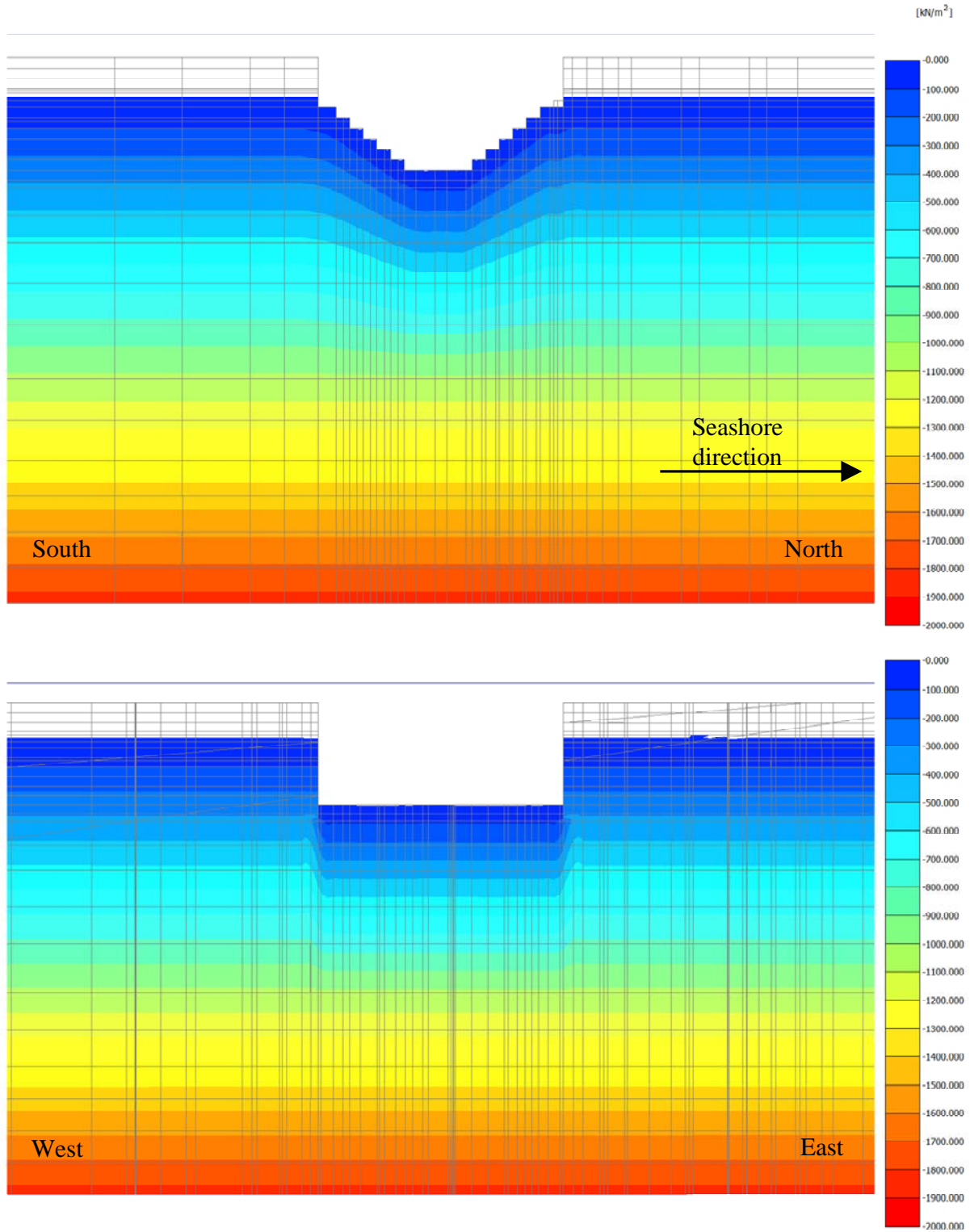


Figure 58: pore water pressure at end of excavation along longitudinal and transversal sections

 Stretto di Messina		Ponte sullo Stretto di Messina PROGETTO DEFINITIVO		
Calabria Anchor Block – evaluation of block behaviour via 3D FE analyses and of bearing capacity, Annex	<i>Codice documento</i> PF0067_F0_ANX	<i>Rev</i> F0	<i>Data</i> 20-06-2011	

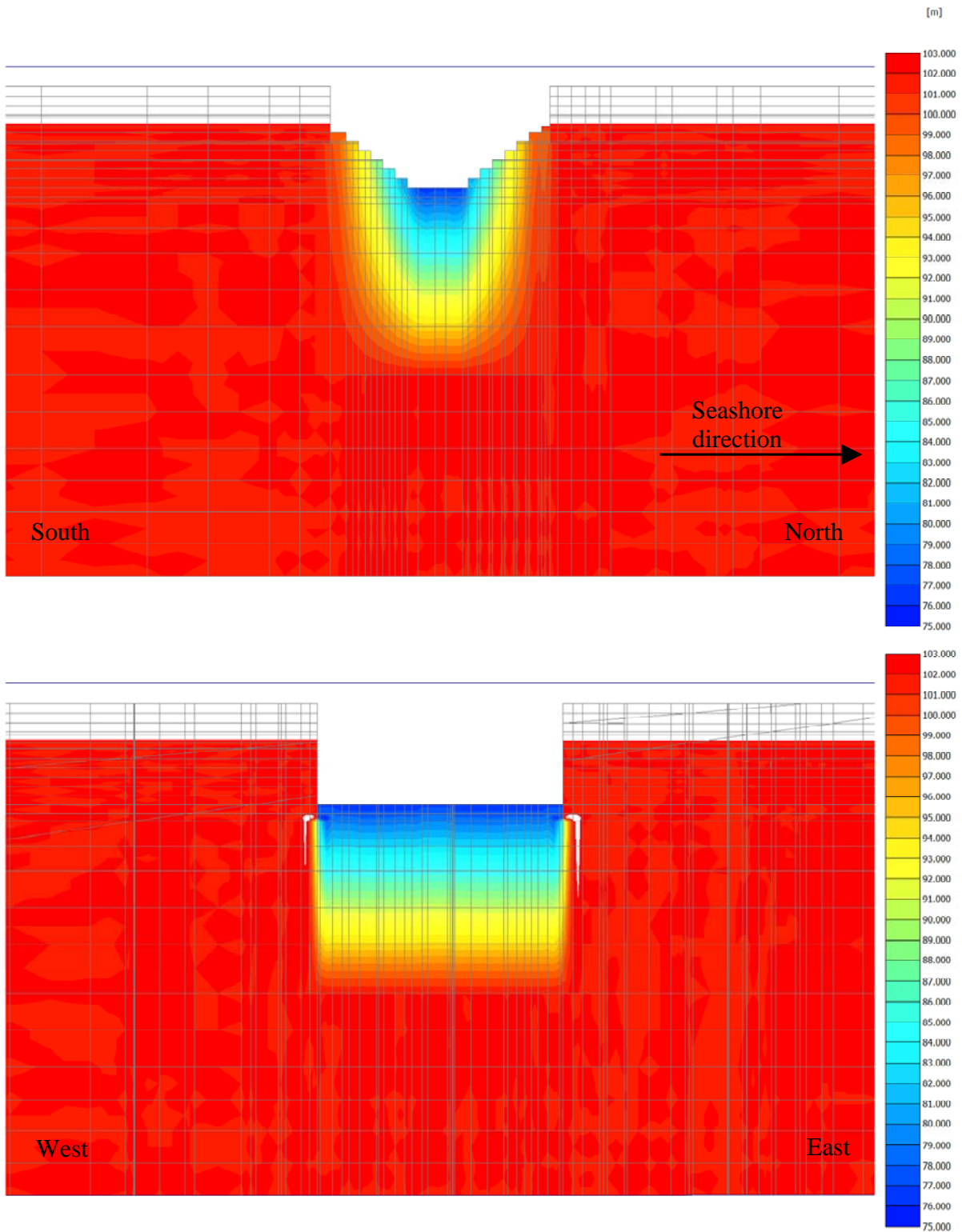


Figure 59: groundwater head at end of excavation along longitudinal and transversal sections

 Stretto di Messina		Ponte sullo Stretto di Messina PROGETTO DEFINITIVO		
Calabria Anchor Block – evaluation of block behaviour via 3D FE analyses and of bearing capacity, Annex	<i>Codice documento</i> PF0067_F0_ANX	<i>Rev</i> F0	<i>Data</i> 20-06-2011	

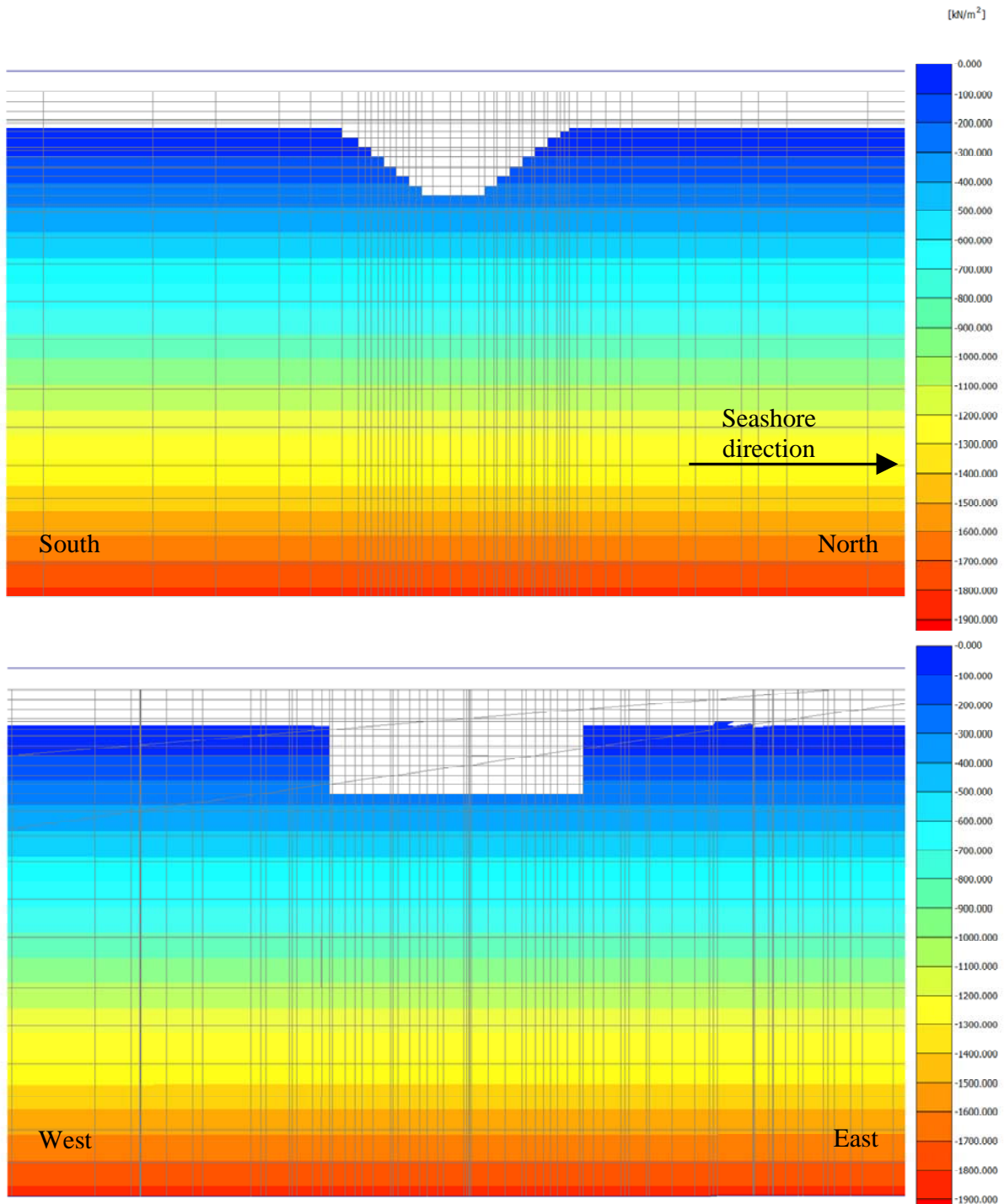


Figure 60: pore water pressure at the end of block construction along longitudinal and transversal sections

		Ponte sullo Stretto di Messina PROGETTO DEFINITIVO		
Calabria Anchor Block – evaluation of block behaviour via 3D FE analyses and of bearing capacity, Annex	<i>Codice documento</i> PF0067_F0_ANX		<i>Rev</i> F0	<i>Data</i> 20-06-2011

APPENDIX A – Updated cable forces obtained from global IBDAS model version 3.3b

The forces transmitted by the main cables to the Calabria Anchor Block have been re-evaluated using the global IBDAS model version 3.3b. The worst load combinations were selected for each limit state (SILS, SLS2 and ULS) for both static and seismic conditions, using 6 different criteria. Table A.1 resumes the values obtained for static loading conditions, while Table A.2 refers to seismic loading conditions.

Low differences are observed between values of the cable forces computed in the Tender Design and those recently provided by the global IBDAS model version 3.3b. Considering the maximum values of cable forces given by the different criteria for each load case, the ratio of the Tender Design cable forces to those provided by IBDAS model are in the range 1.05 to 0.96 (Table A.3); the higher ratio refers to the ULS load combination, while the lower is obtained for the SILS load combination.

For the Ultimate Limit State (ULS) cable forces provided by the Tender Design, referred to in the 3D FE analyses, are 5% higher than the corresponding IBDAS values, this resulting in a conservative estimate of the behaviour of the Calabria Anchor Block. Performance of the anchor block under SILS and SLS2 load cases are also discussed in § 4.

		Ponte sullo Stretto di Messina PROGETTO DEFINITIVO		
Calabria Anchor Block – evaluation of block behaviour via 3D FE analyses and of bearing capacity, Annex	<i>Codice documento</i> PF0067_F0_ANX	<i>Rev</i> F0	<i>Data</i> 20-06-2011	

Table A.1 – Static Loading Conditions – updated global IBDAS model version 3.3b

Criteria	Load case	F_{long} (MN)	F_{vert} (MN)	F (MN)
min u_{vert}	ULS	-2183	593	2262
max u_{vert}		-3578	1059	3731
min u_{hor}		-3578	1058	3731
max u_{hor}		-2183	594	2262
min R_{transv}		-3578	1058	3731
max R_{transv}		-2183	594	2262
min u_{vert}	SILS	-2479	692	2574
max u_{vert}		-3246	946	3381
min u_{hor}		-3246	946	3381
max u_{hor}		-2479	693	2574
min R_{transv}		-3246	946	3381
max R_{transv}		-2479	693	2574
min u_{vert}	SLS2	-2187	595	2267
max u_{vert}		-3217	938	3351
min u_{hor}		-3217	938	3351
max u_{hor}		-2187	595	2267
min R_{transv}		-3217	938	3351
max R_{transv}		-2187	595	2267

		Ponte sullo Stretto di Messina PROGETTO DEFINITIVO		
Calabria Anchor Block – evaluation of block behaviour via 3D FE analyses and of bearing capacity, Annex		<i>Codice documento</i> PF0067_F0_ANX	<i>Rev</i> F0	<i>Data</i> 20-06-2011

Table A.2 – Seismic Loading Conditions – updated global IBDAS model version 3.3b

Criteria	Load case	F_{long} (MN)	F_{vert} (MN)	F (MN)
min u_{vert}	ULS	-2093	533	2160
max u_{vert}		-3467	1052	3623
min u_{hor}		-3434	989	3574
max u_{hor}		-2125	596	2207
min R_{transv}		-3439	989	3578
max R_{transv}		-2121	596	2203
min u_{vert}	SILS	-2383	627	2464
max u_{vert}		-3316	1002	3464
min u_{hor}		-3281	934	3411
max u_{hor}		-2418	696	2516
min R_{transv}		-3285	933	3415
max R_{transv}		-2413	697	2512
min u_{vert}	SLS2	-2152	570	2227
max u_{vert}		-3235	958	3374
min u_{hor}		-3220	929	3351
max u_{hor}		-2167	598	2248
min R_{transv}		-3222	929	3353
max R_{transv}		-2165	598	2246

Table A.3: Cable forces in the Calabria Anchor Block: Tender Design and IBDAS values (model version 3.3b)

	Tender Design	Static IBDAS	Seismic IBDAS	
Load case	F (MN)	F (MN)	F (MN)	F_{TD}/F_{IBDAS}
ULS	3933	3731	3623	1.05
SILS	3142	3381	3464	0.91
SLS2	3232	3351	3374	0.96

		Ponte sullo Stretto di Messina PROGETTO DEFINITIVO		
Calabria Anchor Block – evaluation of block behaviour via 3D FE analyses and of bearing capacity, Annex	<i>Codice documento</i> PF0067_F0_ANX		<i>Rev</i> F0	<i>Data</i> 20-06-2011

APPENDIX B – Updated cable forces obtained from global IBDAS model version 3.3f

The forces transmitted by the main cables to the Calabria Anchor Block have been further re-evaluated using the global IBDAS model version 3.3f. The worst load combinations were selected for each limit state (SILS, SLS2 and ULS) for both static and seismic conditions, using 6 different criteria. Table B.1 resumes the values obtained for static loading conditions, while Table B.2 refers to seismic loading conditions.

Low differences are observed between values of the cable forces computed in the Tender Design and those recently provided by the global IBDAS model version 3.3f. Considering the maximum values of cable forces given by the different criteria for each load case, the ratio of the Tender Design cable forces to those provided by IBDAS model are in the range 1.07 to 0.93 (Table B.3); the higher ratio refers to the ULS load combination, while the lower is obtained for the SILS load combination.

For the Ultimate Limit State (ULS) cable forces provided by the Tender Design, referred to in the 3D FE analyses, are 7% higher than the corresponding IBDAS values, this resulting in a conservative estimate of the behaviour of the Calabria Anchor Block. Performance of the anchor block under SILS and SLS2 load cases are also discussed in § 4.

		Ponte sullo Stretto di Messina PROGETTO DEFINITIVO		
Calabria Anchor Block – evaluation of block behaviour via 3D FE analyses and of bearing capacity, Annex	<i>Codice documento</i> PF0067_F0_ANX	<i>Rev</i> F0	<i>Data</i> 20-06-2011	

Table B.1 – Static Loading Conditions – updated global IBDAS model version 3.3f

Criteria	Load case	F _{long} (MN)	F _{vert} (MN)	F (MN)
min u _{vert}	ULS	-2176	590	2254
max u _{vert}		-3528	1041	3678
min u _{hor}		-3528	1041	3678
max u _{hor}		-2175	591	2254
min R _{transv}		-3528	1041	3678
max R _{transv}		-2175	591	2254
min u _{vert}	SILS	-2440	679	2532
max u _{vert}		-3206	932	3338
min u _{hor}		-3206	932	3338
max u _{hor}		-2439	679	2532
min R _{transv}		-3206	932	3338
max R _{transv}		-2439	679	2532
min u _{vert}	SLS2	-2180	592	2259
max u _{vert}		-3177	924	3308
min u _{hor}		-3177	924	3308
max u _{hor}		-2180	592	2259
min R _{transv}		-3177	924	3308
max R _{transv}		-2180	592	2259

		Ponte sullo Stretto di Messina PROGETTO DEFINITIVO		
Calabria Anchor Block – evaluation of block behaviour via 3D FE analyses and of bearing capacity, Annex		<i>Codice documento</i> PF0067_F0_ANX	<i>Rev</i> F0	<i>Data</i> 20-06-2011

Table B.2 – Seismic Loading Conditions – updated global IBDAS model version 3.3f

Criteria	Load case	F _{long} (MN)	F _{vert} (MN)	F (MN)
min u _{vert}	ULS	-2114	540	2182
max u _{vert}		-3390	1024	3541
min u _{hor}		-3371	983	3512
max u _{hor}		-2132	581	2210
min R _{transv}		-3319	957	3454
max R _{transv}		-2185	608	2268
min u _{vert}	SILS	-2374	624	2454
max u _{vert}		-3245	977	3389
min u _{hor}		-3225	932	3357
max u _{hor}		-2394	670	2486
min R _{transv}		-3166	903	3292
max R _{transv}		-2452	699	2550
min u _{vert}	SLS2	-2158	571	2232
max u _{vert}		-3182	939	3318
min u _{hor}		-3174	920	3304
max u _{hor}		-2166	590	2245
min R _{transv}		-3150	908	3278
max R _{transv}		-2190	602	2272

Table B.3: Cable forces in the Calabria Anchor Block: Tender Design and IBDAS values (model version 3.3f)

	Tender Design	Static IBDAS	Seismic IBDAS	
Load case	F (MN)	F (MN)	F (MN)	F _{TD} /F _{IBDAS}
ULS	3933	3678	3541	1.07
SILS	3142	3338	3389	0.93
SLS2	3232	3308	3318	0.97

		Ponte sullo Stretto di Messina PROGETTO DEFINITIVO		
Calabria Anchor Block – evaluation of block behaviour via 3D FE analyses and of bearing capacity, Annex	<i>Codice documento</i> PF0067_F0_ANX	<i>Rev</i> F0	<i>Data</i> 20-06-2011	

REFERENCES

Berezantzev W.G. (1964). *Calculation of foundation basis*. Construction Literature, Leningrad, U.S.S.R.

Bustamante M., Doix B. (1985). *Une méthode pour le calcul des tirants et des micropieux injectés*. Bull. Liaison Labs. Ponts et Chaussées, 140, pp. 75-95.

Cubrinovski M. and Ishihara K. (1999). *Empirical correlation between SPT N-value and relative density for sandy soils*. Soils and Foundations, 39 n. 5, 61 – 71.

Jamiolkowski M., Leroueil S., and Lo Presti D. C. F. (1991). "Theme lecture: Design parameters from theory to practice." Proc., Geo-Coast'91, 1–41.

Rowe P.W. (1962). *The stress – dilatancy relation for static equilibrium of an assembly of particles in contact*. Proceedings Royal Society, London, Ser. A 269, 500 – 527.

Schmertmann J.H. (1975). *Measurement of in situ shear strength. State – of – the – art report*. ASCE Speciality Conference on in Situ Measurements of Soil Properties, 2, 57 – 138

Tanaka Y., Kudo Y., Yoshida Y. & Ikemi M. (1987). *A study on the mechanical properties of sandy gravel – dynamic properties of reconstituted samples*. Central Research Institute of Electric Power Industry, Report U87019.

		Ponte sullo Stretto di Messina PROGETTO DEFINITIVO		
Calabria Anchor Block – evaluation of block behaviour via 3D FE analyses and of bearing capacity, Annex	<i>Codice documento</i> PF0067_F0_ANX		<i>Rev</i> F0	<i>Data</i> 20-06-2011